UNIVERSITY OF OKLAHOMA

GRADUATE COLLEGE

THE FABRICATION AND APPLICATIONS OF PROTEIN PATTERNS PRODUCED VIA PARTICLE LITHOGRAPHY

A DISSERTATION

SUBMITTED TO THE GRADUATE FACULTY

in partial fulfillment of the requirements for the

Degree of

DOCTOR OF PHILOSOPHY

By

ZACHARY R. TAYLOR
Norman, Oklahoma
2012

THE FABRICATION AND APPLICATIONS OF PROTEIN PATTERNS PRODUCED VIA PARTICLE LITHOGRAPHY

A DISSERTATION APPROVED FOR THE
DEPARTMENT OF BIOENGINEERING

BY

_____
Dr. David Schmidtke

_____
Dr. Matthew Johnson

_____
Dr. Roger Harrison

_____
Dr. Edgar O'Rear, III

_____
Dr. Binil Starly

© Copyright by ZACHARY R. TAYLOR 2012
All Rights Reserved.

This work is dedicated to my father, David Taylor,
and my grandfather JD Taylor

Acknowledgements

I would like to thank Dr. David Schmidtke for his guidance and support not only as an advisor but also as a friend. I would also like to thank Dr. Matthew Johnson for providing additional guidance and perspective, which was the perfect complement to Dr. Schmidtke's contribution to my development as a scientist. I would like to thank the other members of my committee, Drs. Roger Harrison, Edgar O'Rear, III, and Binil Starly for their time and advice. I would also like to thank my labmates Krupa Patel, Phillip Coghill, Jeffrey Fontenot, and Travis Spain for their assistance and for helping make my time at the University of Oklahoma enjoyable. I would like to give a special thanks to Dr. Joel Keay for his collaboration and expertise. I would also like to thank Ernest Sanchez for his help with AFM imaging and Dr. Preston Larson for his help with SEM imaging. I would also like to thank Dr. Rodger McEver and his group at the Oklahoma Medical Research Foundation for their suggestions and advice. I would also like to thank the School of Chemical, Biological and Materials Engineering support staff for their assistance and Terri Colliver in particular for her kindness. I would like to thank Dora Rapp for her help ordering materials and equipment. I am especially grateful to my parents and family for their love and support. My father David Taylor and grandfather JD Taylor were and are my examples of the work ethic, perseverance, and integrity that were required to finish this dissertation. In addition, this work could not have been completed without the love, thoughtfulness, and patience of my wife Ashley or the help of my daughter Addison, who was an outstanding distraction when I needed a break. Finally, and most importantly, I would like to thank the Lord for bringing all of the aforementioned people into my life and for giving me the ability to start and finish this dissertation.

Table of Contents

List of Tables

Table **Page**

List of Figures

Figure **Page**

Abstract

A novel particle lithography technique with the ability to pattern protein in hexagonal dot arrays was developed. The patterning method consists of a simple three-step procedure: (1) formation of a close-packed polystyrene microsphere monolayer, (2) grafting of a protein-resistant layer of poly(ethylene glycol) (PEG), and (3) selective adsorption of protein into the resulting PEG holes. The diameter and center-to-center spacing of the patterned features was varied simultaneously by changing the diameter of the spheres used in the lithographic mask or independently using a simple heating modification. A combination of the original and modified procedures was used to produce patterns of protein dots with diameters of 450 nm – 9 μm and center-to-center spacings of 2 – 10 μm. To demonstrate the applicability of the particle lithography technique, a fluorescent-based immunoassay was created using quantum dot bioconjugates (QDBCs). The millions of protein dot features per patterned substrate served as redundant sampling points that produced a subpicomolar detection limit. Finally, the QDBC patterns were also used to investigate the differences between neutrophil spreading on patterned and homogenously coated anti-PSGL-1 (PL1) surfaces.

Chapter 1: Introduction

Why is Protein Patterning Important?

Many cellular processes are affected by the spatial arrangement of proteins including life cycle events (growth, differentiation, proliferation, and apoptosis);[1-8] movement (migration and chemotaxis);[9-15] protein synthesis;[7,16,17] respiration;[18] immunological response (antigen recognition and synapse formation);[19-25] and adhesion (capture, alignment, rolling, confinement, and spreading).[10,26-32] In addition, several biosensor[33-43] and cell culture[44-49] platforms rely on the organization of proteins into distinct regions. In order to further elucidate the relationship between cellular functions and protein spatial presentation and to produce new biological technologies, reliable methods of patterning protein in discrete domains are needed.

Purpose and Motivation

The primary objective of our work was to design a protein-patterning technique with the versatility to be used in a wide array of applications, including the investigation of cellular phenomena and the development of advanced technologies, like those listed above. While broad applicability was a major design consideration for our patterning process, we chose to demonstrate the use our protein-patterned substrates by studying the effects of ligand clustering on neutrophil adhesion.

Although the effects of protein spatial arrangement have been reported for other immunological cell types (e.g. lymphocytes),[14,15,19-21,23-25,40-43,50,51] relatively few

studies have been published detailing the response of neutrophils or neutrophil mimics to protein-patterned surfaces.[29,52,53] Consequently, there are several important physiological processes involving neutrophils that remain to be investigated. For example, as part of the inflammatory response, neutrophils transiently adhere to activated endothelial cells expressing the adhesion molecule P-selectin.[54] The rapid formation and breakage of bonds between P-selectin glycoprotein ligand-1 (PSGL-1) constitutively expressed on neutrophils and endothelial P-selectin causes neutrophils to roll before firmly adhering to the endothelium.[55] Activated endothelial cells express P-selectin in a punctated fashion in structures called clathrin-coated pits that have lateral dimensions on the order of tens of nanometers to several hundred nanometers.[56-58] Protein-patterned substrates can be used experimentally to mimic activated endothelial cells and to determine the relationship between P-selectin feature dimensions (e.g. patch size and spacing) and neutrophil rolling behavior (e.g. velocity and fluidity).

The applications of protein-patterned substrates, such as neutrophil-rolling experiments, provided the motivation for our patterning-process design criteria. We identified several characteristics of an ideal patterning technique including:

- Capability to pattern protein in both nanometer- (e.g. single proteins, clathrin coated pits) and micrometer-scale (e.g. full-cell size) domains of any desired shape.
- Flexibility to vary feature spacing and geometry to control the number of features with which cells can interact simultaneously.

- Ability to pattern multiple proteins on a single substrate.
- Biomolecule-friendly processing to preserve protein conformation and activity and to produce the correct protein orientation.
- High throughput production of both individual features and whole substrates.
- Low cost, simple equipment and methods to maximize accessibility in the scientific community.

Protein Patterning Techniques

With these criteria in mind, we considered the numerous methods that have been utilized to pattern protein on the micro- and nanometer scales to identify a starting point to develop our patterning procedure. Each technique has an associated cost, throughput, availability, resolution, and set of available feature geometries. For comparison, the basic characteristics of the most common techniques with at least sub-micron resolution are qualitatively summarized in Table 1.1. A more thorough discussion of the basic protocols, advantages, and disadvantages of each technique is also provided.

Microcontact Printing (μCP) (Figure 1.1) is a "soft lithography" technique that utilizes a stamp to transfer protein to surfaces.[59] To create protein patterns, a silicon master is first produced using a lithographic technique,[7,60,61] micromachining,[62] or a variety of less conventional methods.[63] Next, an elastomeric stamp, most commonly made from poly(dimethylsiloxane) (PDMS), is produced by pouring a pre-polymer and a curing agent over the master and allowing it to solidify. The stamp is then removed from the master, inked with the desired protein or chemical solution, and stamped onto the surface to be patterned. After the stamp is removed, the area of the substrate not

Table 1.1: Methods Used to Pattern Protein[a]

Technique	Resolution	Throughput	Expense	Available Geometries
Microcontact Printing (μCP)	50 nm	+++*	$$*	++
Nanoimprint Lithography (NIL)	<10 nm	+++*	$$*	++
Photolithography	100 nm	++-+++	$$-$$$$	++
Electron-Beam Lithography (EBL)	<10 nm	+	$$$	+++
Scanning Probe Lithography (SPL)	10 nm	+	$$	+++
Block Copolymer Lithographic Techniques (BCL / BCML)	<10 nm	+++	$	+
Particle Lithography	30 nm	+++	$	+

[a] The most well-characterized techniques with at least sub-micron resolution
*** Requires mask fabrication by another lithographic method**

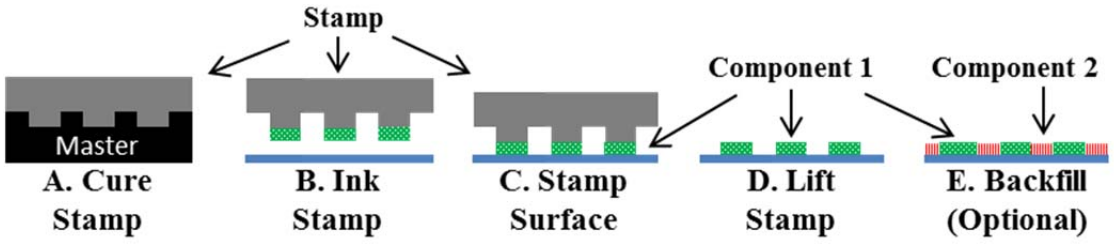

Figure 1.1: Microcontact Printing (μCP) Schematic.

exposed to the stamp can be backfilled with a different protein[64] or a protein-repellant species.[65]

Once formed, both the μCP pattern master and the stamps produced with it can typically be reused. This quality, combined with the straightforward procedure for making the stamps, makes μCP relatively inexpensive and simple to perform. The technique also has a nanometer-scale resolution limit and is versatile in the types of patterns it can produce. To date, microcontact printing has been used to pattern protein features as

small as approximately 50 nm with a high degree of reproducibility.[66,67] Using multiple stamps[64] or staggered features on one stamp,[60] multiple proteins can be patterned on a single substrate. Finally, numerous μCP patterning geometries are available and are restricted only by the limitations of the technique used to produce the master and by the properties of the elastomer used for the stamp.

Although μCP has many advantages, there are also drawbacks to the technique. While the creation of stamps from a master and the stamping process itself is relatively simple, the fabrication of the master often requires processes that are more advanced and more expensive. This issue is compounded by the fact that a new master is required whenever a new pattern geometry is desired. In addition to the difficulty and expense of producing masters, the elastomer stamps are subject to deformation that can lead to changes in feature sizes (although this is sometimes useful)[68] or structural failure of stamp features.[69-71] Finally, when a protein solution is used as the stamp "ink," the transferred protein can lose activity and specificity and cover the surface less densely and less homogeneously than protein adsorbed from solution.[72,73] Regardless of the ink used, μCP transfers contaminants, such as silicone oligomers, from the stamp to the patterned surface, which can affect the functionality of the final patterns.[73,74]

Nanoimprint Lithography (NIL) is a derivative of μCP that uses rigid masters instead of elastomeric stamps to transfer patterns to substrates. In NIL (Figure 1.2), a pattern master is pressed onto a polymer-coated substrate heated above the glass transition temperature of the polymer. After the substrate is allowed to cool, the master is

removed to reveal the imprinted design. The design features then serve as a lithographic mask or mold to pattern protein,[75] protein adherent molecules,[76-79] or protein repellant molecules.[77,80-82]

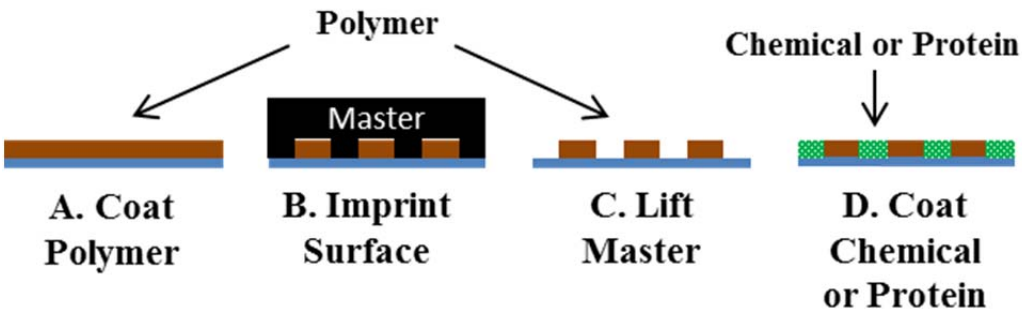

Figure 1.2: Nanoimprint Lithography (NIL) Schematic.

Due to its similarity to μCP, NIL has roughly the same advantages and disadvantages but with a few notable differences. At just several nanometers, the resolution limit of NIL is an order of magnitude lower than μCP and allows for single protein molecule patterning.[79,83] Also, NIL masters are rigid, so they are not subject to the same failure events as μCP stamps, but it is more difficult to maintain conformal contact during pattern transfer.[84] Since NIL masters are not inked directly and are made from materials (e. g. silicon) that do not leach impurities, the risk of contaminating a surface during printing is eliminated. As in μCP, a new master is needed for each desired pattern geometry. Since NIL masters include smaller features than μCP masters, the techniques used to fabricate them are typically more advanced and thus may require more expensive and specialized processing.

Photolithography exploits the light-sensitive properties of chemicals called resists to transfer patterns from a mask to a surface (Figure 1.3). In conventional photolithography, a homogeneous layer of a photoresist is formed on a substrate, often by spin-coating, that may be pre-coated with a protein adherent or repellant species.[48,85-87] Next, a photomask is used to selectively expose areas of the resist to light. Depending on the resist used, the exposed areas will degrade and become more soluble (positive photolithography) to a developer or will polymerize and become less soluble (negative photolithography). When the resist is subsequently exposed to the developer, the soluble regions of the resist will dissolve and reveal the pattern transferred from the photomask. This pattern can be used to selectively adsorb or graft protein,[88,89] a protein adherent layer,[38,48,90] or a protein repellant layer[8,17,91] to the underlying surface. Finally, the remaining resist is removed, and the newly exposed areas can be left unaltered or backfilled with protein,[87] a protein adherent species,[8,17] or a protein repellant species.[92,93]

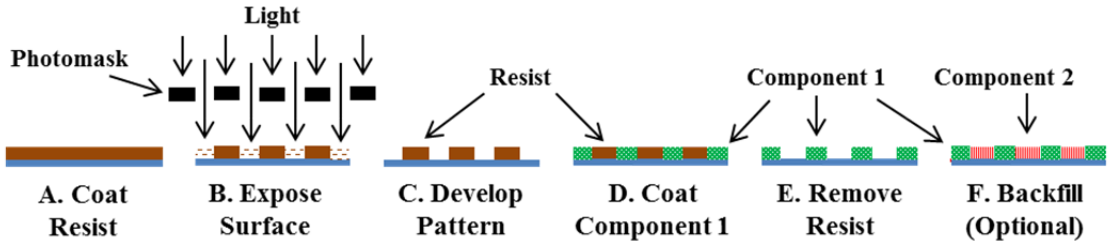

Figure 1.3: Photolithography Schematic (Positive Resist Shown).

Traditionally, the resolution limit of photolithography has been defined by the Rayleigh limit, which, for practical purposes, is often estimated as half the wavelength of the light source.[94] Thus, for a UV light source, the resolution limit would be on the order of hundreds of nanometers, and that size scale has been achieved in protein

patterning.[95] Recently, advanced techniques such as scanning near-field photolithography have been used to produce feature sizes on the order of tens of nanometers in electronic circuits and approximately 100 nanometers in protein patterns.[94,96,97] As these technologies become better developed, it is likely they will be further extended to protein patterning applications.

In addition to a sub-micron resolution limit, other advantages of photolithography include the ability to pattern complicated geometries and the ability to pattern multiple proteins on a single substrate.[20,86,88,98,99] The geometries available for patterning are limited only by the previously discussed resolution limit, the time and expense of fabricating or purchasing photomasks, and the cost of the lithographic system. It is possible to reduce or eliminate the cost of photomasks by using "maskless" techniques that utilize moving mirrors[100] or microscope components[86,88] to direct light. Additional reductions in cost and processing times can be achieved by using photoreactive chemicals that are components of the desired end-product in place of resists that must be removed.[5,86,88,95,97,98,100,101]

Unfortunately, even with cost-saving modifications, the price of the specialized equipment necessary for photolithography can be prohibitive. These expenses increase substantially as the resolution limit of the photolithographic system decreases with the most advanced commercial systems costing tens of millions of dollars.[96] Furthermore, to ensure even application of photoresist during spin-coating, photolithography must be performed in dust free cleanroom facilities that add additional costs to the process.[102]

In addition to high cost, patterns produced by photolithography must be exposed serially, which can contribute to long processing times. This restriction can be partially overcome by the use of automated systems but not without additional specialized, expensive equipment.

Electron-Beam Lithography (EBL) (Figure 1.4) is similar to photolithography in that designs can be created in a resist that is later removed[103-105] or generated directly in an

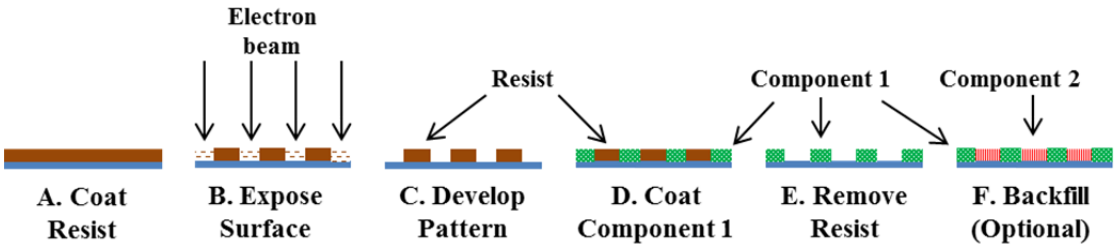

Figure 1.4: Electron-Beam Lithography (EBL) Schematic.

electron-sensitive compound that is a desired component of the final protein pattern.[106-116] However, there are two important differences between EBL and photolithography. First, EBL utilizes an electron beam instead of a light source. Electrons have a wavelength approximately 100,000 times smaller than that of light, so EBL is not a diffraction limited technique. Instead, the minimum feature size achievable with EBL is determined by the size of resist molecules and secondary electron interactions, which produce a resolution limit on the order of a few nanometers.[117,118] The second significant difference is that an electron beam is constantly repositioned to create patterns in EBL instead of features being transferred via a photomask. Since EBL is a maskless technique, nanometer-scale structures can be created in virtually any geometry, and the patterns can be altered by simply changing software inputs.

The primary disadvantages of EBL are the need for expensive equipment that requires specialized training and low sample throughput due to serial processing. Furthermore, the nature of electron beam instruments restricts the types of materials that can be patterned by EBL. In order to prevent charging, substrates must either be intrinsically conductive or treated with a conductive material. For this reason, most EBL protein patterns have been created on silicon even though other materials, such as transparent glass, are more convenient for laboratory applications. Thin layers of gold[116] and indium tin oxide[119] have been deposited on glass to eliminate charging during EBL but at the cost of additional processing time and equipment. Finally, the high-vacuum environment necessary for EBL can denature proteins, which restricts the serial patterning of multiple proteins on a single surface.[117] Protocols have been developed to overcome this limitation, but only for proteins whose functionality is not altered by drying[112] or that selectively adhere to specific chemical moieties.[120]

Scanning Probe Lithography (SPL) encompasses multiple techniques that utilize atomic force microscope (AFM) tips to pattern proteins on the micro- and nanometer scales. In SPL, a cantilever with a sharp tip (radius of curvature on the order of a few nanometers) is positioned close enough to a surface that an "ink" can be transferred from the tip to the surface or that the tip can deform the surface. By manipulating the characteristics of the sample surface, the properties of the AFM tip, and the way in which the AFM tip interacts with the sample surface, patterns may be formed by addition (dip-pen nanolithography [DPN]),[121-127] subtraction (nanoshaving),[128-130] or

substitution (nanografting, either physical[131,132] or chemical[133,134]) of protein or organic molecules.[117,135,136]

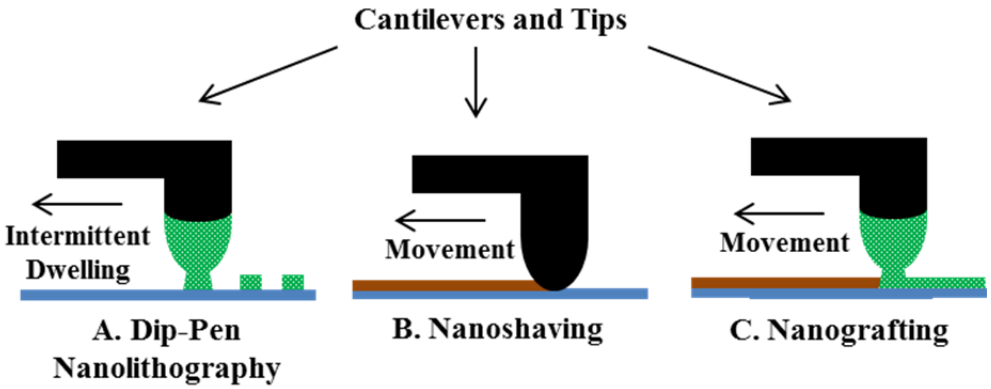

Figure 1.5: Scanning Probe Lithography (SPL) Variations.

SPL techniques have been used to pattern features with dimensions as small as ten nanometers, which allows for the immobilization of single proteins.[137,138] Since SPL systems are maskless, features can be patterned in any desired geometry so long as they are above the resolution limit of the particular instrument. Furthermore, multi-protein arrangements can be created by iterative processing or by simply changing inks during the writing process.[139-142]

Most SPL setups are also used for AFM imaging and thus contain only a single cantilever. Since only a small sample area (approximately 100 μm x 100 μm) can be patterned during each cycle with a single cantilever, SPL throughput is limited on traditional AFMs.[84] To address this issue, parallel DPN systems have been developed with as many as 55,000 cantilevers, but the scheme still has weaknesses.[143] First, the cantilevers cannot be controlled individually, so the same design must be produced by each tip. In addition, the cantilevers can only contact one sample at a time.

Consequently, while the time required to pattern a single substrate is decreased, samples must still be processed serially. Finally, the cantilever arrays and the self-leveling system necessary to produce uniform contact between the cantilevers and the surface to be patterned add extra cost to the already expensive AFM platform.[144] All SPL systems, regardless of the number of cantilevers mounted, require specialized training to use and constant tip cleaning and/or re-inking to ensure pattern uniformity.[84]

Block Copolymer Lithography (BCL) and Block Copolymer Micelle Lithography (BCML) employ copolymer molecules to create nanometer-scale arrays of single-polymer domains or arrays of micelles, respectively.[145,146] The copolymer molecules are formed by covalently linking "blocks" of polymers with varying degrees of polarity to create hybrid amphiphilic molecules. These molecules phase-separate when coated on a surface (BCL) or above critical concentrations in solution (BCML). In BCL, the copolymer molecules form distinct domains of the individual polymer moieties of which they are composed. The resulting arrangement can be used, as is, to selectively graft protein[147-153] or can serve as a mask for modification of the underlying substrate before protein attachment.[154] In BCML, copolymer micelles with metal salt cores are formed in solution before they are transferred to the surface to be patterned. The copolymer molecules are then chemically removed to form an array of metal particles that serve as protein anchoring points.[155-160]

The self-assembly of copolymer molecules in BCL and BCML does not require specialized equipment, which makes the techniques two of the most high throughput,

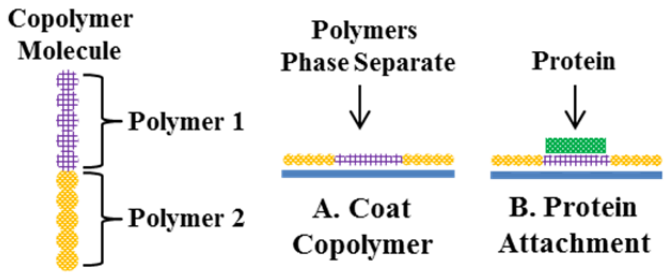

Figure 1.6: Block Copolymer Lithography (BCL) Schematic.

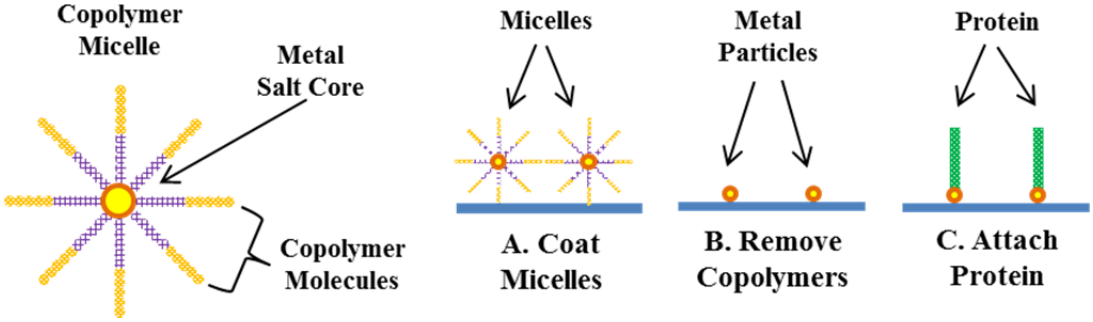

Figure 1.7: Block Copolymer Micelle Lithography (BCML) Schematic.

inexpensive, and technologically simple methods to form nanometer-scale protein patterns with down to single protein molecule resolution.[84] The dimensions and shapes of BCL structures can be varied to a degree by changing the molecular weight of the polymer blocks or the concentration of copolymer in solution.[146,150,151] BCML features can be altered through similar modifications and by adjusting the metal salt concentration, the water concentration, or the dip-coating speed of the micellar solution.[161]

Although the lengths of the copolymer molecules give block copolymer lithographic techniques a nanometer-scale resolution limit, they also limit the ability of BCL and BCML to produce larger protein-coated features or spacing between features. In order to define protein-coated areas measuring greater than approximately 100 nm or with

spacing greater than several hundred nanometers, BCL and BCML must be combined with more traditional lithographic techniques that decrease the throughput and add complexity and expense to the processes.[161] Furthermore, without further lithographic treatment, the available pattern geometries are extremely limited. Finally, to date, BCL and BCML have not been used to create multi-protein patterns, which further restricts the versatility of the techniques.

Particle Lithography utilizes micro- or nanometer-scale spheres as a lithographic mask to pattern protein. The basic procedure begins with the deposition of the spherical particles, which is typically accomplished by drop-casting,[162-169] dip-coating,[170,171] or spin-coating[171-174] a colloidal suspension onto the surface to be patterned. Next, the protein,[165,167,171] protein adherent chemical,[168] or protein repellant chemical[162,169,172-174] that will comprise the background of the pattern is applied to the surface if it was not a component of the sphere suspension.[163,164,166] When the spheres are subsequently removed, the newly uncovered areas of the substrate can be left bare[163-167,171] or covered with a protein[162,169,172-175] or another chemical species.[170]

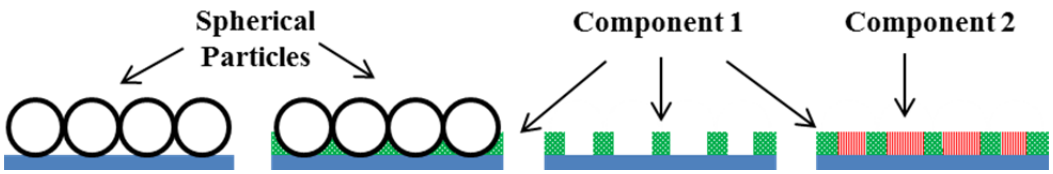

Figure 1.8: Particle Lithography Schematic.

Regardless of the deposition technique applied, the spheres used in particle lithography ultimately self-assemble into close-packed arrangements that can be used as a

lithographic mask to create millions of duplicate features simultaneously. As a result, particle lithography only requires relatively simple, inexpensive equipment and techniques and can be used to create samples in parallel. In addition, particle lithography has been used to create features with dimensions as small as tens of nanometers.[176-178]

Although particle lithography is a versatile technique to pattern protein, it is not without limitations. To date, particle lithography has not been used to pattern multiple proteins on the same substrate. Furthermore, the available patterning geometries, including the shape, size, spacing, and spatial arrangement of the protein coated areas, are restricted by the shape and size of the spherical particles that compose the mask. Consequently, particle lithography has only been used to pattern protein in or around circular,[162,164-166,168-170,172-175,179] triangular,[180] and ring[162,163,166] domains. Other materials have been deposited in more complexly shaped regions (e.g. ellipses,[181] crescents,[182] hexagons,[183] trapezoids,[184] rods,[176] shuttlecocks,[184] zigzag lines,[184] chains,[177]), but these techniques have not yet been extended to protein patterning.

Without mask modification, the spacing and size of protein coated areas are dependent on the mask particles' diameter. To vary these properties independently, heating[179] and etching[170,172-175] techniques have been used to enlarge or reduce feature sizes, respectively, without affecting feature spacing. Methods have also been developed to alter particle spacing without altering particle dimensions (and thus, theoretically, not

altering the transferred feature sizes), but they have not yet been applied to protein patterning.[185]

Close-packed spherical particles form hexagonal arrays that define the spatial orientation of patterned structures. Protocols have been developed to create line,[185-187] square,[187] and ring[185-187] arrangements of close-packed particles. In addition, arrays of non-close-packed particles with random,[188] square,[185] and hexagonal[185] periodicities have been formed. Unfortunately, none of these modifications have been applied to protein patterning.

Overview

A nanometer-scale resolution limit, high throughput, and "bench-top" technology make particle lithography an attractive alternative to other protein patterning methods. Thus, we chose particle lithography as the basic platform for our protein patterning procedures. However, as discussed above, particle lithography has inherent limitations that must be resolved to maximize the applicability of the technique. The subsequent chapters in this dissertation detail the development of our basic patterning procedure, modifications to overcome some of the major drawbacks of the technique, and the application of protein patterns produced by particle lithography to cell adhesion experiments. Each chapter includes an introduction to provide the relevant background information and motivation for the particular study.

Chapter 2 introduces our basic particle lithography protein patterning technique. We characterized the three steps of our procedure: lithographic mask formation, passivation of the unblocked surface by grafting a protein-repellant layer of poly(ethylene glycol) (PEG), and adsorption of protein in the domains protected by the spheres. We demonstrate the ability of our technique to create hexagonal protein "dot" patterns with sub-micron to micron-sized dimensions that are independent of the protein used. In addition, we discuss the importance of removing residual surfactant from substrate surfaces in order to obtain uniform features. The patterning protocol presented in this chapter was the basis for the remainder of the work in this dissertation.

Chapter 3 describes an extension of our particle lithography technique to pattern quantum dot bioconjugates (QDBCs). This variation of our technique allows for the patterning of proteins, antibodies, and small biological molecules, such as biotin, in sub-micron domains. We utilized the relatively-high quantum efficiency and photostability of quantum dots relative to traditional fluorophores to construct a sensitive fluorescent immunoassay with a sub-picomolar detection limit. Although a slight departure from our goal of creating cell adhesion substrates, this study demonstrates the broad applicability of our patterning procedure that we achieved. In addition, patterned QDBCs allow relatively long-term fluorescent visualization of protein coated areas in cell adhesion studies discussed in later chapters.

Chapter 4 discusses a modification of our patterning process to independently-control protein-dot diameters and center-to-center distances. By heating the sphere lithographic

mask beyond its glass transition temperature, we induced deformation that expanded the "footprint" of the spheres in the PEG background. We used both uniform heating to create single-diameter protein dot patterns and gradient heating to create a continuum of protein dot diameters on a single substrate. This chapter also includes our first application of our patterning technique to cell-adhesion experiments. We demonstrated the spreading of isolated human neutrophils on anti-PSGL-1 (PL1 antibody) patterned surfaces and found that adhesion was limited to PL1-coated areas.

Chapters 5 and 6 examine the results of other preliminary studies, provide suggestions for future directions, and present the major conclusions of this dissertation.

Summary of Scientific Contributions

The major scientific contributions of this work are:

- The development of a low cost, "bench-top" protein patterning technique capable of producing sub-micron features quickly and easily compared to other patterning techniques.
- The extension of the patterning technique to multiple proteins and biomolecule-conjugated particles (i.e. CdSe quantum dots and nanogold).
- The modification of the technique with a deformation heating step to change protein dot diameters without altering their center-to-center spacing. The heat can be applied uniformly to create patterns with dots of a single diameter or as a gradient to create a continuous gradient of dot sizes across a sample.

- The application of the technique to a proof-of-concept novel fluorescent binding assay with a sub-picomolar detection limit. The binding assay could theoretically be used for a number of different analytes of interest from various biological fluids.
- The application of the technique to a proof-of-concept neutrophil spreading assay. The assay could theoretically be used to study adhesion interactions in a wide array of physiologically relevant situations (e.g. different ligands, ligand geometries, cell types, flow conditions, etc.).

References

1. Chen, C. S.; Mrksich, M.; Huang, S.; Whitesides, G. M.; Ingber, D. E. Geometric Control of Cell Life and Death. *Science.* **1997**, *276*, 1425-1428.

2. Nelson, C. M.; Chen, C. S. Cell-cell signalling by direct contact increases cell proliferation via a PI3K-dependent signal. *FEBS Lett.* **2002**, *514*, 238-242.

3. Chen, C. S.; Mrksich, M.; Huang, S.; Whitesides, G. M.; Ingber, D. E. Micropatterned Surfaces for Control of Cell Shape, Position, and Function. *Biotechnol. Prog.* **1998**, *14*, 356-363.

4. Dike, L. E.; Chen, C. S.; Mrksich, M.; Tien, J.; Whitesides, G. M.; Ingber, D. E. Geometric control of switching between growth, apoptosis, and differentiation during angiogenesis using micropatterned substrates. *In Vitro Cell Dev.-An.* **1999**, *35*, 441-448.

5. Ito, Y.; Chen, G.; Imanishi, Y. Micropatterned Immobilization of Epidermal Growth Factor To Regulate Cell Function. *Bioconjugate Chem.* **1998**, *9*, 277-282.

6. Kandere-Grzybowska, K.; Campbell, C.; Komarova, Y.; Grzybowski, B. A.; Borisy, G. G. Molecular dynamics imaging in micropatterned living cells. *Nat. Methods.* **2005**, *2*, 739-741.

7. Singhvi, R.; Kumar, A.; Lopez, G. P.; Stephanopoulos, G. N.; Wang, D. C.; Whitesides, G. M.; Ingber, D. E. Engineering Cell Shape and Function. *Science.* **1994**, *264*, 696-698.

8. Thomas, C. H.; Lhoest, J.-B.; Castner, D. G.; McFarland, C. D.; Healy, K. E. Surfaces Designed to Control the Projected Area and Shape of Individual Cells. *J. Biomech. Eng.-T. ASME.* **1999**, *121*, 40-48.

9. Doyle, A. D.; Wang, F. W.; Matsumoto, K.; Yamada, K. M. One-dimensional topography underlies three-dimensional fibrillar cell migration. *J. Cell Biol.* **2009**, *184*, 481-490.

10. Saux, G. L.; Magenau, A.; Gunaratnam, K.; Kilian, K. A.; Böcking, T.; Gooding, J. J.; Gaus, K. Spacing of Integrin Ligands Influences Signal Transduction in Endothelial Cells. *Biophys. J.* **2011**, *101*, 764-773.

11. Tan, J.; Shen, H.; Saltzman, W. M. Micron-Scale Positioning of Features Influences the Rate of Polymorphonuclear Leukocyte Migration. *Biophys. J.* **2001**, *81*, 2569-2579.

12. Jeon, N. L.; Baskaran, H.; Dertinger, S. K. W.; Whitesides, G. M.; Water, L. V. D.; Toner, M. Neutrophil chemotaxis in linear and complex gradients of interleukin-8 formed in a microfabricated device. *Nat. Biotechnol.* **2002**, *20*, 826-830.

13. Miller, E. D.; Li, K.; Kanade, T.; Weiss, L. E.; Walker, L. M.; Campbell, P. G. Spatially directed guidance of stem cell population migration by immobilized patterns of growth factors. *Biomaterials.* **2011**, *32*, 2775-2785.

14. Stachowiak, A. N.; Irvine, D. J. Inverse opal hydrogel-collagen composite scaffolds as a supportive microenvironment for immune cell migration. *J. Biomed. Mater. Res. A.* **2008**, *85*, 815-828.

15. Swiston, A. J.; Cheng, C.; Um, S. H.; Irvine, D. J.; Cohen, R. E.; Rubner, M. F. Surface Functionalization of Living Cells with Multilayer Patches. *Nano Lett.* **2008**, *8*, 4446-4453.

16. Li, F.; Li, B.; Wang, Q.-M.; Wang, J. H.-C. Cell Shape Regulates Collagen Type I Expression in Human Tendon Fibroblasts. *Cell Motil. Cytoskel.* **2008**, *65*, 332-341.

17. Thomas, C. H.; Collier, J. H.; Sfeir, C. S.; Healy, K. E. Engineering gene expression and protein synthesis by modulation of nuclear shape. *P. Natl. Acad. Sci. USA.* **2002**, *99*, 1972-1977.

18. Nishizawa, M.; Takoh, K.; Matsue, T. Micropatterning of HeLa Cells on Glass Substrates and Evaluation of Respiratory Activity Using Microelectrodes. *Langmuir.* **2002**, *18*, 3645-3649.

19. DeMond, A. L.; Mossman, K. D.; Starr, T.; Michael L. Dustin; Groves, J. T.; Yager, P. T Cell Receptor Microcluster Transport through Molecular Mazes Reveals Mechanism of Translocation. *Biophys. J.* **2008**, *94*, 3286-3292.

20. Doh, J.; Irvine, D. J. Immunological synapse arrays: Patterned protein surfaces that modulate immunological synapse structure formation in T cells. *P. Natl. Acad. Sci. USA.* **2006**, *103*, 5700-5705.

21. Hartman, N. C.; Nye, J. A.; Groves, J. T. Cluster size regulates protein sorting in the immunological synapse. *P. Natl. Acad. Sci. USA.* **2009**, *106*, 12729-12734.

22. Hammond, S.; Wagenknecht-Wiesner, A.; Veatch, S. L.; Holowka, D.; Baird, B. Roles for SH2 and SH3 domains in Lyn kinase association with activated FceRI in RBL mast cells revealed by patterned surface analysis. *J. Struct. Biol. 168*, 161-167.

23. Manz, B. N.; Jackson, B. L.; Petit, R. S.; Dustin, M. L.; Groves, J. T-cell triggering thresholds are modulated by the number of antigen within individual T-cell receptor clusters. *P. Natl. Acad. Sci. USA.* **2011**, *108*, 9089-9094.

24. Mossman, K. D.; Campi, G.; Groves, J. T.; Dustin, M. L. Altered TCR Signaling from Geometrically Repatterned Immunological Synapses. *Science.* **2005**, *310*, 1191-1193.

25. Yu, C.-h.; Wu, H.-J.; Kaizuka, Y.; Vale, R. D.; Groves, J. T. Altered Actin Centripetal Retrograde Flow in Physically Restricted Immunological Synapses. *PLoS ONE.* **2010**, *5*, e11878.

26. Cuvelier, D.; Rossier, O.; Bassereau, P.; Nassoy, P. Micropatterned ‘‘adherent /repellent’’ glass surfaces for studying the spreading kinetics of individual red blood cells onto protein-decorated substrates. *Eur. Biophys. J.* **2003**, *32*, 342-354.

27. Kenar, H.; Kocabas, A.; Aydinli, A.; Hasirc, V. Chemical and topographical modification of PHBV surface to promote osteoblast alignment and confinement. *J. Biomed. Mater. Res. A.* **2007**, *85*, 1001-1010.

28. Lee, K.-B.; Park, S.-J.; Mirkin, C. A.; Smith, J. C.; Mrksich, M. Protein Nanoarrays Generated By Dip-Pen Nanolithography. *Science.* **2002**, *295*, 1702-1705.

29. Nalayanda, D. D.; Kalukanimuttam, M.; Schmidtke, D. W. Micropatterned surfaces for controlling cell adhesion and rolling under flow. *Biomed. Microdevices.* **2007**, *9*, 207-214.

30. Wang, Y. C.; Ho, C.-C. Micropatterning of proteins and mammalian cells on biomaterials *FASEB J.* **2004**, *18*, 525-527.

31. Zheng, H.; Berg, M. C.; Rubner, M. F.; Hammond, P. T. Controlling Cell Attachment Selectively onto Biological Polymer-Colloid Templates Using Polymer-on-Polymer Stamping. *Langmuir.* **2004**, *20*, 7215-7222.

32. Kita, A.; Sakurai, Y.; Myers, D. R.; Rounsevell, R.; Huang, J. N.; Seok, T. J.; Yu, K.; Wu, M. C.; Fletcher, D. A.; Lam, W. A. Microenvironmental Geometry Guides Platelet Adhesion and Spreading: A Quantitative Analysis at the Single Cell Level. *PLoS ONE.* **2011**, *6*, e26437.

33. Howell, S. W.; Inerowicz, H. D.; Regnier, F. E.; Reifenberger, R. Patterned Protein Microarrays for Bacterial Detection. *Langmuir.* **2003**, *19*, 436-439.

34. Li, X.; Liu, Y.; Zhu, A.; Luo, Y.; Deng, Z.; Tian, Y. Real-Time Electrochemical Monitoring of Cellular H2O2 Integrated with In Situ Selective Cultivation of Living Cells Based on Dual Functional Protein Microarrays at Au-TiO2 Surfaces. *Anal. Chem.* **2010**, *82*, 6512-6518.

35. Liu, X.-h.; Wang, H.-k.; Herron, J. N.; Prestwich, G. D. Photopatterning of Antibodies on Biosensors. *Bioconjugate Chem.* **2000**, *11*, 755-761.

36. Rowe, C. A.; Tender, L. M.; Feldstein, M. J.; Golden, J. P.; Scruggs, S. B.; MacCraith, B. D.; Cras, J. J.; Ligler, F. S. Array Biosensor for Simultaneous Identification of Bacterial, Viral, and Protein Analytes. *Anal. Chem.* **1999**, *71*, 3846-3852.

37. Delehanty, J. B.; Ligler, F. S. A Microarray Immunoassay for Simultaneous Detection of Proteins and Bacteria. *Anal. Chem.* **2002**, *74*, 5681-5687.

38. Veiseh, M.; Zareie, M. H.; Zhang, M. Highly Selective Protein Patterning on Gold-Silicon Substrates for Biosensor Applications. *Langmuir.* **2002**, *18*, 6671-6678.

39. Chuang, Y.-H.; Chang, Y.-T.; Liu, K.-L.; Chang, H.-Y.; Yew, T.-R. Electrical impedimetric biosensors for liver function detection. *Biosens. Bioelectron.* **2011**, *28*, 368-372.

40. Kim, H.; Cohen, R. E.; Hammond, P. T.; Irvine, D. J. Live Lymphocyte Arrays for Biosensing. *Adv. Funct. Mater.* **2006**, *16*, 1313-1323.

41. Liu, Y.; Yan, J.; Howland, M. C.; Kwa, T.; Revzin, A. Micropatterned Aptasensors for Continuous Monitoring of Cytokine Release from Human Leukocytes. *Anal. Chem.* **2011**, *83*, 8286-8292.

42. Zhu, H.; Stybayeva, G.; Silangcruz, J.; Yan, J.; Ramanculov, E.; Dandekar, S.; George, M. D.; Revzin, A. Detecting Cytokine Release from Single T-cells. *Anal. Chem.* **2009**, *81*, 8150-8156.

43. Zhu, H.; Macal, M.; Jones, C. N.; George, M. D.; Dandekar, S.; Revzin, A. A miniature cytometry platform for capture and characterization of T-lymphocytes from human blood. *Anal. Chim. Acta.* **2008**, *608*, 186-196.

44. Johnson, D. M.; Maurer, J. A. Recycling and reusing patterned self-assembled monolayers for cell culture. *Chem. Commun.* **2011**, *47*, 520-522.

45. Chiu, D. T.; Jeon, N. L.; Huang, S.; Kane, R. S.; Wargo, C. J.; Choi, I. S.; Ingber, D. E.; Whitesides, G. M. Patterned deposition of cells and proteins onto surfaces by using three-dimensional microfluidic systems. *P. Natl. Acad. Sci. USA.* **2000**, *97*, 2408-2413.

46. Folch, A.; Toner, M. Cellular Micropatterns on Biocompatible Materials. *Biotechnol. Prog.* **1998**, *14*, 388-392.

47. Lee, E.-J.; Chan, E. W. L.; Yousaf, M. N. Spatio-Temporal Control of Cell Coculture Interactions on Surfaces. *ChemBioChem.* **2009**, *10*, 1648-1653.

48. Sorribas, H.; Padeste, C.; Tiefenauer, L. Photolithographic generation of protein micropatterns for neuron culture applications. *Biomaterials.* **2002**, *23*, 893-900.

49. Hui, E. E.; Bhatia, S. N. Microscale Control of Cell Contact and Spacing via Three-Component Surface Patterning. *Langmuir.* **2007**, *23*, 4103-4107.

50. Kim, H.; Doh, J.; Irvine, D. J.; Cohen, R. E.; Hammond, P. T. Large Area Two-Dimensional B Cell Arrays for Sensing and Cell-Sorting Applications. *Biomacromolecules.* **2004**, *5*, 822-827.

51. Shen, K.; Tsai, J.; Shi, P.; Kam, L. C. Self-Aligned Supported Lipid Bilayers for Patterning the Cell-Substrate Interface. *J. Am. Chem. Soc.* **2009**, *131*, 13204-13205.

52. Lee, D.; King, M. R. Microcontact Printing of P-Selectin Increases the Rate of Neutrophil Recruitment Under Shear Flow. *Biotechnol. Prog.* **2008**, *24*, 1052-1059.

53. Schmidt, B. J.; Huang, P.; Breuer, K. S.; Lawrence, M. B. Catch Strip Assay for the Relative Assessment of Two-Dimensional Protein Association Kinetics. *Anal. Chem.* **2008**, *80*, 944-950.

54. McEver, R. P.; Beckstead, J. H.; Moore, K. L.; Marshall-Carlson, L.; Bainton, D. F. GMP-140, a Platelet a-Granule Membrane Protein, Is Also Synthesized by Vascular Endothelial Cells and Is Localized in Weibel-Palade Bodies. *J. Clin. Invest.* **1989**, *84*, 92-99.

55. Moore, K. L.; Patel, K. D.; Bruehl, R. E.; Fugang, L.; Johnson, D. A.; Lichenstein, H. S.; Cummings, R. D.; Bainton, D. F.; McEver, R. P. P-Selectin Glycoprotein Ligand-1 Mediates Rolling of Human Neutrophils on P-Selectin. *J. Cell Biol.* **1995**, *128*, 661-671.

56. Setiadi, H.; Disdier, M.; Green, S. A.; Canfield, W. M.; McEver, R. P. Residues Throughout the Cytoplasmic Domain Affect the Internalization Efficiency of P-selectin. *J. Biol. Chem.* **1995**, *45*, 26818-26826.

57. Kim, M. B.; Sarelius, I. H. Role of shear forces and adhesion molecule distribution on P-selectin-mediated leukocyte rolling in postcapillary venules. *Am. J. Physiol.-Heart C.* **2004**, *287*, H2705-H2711.

58. Mettlen, M.; Loerke, D.; Yarar, D.; Danuser, G.; Schmid, S. L. Cargo- and adaptor-specific mechanisms regulate clathrin-mediated endocytosis. *J. Cell Biol.* **2010**, *188*, 919-933.

59. Ruiz, S. A.; Chen, C. S. Microcontact printing: A tool to pattern. *Soft Matter.* **2007**, *3*, 168-177.

60. Chalmeau, J.; Thibault, C.; Carcenac, F.; Vieu, C. Micro-Contact Printing of Two Different Biomolecules in One Step Using Deformable Poly(dimethylsiloxane)-Based Stamp. *Jpn. J. Appl. Phys.* **2008**, *47*, 5221-5225.

61. Miller, J. S.; Bethencourt, M. I.; Hahn, M.; Lee, T. R.; West, J. L. Laser-scanning lithography (LSL) for the soft lithographic patterning of cell-adhesive self-assembled monolayers. *Biotechnol. Bioeng.* **2006**, *93*, 1060-1068.

62. Dyer, P. E.; Maswadi, S. M.; Walton, C. D.; Ersoz, M.; Fletcher, P. D. I.; Paunov, V. N. 157-nm laser micromachining of N-BK7 glass and replication for microcontact printing. *Appl. Phys. A-Mater.* **2003**, *77*, 391-394.

63. Xia, Y.; Tien, J.; Qin, D.; Whitesides, G. M. Non-Photolithographic Methods for Fabrication of Elastomeric Stamps for Use in Microcontact Printing. *Langmuir.* **1996**, *12*, 4033-4038.

64. Shen, K.; Thomas, V. K.; Dustin, M. L.; Kam, L. C. Micropatterning of costimulatory ligands enhances CD4+ T cell function. *P. Natl. Acad. Sci. USA.* **2008**, *105*, 7791-7796.

65. Rozkiewicz, D. I.; Kraan, Y.; Werten, M. W. T.; Wolf, F. A. d.; Subramaniam, V.; Ravoo, B. J.; Reinhoudt, D. N. Covalent Microcontact Printing of Proteins for Cell Patterning. *Chem.-Eur. J.* **2006**, *12*, 6290-6297.

66. Li, H.-W.; Muir, B. V. O.; Fichet, G.; Huck, W. T. S. Nanocontact Printing: A Route to Sub-50-nm-Scale Chemical and Biological Patterning. *Langmuir.* **2003**, *19*, 1963-1965.

67. Kuo, C. W.; Chien, F.-C.; Shiu, J.-Y.; Tsai, S.-M.; Chueh, D.-Y.; Hsiao, Y.-S.; Yang, Z.-H.; Chen, P. Investigation of the growth of focal adhesions using protein nanoarrays fabricated by nanocontact printing using size tunable polymeric nanopillars. *Nanotechnology.* **2011**, *22*, 265302.

68. Hong, J. M.; Ozkeskin, F. M.; Zou, J. A micromachined elastomeric tip array for contact printing with variable dot size and density. *J. Micromech. Microeng.* **2008**, *18*, 015003.

69. Bietsch, A.; Michel, B. Conformal contact and pattern stability of stamps used for soft lithography. *J. Appl. Phys.* **2000**, *88*, 4310-4318.

70. Delamarche, E.; Schmid, H.; Michel, B.; Biebuyck, H. Stability of Molded Polydimethylsiloxane Microstructures. *Adv. Mater.* **1997**, *9*, 741-746.

71. Hui, C. Y.; Jagota, A.; Lin, Y. Y.; Kramer, E. J. Constraints on Microcontact Printing Imposed by Stamp Deformation. *Langmuir.* **2002**, *18*, 1394-1407.

72. Graber, D. J.; Zieziulewicz, T. J.; Lawrence, D. A.; Shain, W.; Turner, J. N. Antigen Binding Specificity of Antibodies Patterned by Microcontact Printing. *Langmuir.* **2003**, *19*, 5431-5434.

73. Foley, J. O.; Fu, E.; Gamble, L. J.; Yager, P. Microcontact Printed Antibodies on Gold Surfaces: Function, Uniformity, and Silicone Contamination. *Langmuir.* **2008**, *24*, 3628-3635.

74. Hale, P. S.; Kappen, P.; Prissanaroon, W.; Brack, N.; Pigram, P. J.; Liesegang, J. Minimizing silicone transfer during micro-contact printing. *Appl. Surf. Sci.* **2007**, *253*, 3746-3750.

75. Duan, X.; Zhao, Y.; Berenschot, E.; Tas, N. R.; Reinhoudt, D. N.; Huskens, J. Large-Area Nanoscale Patterning of Functional Materials by Nanomolding in Capillaries. *Adv. Funct. Mater.* **2010**, *20*, 2519-2526.

76. Falconnet, D.; Pasqui, D.; Park, S.; Eckert, R.; Schift, H.; Gobrecht, J.; Barbucci, R.; Textor, M. A Novel Approach to Produce Protein Nanopatterns by Combining Nanoimprint Lithography and Molecular Self-Assembly. *Nano Lett.* **2004**, *4*, 1909-1914.

77. Maury, P.; Escalante, M.; Péter, M.; Reinhoudt, D. N.; Subramaniam, V.; Huskens, J. Creating Nanopatterns of His-Tagged Proteins on Surfaces by Nanoimprint Lithography Using Specific NiNTA-Histidine Interactions. *Small.* **2007**, *3*, 1584-1592.

78. Schvartzman, M.; Nguyen, K.; Palma, M.; Abramson, J.; Sable, J.; Hone, J.; Sheetz, M. P.; Wind, S. J. Fabrication of nanoscale bioarrays for the study of cytoskeletal protein binding interactions using nanoimprint lithography. *J. Vac. Sci. Technol. B.* **2009**, *27*, 61-65.

79. Schvartzman, M.; Palma, M.; Sable, J.; Abramson, J.; Hu, X.; Sheetz, M. P.; Wind, S. J. Nanolithographic Control of the Spatial Organization of Cellular Adhesion Receptors at the Single-Molecule Level. *Nano Lett.* **2011**, *11*, 1306-1312.

80. Hoff, J. D.; Cheng, L.-J.; Meyhöfer, E.; Guo, L. J.; Hunt, A. J. Nanoscale Protein Patterning by Imprint Lithography. *Nano Lett.* **2004**, *4*, 853-857.

81. Escalante, M.; Maury, P.; Bruinink, C. M.; Werf, K. v. d.; Olsen, J. D.; Timney, J. A.; Huskens, J.; Hunter, C. N.; Subramaniam, V.; Otto, C. Directed assembly of functional light harvesting antenna complexes onto chemically patterned surfaces. *Nanotechnology.* **2008**, *19*, 025101.

82. Merino, S.; Retolaza, A.; Trabadelo, V.; Cruz, A.; Heredia, P.; Alduncín, J. A.; Mecerreyes, D.; Fernández-Cuesta, I.; Borrisé, X.; Pérez-Murano, F. Protein patterning on the micro- and nanoscale by thermal nanoimprint lithography on a new functionalized copolymer. *J. Vac. Sci. Technol. B.* **2009**, *27*, 2439-2443.

83. Schvartzman, M.; Wind, S. J. Robust Pattern Transfer of Nanoimprinted Features for Sub-5-nm Fabrication. *Nano Lett.* **2009**, *9*, 3629-3634.

84. Schmidt, R. C.; Healy, K. E. Controlling biological interfaces on the nanometer length scale. *J. Biomed. Mater. Res. A.* **2009**, *90*, 1252-1261.

85. Andruzzi, L.; Senaratne, W.; Hexemer, A.; Sheets, E. D.; Ilic, B.; Kramer, E. J.; Baird, B.; Ober, C. K. Oligo(ethylene glycol) Containing Polymer Brushes as Bioselective Surfaces. *Langmuir.* **2005**, *21*, 2495-2504.

86. Kim, M.; Choi, J.-C.; Jung, H.-R.; Katz, J. S.; Kim, M.-G.; Doh, J. Addressable Micropatterning of Multiple Proteins and Cells by Microscope Projection Photolithography Based on a Protein Friendly Photoresist. *Langmuir.* **2010**, *26*, 12112-12118.

87. Hucknall, A.; Simnick, A. J.; Hill, R. T.; Chilkoti, A.; Garcia, A.; Johannes, M. S.; Clark, R. L.; Zauscher, S.; Ratner, B. D. Versatile synthesis and micropatterning of nonfouling polymer brushes on the wafer scale. *Biointerphases.* **2009**, *4*, FA50-FA57.

88. Kwon, K. W.; Choi, J.-C.; Suh, K.-Y.; Doh, J. Multiscale Fabrication of Multiple Proteins and Topographical Structures by Combining Capillary Force Lithography and Microscope Projection Photolithography. *Langmuir.* **2011**, *27*, 3238-3243.

89. Ionov, L.; Diez, S. Environment-Friendly Photolithography Using Poly(N-isopropylacrylamide)-Based Thermoresponsive Photoresists. *J. Am. Chem. Soc.* **2009**, *131*, 13315-13319.

90. Shuster, M. J.; Vaish, A.; Cao, H. H.; Guttentag, A. I.; McManigle, J. E.; Gibb, A. L.; Martinez, M. M.; Nezarati, R. M.; Hinds, J. M.; Liao, W.-S.; Weiss, P. S.; Andrews, A. M. Patterning small-molecule biocapture surfaces: microcontact insertion printing vs. photolithography. *Chem. Commun.* **2011**, *47*, 10641-10643.

91. Guillaume-Gentil, O.; Gabi, M.; Zenobi-Wong, M.; Vörös, J. Electrochemically switchable platform for the micro-patterning and release of heterotypic cell sheets. *Biomed. Microdevices.* **2011**, *13*, 221-230.

92. Vail, T. L.; Cushing, K.; Ingram, J. C.; Omer, I. S. Micropatterned avidin arrays on silicon substrates via photolithography, self-assembly and bioconjugation. *Biotechnol. Appl. Bioc.* **2006**, *43*, 85-91.

93. Falconnet, D.; Koenig, A.; Assi, F.; Textor, M. A Combined Photolithographic and Molecular-Assembly Approach to Produce Functional Micropatterns for Applications in the Biosciences. *Adv. Funct. Mater.* **2004**, *14*, 749-756.

94. Leggett, G. J. Scanning near-field photolithography—surface photochemistry with nanoscale spatial resolution. *Chem. Soc. Rev.* **2006**, *35*, 1150-1161.

95. Christman, K. L.; Requa, M. V.; Enriquez-Rios, V. D.; Ward, S. C.; Bradley, K. A.; Turner, K. L.; Maynard, H. D. Submicron Streptavidin Patterns for Protein Assembly. *Langmuir.* **2006**, *22*, 7444-7450.

96. Seisyan, R. P. Nanolithography in Microelectronics: A Review. *Tech. Phys.* **2011**, *56*, 1061-1073.

97. Reynolds, N. P.; Janusz, S.; Escalante-Marun, M.; Timney, J.; Ducker, R. E.; Olsen, J. D.; Otto, C.; Subramaniam, V.; Leggett, G. J.; Hunter, C. N. Directed Formation of Micro- and Nanoscale Patterns of Functional Light-Harvesting LH2 Complexes. *J. Am. Chem. Soc.* **2007**, *129*, 14625-14631.

98. Bhatnagar, P.; Malliaras, G. G.; Kim, I.; Batt, C. A. Multiplexed Protein Patterns on a Photosensitive Hydrophilic Polymer Matrix. *Adv. Mater.* **2009**, *22*, 1242-1246.

99. Zou, Y.; Yeh, P.-Y. J.; Rossi, N. A. A.; Brooks, D. E.; Kizhakkedathu, J. N. Nonbiofouling Polymer Brush with Latent Aldehyde Functionality as a Template for Protein Micropatterning. *Biomacromolecules.* **2010**, *11*, 284-293.

100. Shin, D.-S.; Lee, K.-N.; Jang, K.-H.; Kim, J.-K.; Chung, W.-J.; Kim, Y.-K.; Lee, Y.-S. Protein patterning by maskless photolithography on hydrophilic polymer-grafted surface. *Biosens. Bioelectron.* **2003**, *19*, 485-494.

101. Yamazoe, H.; Uemura, T.; Tanabe, T. Facile Cell Patterning on an Albumin-Coated Surface. *Langmuir.* **2008**, *24*, 8402-8404.

102. Folch, A.; Toner, M. Microengineering of Cellular Interactions. *Annu. Rev. Biomed. Eng.* **2000**, *2*, 227-256.

103. Brétagnol, F.; Ceriotti, L.; Valsesia, A.; Sasak, T.; Ceccone, G.; Gilliland, D.; Colpo, P.; Rossi, F. Fabrication of functional nano-patterned surfaces by a combination of plasma processes and electron-beam lithography. *Nanotechnology.* **2007**, *18*, 135303.

104. Denis, F. A.; Pallandre, A.; Nysten, B.; Jonas, A. M.; Dupont-Gillain, C. C. Alignment and Assembly of Adsorbed Collagen Molecules Induced by Anisotropic Chemical Nanopatterns. *Small.* **2005**, *1*, 984-991.

105. Sabella, S.; Brunetti, V.; Vecchio, G.; Torre, A. D.; Rinaldi, R.; Cingolani, R.; Pompa, P. P. Micro/Nanoscale Parallel Patterning of Functional Biomolecules, Organic Fluorophores and Colloidal Nanocrystals. *Nanoscale Res. Lett.* **2009**, *4*, 1222-1229.

106. Ballav, N.; Thomas, H.; Winkler, T.; Terfort, A.; Zharnikov, M. Making Protein Patterns by Writing in a Protein-Repelling Matrix. *Angew. Chem. Int. Edit.* **2009**, *48*, 5833-5836.

107. Brétagnol, F.; Sirghi, L.; Mornet, S.; Sasaki, T.; Gilliland, D.; Colpo, P.; Rossi, F. Direct fabrication of nanoscale bio-adhesive patterns by electron beam surface modification of plasma polymerized poly ethylene oxide-like coatings. *Nanotechnology.* **2008**, *19*, 125306.

108. Ceccone, G.; Leung, B. O.; Perez-Roldan, M. J.; Valsesia, A.; Colpo, P.; Rossi, F.; Hitchcock, A. P.; Scholl, A. X-ray spectromicroscopy study of ubiquitin adsorption to plasma polymerized microstructures. *Surf. Interface Anal.* **2010**, *42*, 830-834.

109. Christman, K. L.; Broyer, R. M.; Schopf, E.; Kolodziej, C. M.; Chen, Y.; Maynard, H. D. Protein Nanopatterns by Oxime Bond Formation. *Langmuir.* **2011**, *27*, 1415-1418.

110. Gao, B.; Bernstein, G. H.; Lieberman, M. Self-assembled monolayers of poly(ethylene glycol) siloxane as a resist for ultrahigh-resolution electron beam lithography on silicon oxide. *J. Vac. Sci. Technol. B.* **2009**, *27*, 2292-2300.

111. Krakert, S.; Ballav, N.; Zharnikov, M.; Terfort, A. Adjustment of the bioresistivity by electron irradiation: self-assembled monolayers of oligo(ethyleneglycol)-terminated alkanethiols with embedded cleavable group. *Phys. Chem. Chem. Phys.* **2010**, *12*, 507-515.

112. Pesen, D.; Haviland, D. B. Modulation of Cell Adhesion Complexes by Surface Protein Patterns. *ACS Appl. Mater. Interfaces.* **2009**, *1*, 543-548.

113. Pesen, D.; Heinz, W. F.; Werbin, J. L.; Hoh, J. H.; Haviland, D. B. Electron beam patterning of fibronectin nanodots that support focal adhesion formation. *Soft Matter.* **2007**, *3*, 1280-1284.

114. Robin, S.; Gandhi, A. A.; Gregor, M.; Laffir, F. R.; Plecenik, T.; Plecenik, A.; Soulimane, T.; Tofail, S. A. M. Charge Specific Protein Placement at Submicrometer and Nanometer Scale by Direct Modification of Surface Potential by Electron Beam. *Langmuir.* **2011**, *27*, 14968-14974.

115. Rundqvist, J.; Mendoza, B.; Werbin, J. L.; Heinz, W. F.; Lemmon, C.; Romer, L. H.; Haviland, D. B.; Hoh, J. H. High Fidelity Functional Patterns of an Extracellular Matrix Protein by Electron Beam-Based Inactivation. *J. Am. Chem. Soc.* **2007**, *129*, 59-67.

116. Verma, V.; Hancock, W. O.; Catchmark, J. M. Nanoscale patterning of kinesin motor proteins and its role in guiding microtubule motility. *Biomed. Microdevices.* **2009**, *11*, 313-322.

117. Mendes, P. M.; Yeung, C. L.; Preece, J. A. Bio-nanopatterning of Surfaces. *Nanoscale Res. Lett.* **2007**, *2*, 373-384.

118. Krsko, P.; Sukhishvili, S.; Mansfield, M.; Clancy, R.; Libera, M. Electron-Beam Surface-Patterned Poly(ethylene glycol) Microhydrogels. *Langmuir.* **2003**, *19*, 5618-5625.

119. Lussi, J. W.; Tang, C.; Kuenzi, P.-A.; Staufer, U.; Csucs, G.; Vörös, J.; Gaudenz Danuser; Hubbell, J. A.; Textor, M. Selective molecular assembly patterning at the nanoscale: a novel platform for producing protein patterns by electron-beam lithography on SiO2/indium tin oxide-coated glass substrates. *Nanotechnology.* **2005**, *16*, 1781-1786.

120. Christman, K. L.; Schopf, E.; Broyer, R. M.; Li, R. C.; Chen, Y.; Maynard, H. D. Positioning Multiple Proteins at the Nanoscale with Electron Beam Cross-Linked Functional Polymers. *J. Am. Chem. Soc.* **2009**, *131*, 521-527.

121. Kim, K. H.; Kim, J. D.; Kim, Y. J.; Kang, S. H.; Jung, S. Y.; Jung, H. Protein Immobilization Without Purification via Dip-Pen Nanolithography. *Small.* **2008**, *4*, 1089-1094.

122. Kramer, M. A.; Park, H. C.; Ivanisevic, A. Dip-Pen Nanolithography on SiOx and Tissue-Derived Substrates: Comparison with Multiple Biological Inks. *Scanning.* **2010**, *32*, 30-34.

123. Lee, K.-B.; Kim, E.-Y.; Mirkin, C. A.; Wolinsky, S. M. The Use of Nanoarrays for Highly Sensitive and Selective Detection of Human Immunodeficiency Virus Type 1 in Plasma. *Nano Lett.* **2004**, *4*, 1869-1872.

124. Li, B.; Zhang, Y.; Hu, J.; Li, M. Fabricating protein nanopatterns on a single DNA molecule with Dip-pen nanolithography. *Ultramicroscopy.* **2005**, *105*, 312-315.

125. Rakickas, T.; Gavutis, M.; Reichel, A.; Piehler, J.; Liedberg, B.; Valiokas, R. Protein-Protein Interactions in Reversibly Assembled Nanopatterns. *Nano Lett.* **2008**, *8*, 3369-3375.

126. Rozhok, S.; Shen, C. K.-F.; Littler, P.-L. H.; Fan, Z.; Liu, C.; Mirkin, C. A.; Holz, R. C. Methods for Fabricating Microarrays of Motile Bacteria. *Small.* **2005**, *1*, 445-451.

127. Senesi, A. J.; Rozkiewicz, D. I.; Reinhoudt, D. N.; Mirkin, C. A. Agarose-Assisted Dip-Pen Nanolithography of Oligonucleotides and Proteins. *ACS Nano.* **2009**, *3*, 2394-2402.

128. Harris, L. G.; Schofield, W. C. E.; Badyal, J. P. S. MultiFunctional Molecular Scratchcards. *Chem. Mater.* **2007**, *19*, 1546-1551.

129. Muir, B. W.; Fairbrother, A.; Gengenbach, T. R.; Rovere, F.; Abdo, M. A.; McLean, K. M.; Hartley, P. G. Scanning Probe Nanolithography and Protein Patterning of Low-Fouling Plasma Polymer Multilayer Films. *Adv. Mater.* **2006**, *2006*, 3079-3082.

130. Zhou, D.; Bruckbauer, A.; Ying, L.; Abell, C.; Klenerman, D. Building Three-Dimensional Surface Biological Assemblies on the Nanometer Scale. *Nano Lett.* **2003**, *3*, 1517-1520.

131. Tinazli, A.; Piehler, J.; Beuttler, M.; Guckenberger, R.; Tampé, R. Native protein nanolithography that can write, read and erase. *Nat. Nanotechnol.* **2007**, *2*, 220-225.

132. Wadu-Mesthrige, K.; Xu, S.; Amro, N. A.; Liu, G.-y. Fabrication and Imaging of Nanometer-Sized Protein Patterns. *Langmuir.* **1999**, *15*, 8580-8583.

133. Braunschweig, A. B.; Senesi, A. J.; Mirkin, C. A. Redox-Activating Dip-Pen Nanolithography (RA-DPN). *J. Am. Chem. Soc.* **2009**, *131*, 922-923.

134. Gao, P.; Cai, Y. The Boundary Molecules in a Lysozyme Pattern Exhibit Preferential Antibody Binding. *Langmuir.* **2008**, *24*, 10334-10339.

135. Krämer, S.; Fuierer, R. R.; Gorman, C. B. Scanning Probe Lithography Using Self-Assembled Monolayers. *Chem. Rev.* **2003**, *103*, 4367-4418.

136. Ngunjiri, J.; Garno, J. C. AFM-Based Lithography for Nanoscale Protein Assays. *Anal. Chem.* **2008**, *80*,

137. Bellido, E.; Miguel, R. d.; Ruiz-Molina, D.; Lostao, A.; Maspoch, D. Controlling the Number of Proteins with Dip-Pen Nanolithography. *Adv. Mater.* **2010**, *22*, 352-355.

138. Chai, J.; Wong, L. S.; Giam, L.; Mirkin, C. A. Single-molecule protein arrays enabled by scannin probe block copolymer lithography. *P. Natl. Acad. Sci. USA.* **2011**, *108*, 19521-19525.

139. Collins, J. M.; Nettikadan, S. Subcellular scaled multiplexed protein patterns for single cell cocultures. *Anal. Biochem.* **2011**, *419*, 339-341.

140. Wagner, H.; Li, Y.; Hirtz, M.; Chi, L.; Fuchs, H.; Studer, A. Site specific protein immobilization into structured polymer brushes prepared by AFM lithography. *Soft Matter.* **2011**, *7*, 9854-9858.

141. Wang, D.; Kodali, V. K.; II, W. D. U.; Jarvholm, J. E.; Okada, T.; Jones, S. C.; Rumi, M.; Dai, Z.; King, W. P.; Marder, S. R.; Curtis, J. E.; Riedo, E. Thermochemical Nanolithography of Multifunctional Nanotemplates for Assembling Nano-Objects. *Adv. Funct. Mater.* **2009**, *19*, 3696-3702.

142. Xing, C.; Zheng, Z.; Zhang, B.; Tang, J. Nanoscale Patterning of Multicomponent Proteins by Bias-Assisted Atomic Force Microscopy Nanolithography. *ChemPhysChem.* **2011**, *12*, 1262-1265.

143. Salaita, K.; Wang, Y.; Fragala, J.; Vega, R. A.; Liu, C.; Mirkin, C. A. Massively Parallel Dip–Pen Nanolithography with 55000-Pen Two-Dimensional Arrays. *Angew. Chem. Int. Edit.* **2006**, *45*, 7220-7223.

144. Haaheim, J.; Val, V.; Bussan, J.; Rozhok, S.; Jang, J.-W.; Fragala, J.; Nelson, M. Self-Leveling Two-Dimensional Probe Arrays for Dip Pen Nanolithography. *Scanning.* **2010**, *32*, 49-59.

145. Glass, R.; Möller, M.; Spatz, J. P. Block copolymer micelle nanolithography. *Nanotechnology.* **2003**, *14*, 1153-1160.

146. Park, M.; Harrison, C.; Chaikin, P. M.; Register, R. A.; Adamson, D. H. Block Copolymer Lithography: Periodic Arrays of ~10^{11} Holes in 1 Square Centimeter. *Science.* **1997**, *276*, 1401-1404.

147. Gao, X.; Zhu, S.; Sheardown, H.; Brash, J. L. Nanoscale patterning through self-assembly of hydrophilic block copolymers with one chain end constrained to surface. *Polymer.* **2010**, *51*, 1771-1778.

148. Kumar, N.; Hahm, J.-i. Nanoscale Protein Patterning Using Self-Assembled Diblock Copolymers. *Langmuir.* **2005**, *21*, 6652-6655.

149. Kumar, N.; Parajuli, O.; Dorfman, A.; Kipp, D.; Hahm, J.-i. Activity Study of Self-Assembled Proteins on Nanoscale Diblock Copolymer Templates. *Langmuir.* **2007**, *23*, 7416-7422.

150. Lau, K. H. A.; Bang, J.; Kim, D. H.; Knoll, W. Self-assembly of Protein Nanoarrays on Block Copolymer Templates. *Adv. Funct. Mater.* **2008**, *18*, 3148-3157.

151. Liu, D.; Wang, T.; Keddie, J. L. Protein Nanopatterning on Self-Organized Poly(styrene-b-isoprene) Thin Film Templates. *Langmuir.* **2009**, *25*, 4526-4534.

152. Liu, D.; Abdullah, C. A. C.; Sear, R. P.; Keddie, J. L. Cell adhesion on nanopatterned fibronectin substrates. *Soft Matter.* **2010**, *6*, 5408-5416.

153. Parajuli, O.; Gupta, A.; Kumar, N.; Hahm, J.-i. Evaluation of Enzymatic Activity on Nanoscale Polystyrene-block-Polymethylmethacrylate Diblock Copolymer Domains. *J. Phys. Chem. B.* **2007**, *111*, 14022-14027.

154. Jung, J.-M.; Kwon, K. Y.; Ha, T.-H.; Chung, B. H.; Jung, H.-T. Gold-Conjugated Protein Nanoarrays through Block-Copolymer Lithography: From Fabrication to Biosensor Design. *Small.* **2006**, *2*, 1010-1015.

155. Hu, Y.; Chen, D.; Park, S.; Emrick, T.; Russell, T. P. Guided Assemblies of Ferritin Nanocages: Highl Ordered Arrays of Monodisperse Nanoscopic Elements. *Adv. Mater.* **2010**, *22*, 2583-2587.

156. Lohmüller, T.; Triffo, S.; O'Donoghue, G. P.; Xu, Q.; Coyle, M. P.; Groves, J. T. Supported Membranes Embedded with Fixed Arrays of Gold Nanoparticles. *Nano Lett.* **2011**, *11*, 4912-4918.

157. Aydin, D.; Schwieder, M.; Louban, I.; Knoppe, S.; Ulmer, J.; Haas, T. L.; Walczak, H.; Spatz, J. P. Micro-Nanostructured Protein Arrays: A Tool for Geometrically Controlled Ligand Presentation**. *Small.* **2009**, *5*, 1014-1018.

158. Wolfram, T.; Belz, F.; Schoen, T.; Spatz, J. P. Site-specific presentation of single recombinant proteins in defined nanoarrays. *Biointerphases.* **2007**, *2*, 44-48.

159. Jaehrling, S.; Thelen, K.; Wolfram, T.; Pollerberg, G. E. Nanopatterns Biofunctionalized with Cell Adhesion Molecule DM-GRASP Offered as Cell Substrate: Spacing Determines Attachment and Differentiation of Neurons. *Nano Lett.* **2009**, *9*, 4115-4121.

160. Thelen, K.; Wolfram, T.; Maier, B.; Jährling, S.; Tinazli, A.; Piehler, J.; Spatz, J. P.; Pollerberg, G. E. Cell adhesion molecule DM-GRASP presented as nanopatterns to neurons regulates attachment and neurite growth. *Soft Matter.* **2007**, *3*, 1486-1491.

161. Lohmüller, T.; Aydin, D.; Schwieder, M.; Morhard, C.; Louban, I.; Pacholski, C.; Spatz, J. P. Nanopatterning by block copolymer micelle nanolithography and bioinspired applications. *Biointerphases.* **2011**, *6*, MR1-MR12.

162. Cai, Y.; Ocko, B. M. Large-Scale Fabrication of Protein Nanoarrays Based on Nanosphere Lithography. *Langmuir.* **2005**, *21*, 9274-9279.

163. Daniels, S. L.; Ngunjiri, J. N.; Garno, J. C. Investigation of the magnetic properties of ferritin by AFM imaging with magnetic sample modulation. *Anal. Bioanal. Chem.* **2009**, *394*, 215-223.

164. Garno, J. C.; Amro, N. A.; Wadu-Mesthrige, K.; Liu, G.-Y. Production of Periodic Arrays of Protein Nanostructures Using Particle Lithography. *Langmuir.* **2002**, *18*, 8186-8192.

165. Geng, D. L.; Miao, Y. H.; Helseth, L. E. Influence of Salt on Colloidal Lithography of Albumin. *Langmuir.* **2007**, *23*, 8480-8484.

166. Li, J.-R.; Henry, G. C.; Garno, J. C. Fabrication of nanopatterned films of bovine serum albumin and staphylococcal protein A using latex particle lithography. *Analyst.* **2006**, *131*, 244-250.

167. Miao, Y. H.; Helseth, L. E. Adsorption of bovine serum albumin on polyelectrolyte-coated glass substrates: Applications to colloidal lithography. *Colloid. Surface. B.* **2008**, *66*, 299-303.

168. Singh, G.; Griesser, H. J.; Bremmell, K.; Kingshott, P. Highly Ordered Nanometer-Scale Chemical and Protein Patterns by Binary Colloidal Crystal Lithography Combined with Plasma Polymerization. *Adv. Funct. Mater.* **2011**, *21*, 540-546.

169. Singh, G.; Gohri, V.; Pillai, S.; Arpanaei, A.; Foss, M.; Kingshottz, P. Large-Area Protein Patterns Generated by Ordered Binary Colloidal Assemblies as Templates. *Nano Lett.* **2011**, *5*, 3542-3551.

170. Blättler, T. M.; Binkert, A.; Zimmermann, M.; Textor, M.; Vörös, J.; Reimhult, E. From particle self-assembly to functionalized sub-micron protein patterns. *Nanotechnology.* **2008**, *19*, 075301.

171. Marquez, M.; Patel, K.; Carswell, A. D. W.; Schmidtke, D. W.; Grady, B. P. Synthesis of Nanometer-Scale Polymeric Structures on Surfaces from Template Assisted Admicellar Polymerization: A Comparative Study with Protein Adsorption. *Langmuir.* **2006**, *22*, 8010-8016.

172. Valsesia, A.; Mannelli, I.; Colpo, P.; Bretagnol, F.; Rossi, F. Protein Nanopatterns for Improved Immunodetection Sensitivity. *Anal. Chem.* **2008**, *80*, 7336-7340.

173. Valsesia, A.; Meziani, T.; Bretagnol, F.; Colpo, P.; Ceccone, G.; Rossi, F. Plasma assisted production of chemical nano-patterns by nano-sphere lithography: application to bio-interfaces. *J. Phys. D Appl. Phys.* **2007**, *40*, 2341-2347.

174. Valsesia, A.; Colpo, P.; Silvan, M. M.; Meziani, T.; Ceccone, G.; Rossi, F. Fabrication of Nanostructured Polymeric Surfaces for Biosensing Devices. *Nano Lett.* **2004**, *4*, 1047-1050.

175. Valsesia, A.; Colpo, P.; Meziani, T.; Lisboa, P.; Lejeune, M.; Rossi, F. Immobilization of Antibodies on Biosensing Devices by Nanoarrayed Self-Assembled Monolayers. *Langmuir.* **2006**, *22*, 1763-1767.

176. Kosiorek, A.; Kandulski, W.; Glaczynska, H.; Giersig, M. Fabrication of Nanoscale Rings, Dots, and Rods by Combining Shadow Nanosphere Lithography and Annealed Polystyrene Nanosphere Masks. *Small.* **2005**, *1*, 439-444.

177. Haynes, C. L.; Duyne, R. P. V. Nanosphere Lithography: A Versatile Nanofabrication Tool for Studies of Size-Dependent Nanoparticle Optics. *J. Phys. Chem. B.* **2001**, *105*, 5599-5611.

178. Lusker, K. L.; Li, J.-R.; Garno, J. C. Nanostructures of Functionalized Gold Nanoparticles Prepared by Particle Lithography with Organosilanes. *Langmuir.* **2011**, *27*, 13269-13275.

179. Agheli, H.; Malmström, J.; Larsson, E. M.; Textor, M.; Sutherland, D. S. Large Area Protein Nanopatterning for Biological Applications. *Nano Lett.* **2006**, *6*, 1165-1171.

180. Slater, J. H.; Frey, W. Nanopatterning of fibronectin and the influence of integrin clustering on endothelial cell spreading and proliferation. *J. Biomed. Mater. Res. A.* **2008**, *87*, 176-195.

181. Dmitriev, A.; Hägglund, C.; Chen, S.; Fredriksson, H.; Pakizeh, T.; Käll, M.; Sutherland, D. S. Enhanced Nanoplasmonic Optical Sensors with Reduced Substrate Effect. *Nano Lett.* **2008**, *8*, 3893-3898.

182. Retsch, M.; Tamm, M.; Bocchio, N.; Horn, N.; Förch, R.; Jonas, U.; Kreiter, M. Parallel Preparation of Densely Packed Arrays of 150-nm Gold-Nanocrescent Resonators in Three Dimensions. *Small.* **2009**, *5*, 2105-2110.

183. Cong, C.; Junus, W. C.; Shen, Z.; Yu, T. New Colloidal Lithographic Nanopatterns Fabricated by Combining Pre-Heating and Reactive Ion Etching. *Nanoscale Res. Lett.* **2009**, *4*, 1324-1328.

184. Zhang, G.; Wang, D.; Möhwald, H. Fabrication of Multiplex Quasi-Three-Dimensional Grids of One-Dimensional Nanostructures via Stepwise Colloidal Lithography. *Nano Lett.* **2007**, *7*, 3410-3413.

185. Li, X.; Wang, T.; Zhang, J.; Yan, X.; Zhang, X.; Zhu, D.; Li, W.; Zhang, X.; Yang, B. Modulating Two-Dimensional Non-Close-Packed Colloidal Crystal Arrays by Deformable Soft Lithography. *Langmuir.* **2010**, *26*, 2930-2936.

186. Xia, Y.; Yin, Y.; Lu, Y.; McLellan, J. Template-Assisted Self-Assembly of Spherical Colloids into Complex and Controllable Structures. *Adv. Funct. Mater.* **2003**, *13*, 907-918.

187. Khanh, N. N.; Yoon, K. B. Facile Organization of Colloidal Particles into Large, Perfect One and Two-Dimensional Arrays by Dry Manual Assembly on Patterned Substrates. *J. Am. Chem. Soc.* **2009**, *131*, 14228-14230.

188. Hanarp, P.; Käll, M.; Sutherland, D. S. Optical Properties of Short Range Ordered Arrays of Nanometer Gold Disks Prepared by Colloidal Lithography. *J. Phys. Chem. B.* **2003**, *107*, 5768-5772.

Chapter 2: Fabrication of Protein Dot Arrays via Particle Lithography

This chapter was reproduced in part with permission from:

Taylor, Z. R.; Patel, K.; Spain, T. G.; Keay, J. C.; Jernigen, J. D.; Sanchez, E. S.; Grady, B. P.; Johnson, M. B.; Schmidtke, D. W. Fabrication of Protein Dot Arrays via Particle Lithography. Langmuir. 2009, 25, 10932-10938.

Copyright 2009 American Chemical Society.

Introduction

The fabrication of micro- and nano-scale patterns of proteins has applications in a number of fields. In biology, protein patterning has been used to investigate the role of protein spatial presentation on cell adhesion,[1] chemotaxis,[2] cell proliferation,[3] and cell apoptosis.[4] In the field of biosensors, patterning has been utilized to fabricate multianalyte immunosensor arrays,[5] protein microarrays for bacterial detection,[6] patterned DNA microarrays,[7,8] and to align neuronal cell growth on microelectronic devices.[9] Finally, protein-patterned substrates have been utilized for the growth of cardiomyocyte cultures for myocardial repair,[10] the growth of osteoblast cells for bone tissue engineered constructs,[11] and for growing co-cultures of hepatocytes and fibroblasts.[12]

Current methods of protein patterning include both "top-down techniques" such as microcontact printing,[1,13,14] microfluidic patterning,[15-18] photolithography,[19,20] imprint lithography,[21] and E-beam lithography[22-24] and "bottom-up techniques" such as block copolymer micelle nanolithography[25-27] and particle lithography.[28-30]

Important parameters in choosing one method over another often include the size of the pattern, the shape of the pattern, pattern fidelity and long-range order, processing time, necessity of specialized equipment, and cost. The reader is referred to the reviews of Vörös et al.[31] and Christman et al.[32] for an in-depth analysis of the specific advantages and disadvantages of these methods.

Particle lithography is an attractive technique for protein patterning due to its simplicity, low-cost, and versatility. This technique has been widely used in a number of areas to generate nanometer to micrometer sized patterns with a variety of materials, such as inorganics,[33,34] metals,[35-38] and polymers.[39-41] However, in the area of protein patterning, particle lithography is a relatively new method (Table 2.1). In an initial study by Garno et al.,[28] surfaces with periodic protein nanostructures were prepared by mixing latex spheres with a specific protein followed by deposition on flat surfaces. Upon sphere removal, a honeycomb protein pattern was obtained. This technique has been extended to the fabrication of honeycomb patterns of protein mixtures [(protein A and bovine serum albumin (BSA)][42] and protein rings.[43] Similar honeycomb structures have been obtained by our group by an alternative procedure in which incubation of the protein solution occurs only after the sphere monolayer is formed.[40] Alternatively, particle lithographic methods have been developed to fabricate patterns of protein dots.[29,30,44-46]

A persistent challenge in fabricating useful patterns via particle lithography for both protein and non-protein applications is to create patterns with high fidelity and long-

Table 2.1: Comparison of Particle Lithography Methods of Protein Patterning[a]

Pattern Type	Method of Monolayer Formation	Background/ Grafting Method	Pattern Size	Protein Type(s)	Ref
Dots	Spin Coating	PEO Plasma Polymerization	50 – 200 nm	BSA Human IgG	46
Dots	Computer-Driven Dip Coating	PLL-g-PEG Electrostatic	0.1 – 2.0 μm	Streptavidin	30
Dots Rings	Solvent Evaporation	PEG-silane Liquid or Vapor Phase Grafting	60 – 120 nm	Lysozyme	29
Dot	Electrostatic Solvent Evaporation	PLL-g-PEG Electrostatic	124 nm	Ferritin Laminin	45
Dots	Solvent Evaporation	PVA Photocrosslinking	490 nm	GFP	44
Dots	Patterned Wettability	PEG-silane Liquid Phase Grafting	0.45 – 1.2 μm	BSA Fibrinogen P-selectin	This Work
Honeycomb Rings	Solvent Evaporation	NA	0.2 – 0.8 μm	BSA Rabbit IgG	28
Honeycomb Rings	Solvent Evaporation	NA	0.2 – 0.5 μm	SpA BSA	42
Honeycomb Rings	Spin Coating	NA	0.16 – 2.3 μm	BSA Fibrinogen Anti-mouse IgG	40
Rings	Solvent Evaporation	NA	0.20 – 0.36 μm	Ferritin Apoferritin BSA Rabbit IgG	43

[a] PLL-g-PEG – poly(lysine)-graft-poly(ethylene glycol); PVA – poly(vinylalcohol); PEO – poly(ethylene oxide); GFP – green fluorescent protein; NA – not applicable; BSA – bovine serum albumin; IgG – immunoglobulin; SpA – staphylococcal protein A

range order. In response to this challenge, considerable research has been performed and a diverse set of strategies, such as spin coating,[41,47] confined convective assembly,[48] physical confinement,[49] template assisted assembly,[50,51] chemically

patterned surfaces,[52-54] patterned wettability,[55,56] Langmuir-Blodgett technique,[57,58] and electrodeposition[59,60] have been developed. Excellent reviews of these colloidal techniques are available.[61,62] Despite the fact that these techniques are available, most of the studies that employ particle lithography to pattern proteins have relied on simple solvent evaporation (see Table 2.1). As will be discussed below, we have employed the technique of patterned wettability to produce large areas of well-ordered microspheres and subsequent protein dot patterns.

An additional issue in the fabrication of protein dots via particle lithography is creating a background that repels protein. Because of its protein-resistant properties, most strategies have employed poly(ethylene glycol) (PEG) as the inert background via two different strategies. In the first scheme, particle lithography is employed to initially define hydrophobic regions on a surface (*e.g.* alkane thiols on gold nanodisks[45] or dodecyl phosphates on TiO_2[30]) and then the copolymer poly(L-lysine)-graft-poly(ethylene glycol) (PLL-g-PEG) is electrostatically grafted around these regions to provide an inert and protein-repellant background. Subsequently, proteins are adsorbed to the patterned hydrophobic regions. By contrast, the second scheme involves covalently grafting a layer of poly(ethylene glycol) through silane chemistry around the beads.[29] Upon removal of the beads, holes in the protein-repellant layer are exposed for subsequent protein deposition.

In this work, we report a novel method (Figure 2.1) for fabricating periodic patterns of protein dots, 450 nm – 1.1 μm in diameter. To create patterns with long-range order we

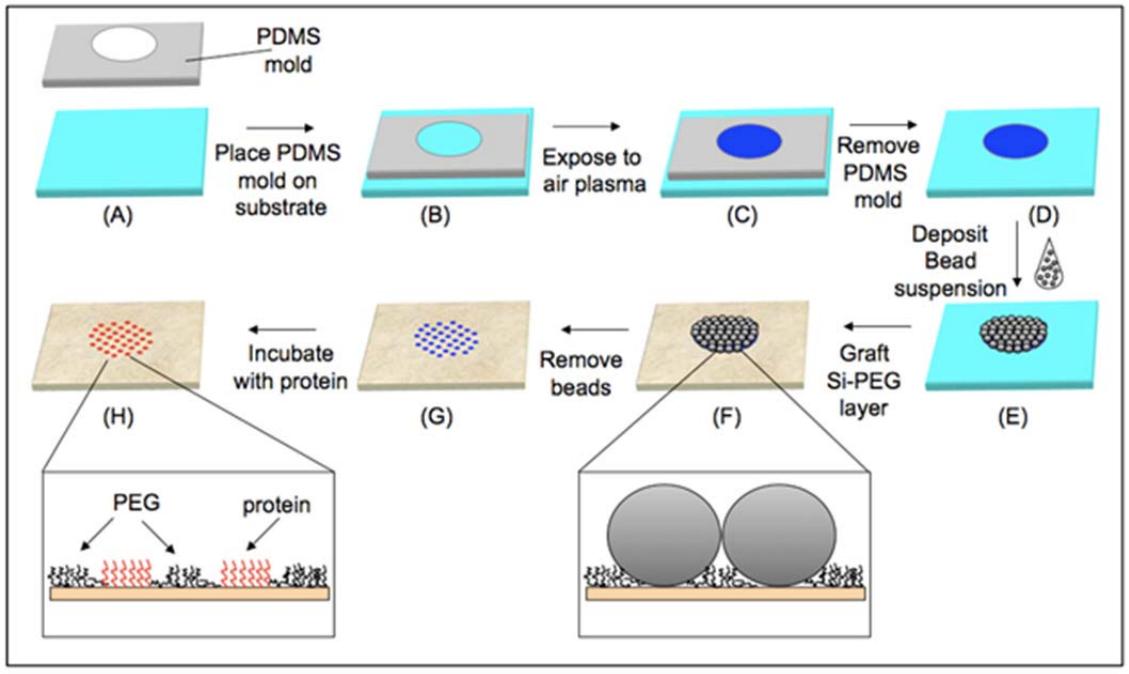

Figure 2.1: Schematic of the Protein Patterning Procedure. Step 1: A circular, hydrophilic region is created on a glass slide (A – D). Step 2: A drop of a bead suspension is deposited on the hydrophilic surface, and as the solvent evaporates, a monolayer of spheres is formed (D and E). Step 3: The monolayer of spheres then serves as a mask to selectively graft a layer of PEG to the glass substrate through silane chemistry (E and F). Step 4: The sphere monolayer is removed, exposing bare glass surrounded by PEG, and the protein is then adsorbed to these bare glass regions (F – H).

first used the method of patterned wettability to self-assemble a monolayer of latex spheres. This sphere monolayer then served as a lithographic mask to selectively graft a nanometer thin layer of PEG. A solution phase grafting procedure with methoxy-poly(ethylene glycol)-(triethoxy)silane (PEG-silane or mPEG-sil) was developed to form a siloxane-anchored self-assembled monolayer of PEG around the beads. In contrast to the method of Cai described above,[29] the PEG layer in our procedure was grafted directly to the glass substrate instead of a previously deposited silane monolayer. A challenge in forming the PEG layer was to find a solvent that would allow for the silanization reaction but that would not dissolve the polystyrene beads. Following sphere removal, periodic patterns of holes in the protein-repellant PEG layer

were exposed, and proteins selectively adsorbed onto the underlying surface in these holes. We demonstrate the versatility of this technique by fabricating dot patterns of different diameters and different proteins.

Experimental Section

Chemicals and Materials. Polystyrene latex spheres (2 μm, 5 μm, and 10 μm mean diameter) were purchased from Duke Scientific, and washed once in DI water by centrifugation before use. Silicon wafers (P type, <111>) were purchased from Wafer World, Inc (West Palm Beach, FL), while mPEG-sil (MW = 5000) was purchased from LaySan Bio (Arab, AL). Poly(dimethylsiloxane) (PDMS; Sylgard-184, Dow-Corning) was purchased from Krayden (Marlborough, MA). AlexaFluor488-labeled Fibrinogen, AlexaFluor488-BSA, and an AlexaFluor 488 protein labeling kit were obtained from Invitrogen (Carlsbad, CA). The labeling kit was used to label P-selectin (R&D Research) according to the manufacturer's instructions. The 1.4 nm FluoroNanogold-anti-mouse Fab'-AlexaFluor 488 and GoldEnhance (GE) EM were purchased from Nanoprobes (Yaphank, NY).

Substrate Preparation and Self-Assembled Monolayer Formation. Microscope glass slides, coverslips, or silicon wafers were sequentially cleaned in trichloroethylene, acetone, methanol, and DI water for 2 min each cycle using an ultrasonic cleaner. A small circular region of each substrate was selectively made hydrophilic by placing a cured PDMS mold containing a 4.5 mm diameter hole onto the surface (Figure 2.1B) and exposing to an air plasma at 400 mTorr (Harrick Scientific Corp., Model PDC-32G,

Ithaca, NY) under low power (0.010 W/cm^3) for 30 seconds (Figure 2.1C). After plasma treatment, the PDMS mold was removed and the substrate was left untouched for ~30 minutes (Figure 2.1D). Next a drop (3–18 μl) of a washed bead suspension was deposited on the patterned region and allowed to dry overnight at 4 °C to form the monolayer of microspheres (Figure 2.1E). The volume and concentration of the bead solution deposited were adjusted so that there were a sufficient number of beads to form a complete monolayer over the plasma treated area. After bead monolayer formation, substrates were heated at 80 °C for 1 h to keep the beads anchored to the surface during washing and wet chemical modification. Finally, each substrate was gently placed in a Petri dish full of DI water and allowed to soak for five minutes to remove residue from the bead suspension. Substrates were gently removed from the DI water and allowed to dry in ambient conditions for at least 1 h before PEG grafting.

PEG Grafting. The bead monolayer then served as a mask to selectively graft a nanometer thin layer of poly(ethylene glycol) (PEG) to the substrate. Briefly, the substrates were exposed to an air plasma at 400 mTorr for 1 min at high power (0.027 W/cm^3), immediately incubated in a 4 mM solution of mPEG-sil in anhydrous acetonitrile, and left overnight at room temperature (Figure 2.1F). For the mPEG-sil incubation, either a 400 μl droplet of the solution was deposited on the surface or the substrate was completely immersed in the liquid. We observed similar results using both techniques. The substrates were then gently placed in three consecutive Petri dishes full of acetonitrile and allowed to soak for 5 min in each to remove any ungrafted mPEG-sil. Finally, the substrates were rinsed with a stream of DI water using a

standard laboratory wash bottle (Nalgene #2401-0500) to further remove any ungrafted mPEG-sil and to remove the beads. The final result was a PEG-coated surface with periodic holes (Figure 2.1G).

Protein Adsorption. AlexaFluor488-labeled proteins were dissolved in Hanks Balanced Salt Solution (HBSS) at concentrations of 10–100 μg/ml. Aliquots of a protein solution were dispensed on the PEG-patterned surface and incubated for 2 hr at room temperature to allow protein to adsorb into the uncoated holes (Figure 2.1H). Following incubation, the substrates were rinsed first with 25 mL HBSS using a transfer pipette and then with 50 mL of DI water using a standard laboratory wash bottle to remove any unbound protein.

Immunogold Labeling. A 1.4 nm FluoroNanogold (FNG) was dissolved in phosphate-buffered saline (PBS), pH 7.4, at concentrations of 20–80 μg/ml. Aliquots of an FNG solution were dispensed on the PEG-patterned surface and incubated for 2 hr at room temperature. Following incubation, the substrates were rinsed first with 25 mL PBS using a transfer pipette and then with 50 mL DI water using a standard laboratory wash bottle. Next, an aliquot of GE EM was mixed according to the manufacturer's instructions using a 1:2:1:1 or 1:3:1:1 ratio of GE EM solutions A, B, C, and D, respectively. The GE EM solution was dispensed on the FNG-patterned surface and allowed to incubate for 20 min at room temperature. Following incubation, the substrates were rinsed with 50 mL DI water using a standard laboratory wash bottle and

then dried under a stream of nitrogen. Finally, substrates were coated with 5 nm of carbon using thermal evaporation.

Substrate Characterization. Bead monolayer formation was characterized by both optical and scanning electron microscopy (SEM). Optical images were acquired with a Zeiss Axiovert 200 inverted microscope equipped with a CoolSnap cf digital camera. SEM images of bead monolayers were obtained by sputtering the monolayers with an Au/Pd layer (5 nm) and then imaging with a Zeiss 960A scanning electron microscope under 15 kV accelerating voltage.

To characterize the coverages of bead monolayers using optical microscopy, bright field images were taken of parts of bead monolayers and then combined to form montages of complete monolayers. The areas covered by close-packed beads were measured with MetaMorph Imaging Software. We defined surface coverage as the percentage of area covered by single layers of close-packed beads with respect to the total area of the substrate. (Small defects and areas of multiple layers of beads were considered reduced coverage).

To characterize the PEG layer formed, small pieces (1 cm x 1 cm) of silicon wafers with a native oxide were modified with a uniform PEG layer by the methods described for the glass substrates. Ellipsometric measurements of the PEG layer film thickness were made using a Gaertner L-117C manual ellipsometer (Gaertner Scientific Corp., Chicago, IL) with a 632.8 nm He–Ne laser at an angle of incidence of 70°. All film

thicknesses were determined using the Gaertner Ellipsometry Measurement Program (GEMP) in the one-layer and two-layer mode. We measured PEG layer thicknesses in two ways. Initially, we modeled the two layers (PEG layer on a native oxide layer on silicon) as a one-layer system, based on the fact that the index of refraction for PEG (n_{PEG} = 1.46)[63] and that for silicon dioxide are very close (n_{SiO_2}= 1.46). Finally, we used better optical data for a native silicon dioxide layer based on the work of Subramanian et al.[64] as part of a two-layer system. The results in both cases were within statistical error. In the latter analysis, we determined the index of refraction and thickness of the native oxide layer by iteration, using the usual parameters for the silicon substrate (n= 3.85 + 0.02i), and the index of refraction versus thickness curve reported by Subramanian et al.[64] Doing this, we determined our native oxide thickness was typically 2.9 nm with n= 2.43 (cf. with a thickness of 3.2 nm assuming an n= 1.46). Using these properties for our native oxide, we used the GEMP program in the two-layer mode to determine the PEG layer thickness. For all measurements of PEG film thickness, we measured the sample in at least two different locations on at least two identically prepared films and these were compared to an out-of-the-box sample from the same silicon wafer prepared and measured with the PEG samples.

Characterization of the protein-patterned substrates was done by fluorescent imaging with a fluorescent microscope (Zeiss Axiovert 200) and analyzed with MetaMorph Imaging Software. Substrates patterned with FluoroNanogold were imaged with a Zeiss 960A scanning electron microscope (SEM) with 20-kV accelerating voltage using a backscattered electron (BSE) detector.

Calculations and Statistics. Values are presented as means ± standard errors of the mean unless otherwise specified, and statistical significance was assessed when appropriate by a Student's *t* test for paired data, with $P < 0.05$ considered as statistically significant.

Results and Discussion

Periodic patterns of protein dots were fabricated on glass or silicon wafers by a three step procedure (Figure 2.1): (1) Formation of a bead monolayer, (2) grafting of a protein-resistant PEG layer, and (3) selective adsorption of protein. A variety of complementary microscopy techniques were employed to characterize the structures produced and to optimize the process.

Bead Monolayer Formation. A persistent challenge in the use of particle lithography is the ability to create large areas of hexagonally packed, defect-free, bead monolayers. Thus, we investigated whether surfaces with patterned wettability[55,56] would result in the formation of large continuous areas of close-packed and ordered bead monolayers. A circular area of glass or silicon substrates was selectively treated with an air plasma via a PDMS mold to create a distinct region of increased hydrophilicity or wettability (Figure 2.1A – D). Aqueous suspensions (~0.05% V/V) of latex beads were dispensed onto the plasma cleaned substrates. As a control, suspensions of latex beads were also dispensed onto substrates that had not been plasma cleaned. As solvent evaporated from the colloidal suspensions, attractive capillary forces between the beads developed and caused them to self-assemble into closely packed and ordered monolayers. In both cases (Figures 2.2A, B), imperfections in bead ordering (e.g. point defects, dislocation, and

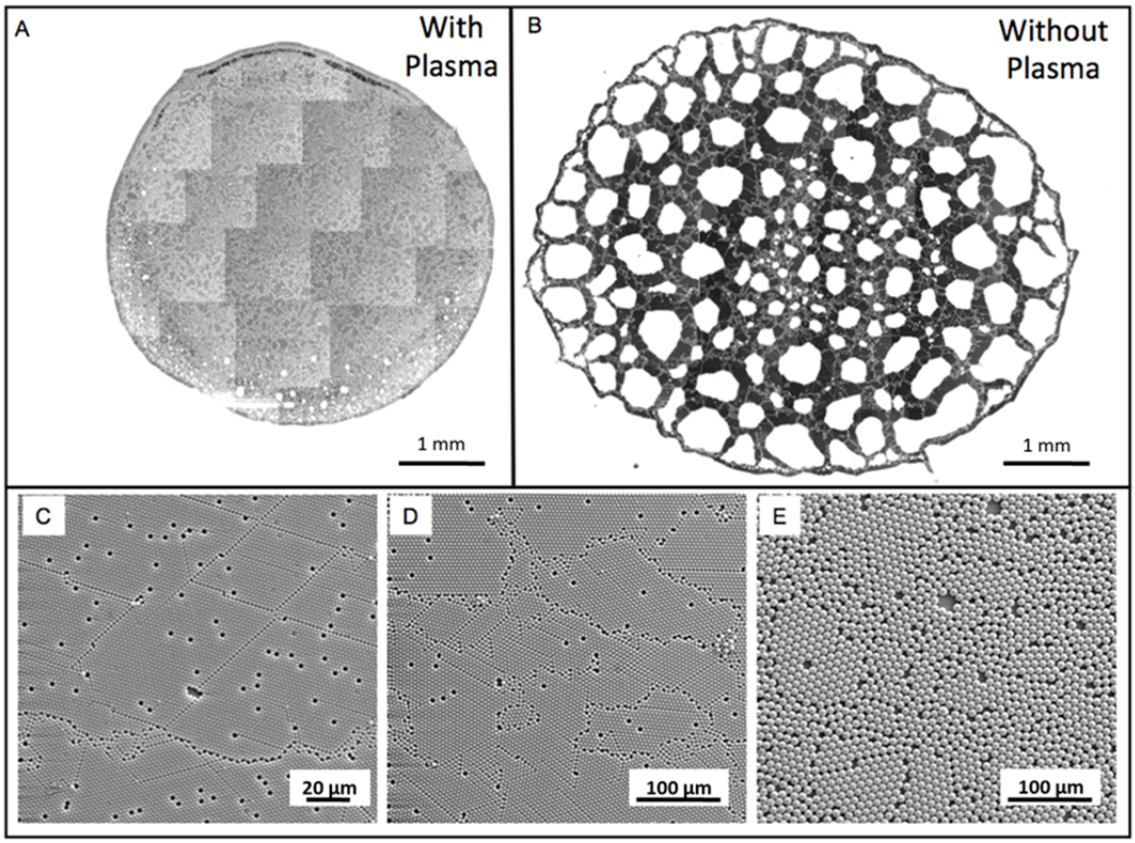

Figure 2.2: Bead Monolayers. Optical image montage of a monolayer formed by 10 µm beads (A) following the plasma cleaning procedure and (B) without plasma cleaning. SEM images of (C) 2, (D), 5, and (E) 10 µm bead monolayers. Panels A and B are both montages composed of several smaller images. The square corner features in panel A are an artifact of piecing together the montage. In panels A and B, white areas contain no beads. The gray and black areas contain beads that are close-packed but contain the defects shown in panels C – E. the larger grain boundary defects are visible in the close-packed areas of panels A and B as lines.

grain boundaries) were observed. On substrates that were not exposed to the plasma cleaning process ("unpatterned substrates"), the bead monolayer was not confined to a specific area, and the monolayer formed included large areas absent of any beads (Figure 2.2B). However, on plasma-cleaned substrates ("patterned substrates"), the monolayer of beads was observed to preferentially nucleate at the edge of the plasma-treated region, resulting in a distinct boundary (Figure 2.2A) of regions with and without beads. Furthermore, patterned substrates exhibited a lower concentration of

defects and an increased surface coverage of bead monolayers as compared to substrates that were not plasma cleaned. For example, patterned surfaces had bead surface coverages >84% with 5 and 10 μm diameter beads whereas untreated glass surfaces exhibited surface coverages of 60 and 38%, respectively. Figure 2.2C – E shows images of periodic arrays formed on patterned substrates with 2, 5, and 10 μm diameter beads. Because of the improved surface coverage subsequent studies were performed with patterned substrates.

Grafting of a Protein-Resistant PEG Layer. Following bead monolayer formation, a protein-repellent background of PEG was created around the beads by chemically grafting mPEG-sil to the surface. Subsequent removal of the bead monolayer uncovered periodic holes in the PEG layer. It should be noted that covalently grafting the PEG-silane to the glass in solution around polystyrene beads was not trivial. Since the original work of Sagiv and co-workers on the formation of SAMs from siloxane compounds,[65,66] subsequent research has shown that the formation of organosliane SAMs depends upon a number of key parameters: water content, solvent, temperature, and deposition time.[67] Furthermore, the reactivity of the silane depends upon its type (e.g. chlorosilanes, alkoxysilanes) and functionality (e.g. mono-, di-, or trifunctional silanes). Normally, silanes are grafted to glass in organic solvents such as toluene to eliminate the problems of multilayer formation or polymerization in the bulk solvent phase in the presence of large amounts of water. However organic solvents such as toluene will dissolve the beads. Therefore, the number of solvents that allow for PEG monolayer formation but do not dissolve the beads is limited. After trying a number of

different solvents, acetonitrile was chosen. To confirm the successful grafting of the PEG layer, we performed ellipsometry on both bulk silicon and silicon modified with a mPEG-sil film. Ellipsometry of the bare silicon provided the refractive index and thickness of the native silicon dioxide layer, which we used to subsequently determine the PEG layer thickness. The oxide thickness was measured to be 2.9 nm, and the PEG layer thickness was 0.5 ± 0.2 nm. This value is smaller than previous measurements of the thickness (1.6–1.7 nm) of a dry PEG layer (MW = 5000) using ellipsometry and atomic force microscopy (AFM).[68] We hypothesize that this difference in thickness is related to variations in the grafting density of PEG.

Protein-Patterned Substrates. The final step of the process was the selective adsorption of protein into the wells of the patterned PEG substrate. Figure 2.3 shows fluorescent images of surfaces that were patterned with PEG via 2, 5, and 10 μm diameter beads and subsequently incubated with solutions of fluorescent fibrinogen. Well-resolved dots of protein in a hexagonal pattern were observed. As the size of the bead increased, both the size of the protein dots formed (450–1050 nm) and the center-to-center spacing between dots increased. To demonstrate the versatility of this technique, we fabricated patterned substrates with two other types of cell adhesion molecules (P-selectin and albumin) and measured the diameter of the dots formed by fluorescent microscopy. As shown in Figure 2.4, the size of the protein dots produced for a given bead size was constant and independent of the protein deposited. These results suggest that the patterning technique could be extended to a number of different proteins, so long as they readily adsorb to glass surfaces. It has previously been shown

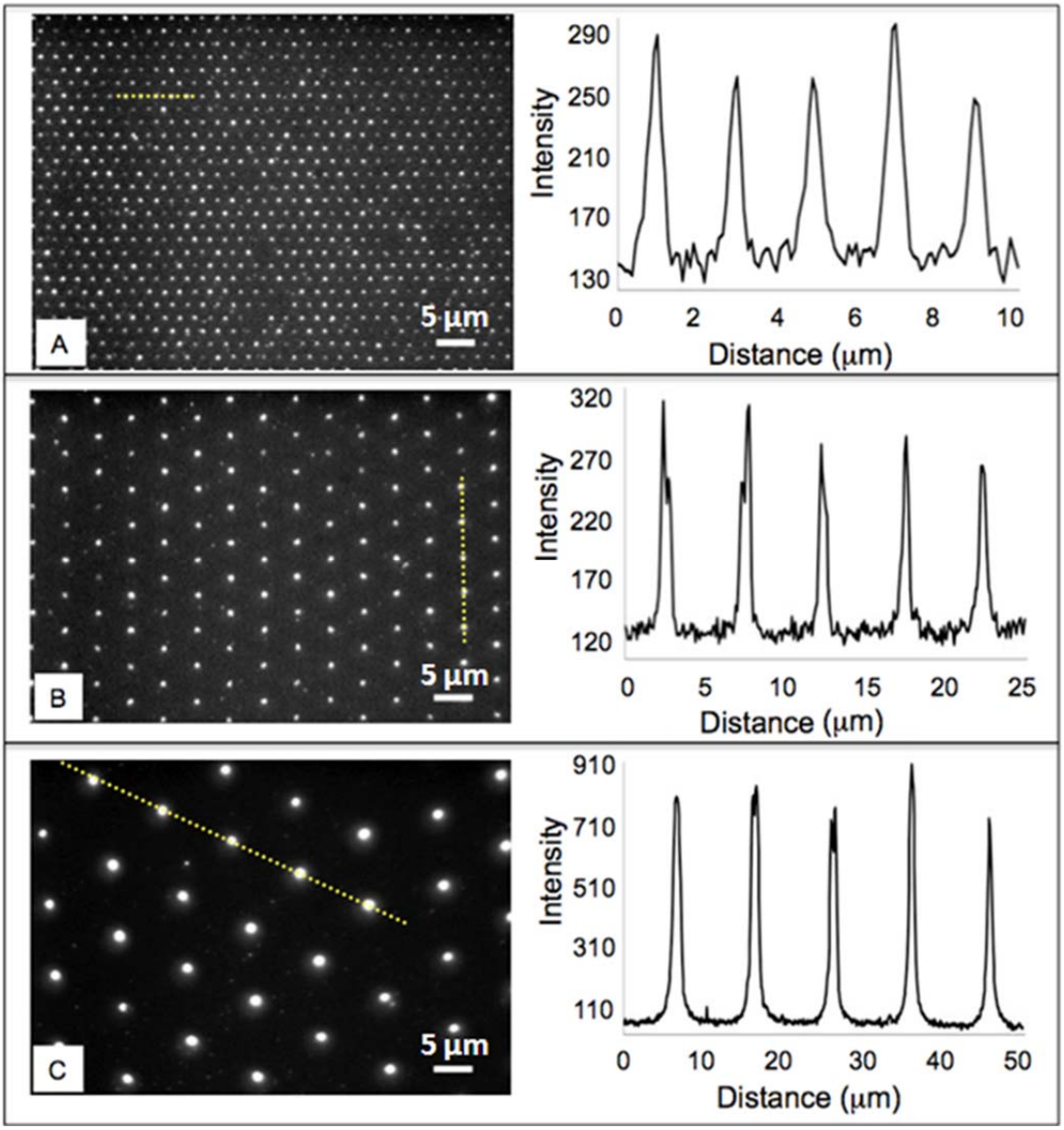

Figure 2.3: Arrays of Protein Dots Fabricated Via Particle Lithography. Fluorescent images of surfaces patterned with fluorescent fibrinogen via particle lithography with (A) 2 µm spheres, (B) 5 µm spheres, and (C) 10 µm spheres. The fluorescent line intensity (arbitrary units) graphs to the right of each image correspond to the dashed lines in each image.

that protein adsorption to glass primarily occurs through ionic interactions, presumably between protein amine groups and glass silanol groups, and that the adsorption of protein increases with increasing isoelectric point.[69] Although proteins with lower isoelectric points may adsorb at a lower rate than those with higher isoelectric points, the majority of proteins will adsorb to glass and thus could be used with the patterning

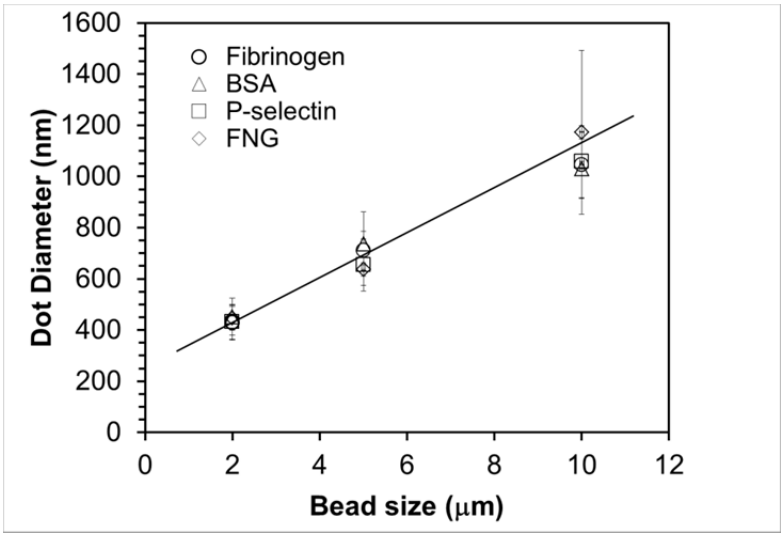

Figure 2.4: Size of Protein Dots is Dependent Upon the Diameter of the Latex Sphere Utilized. Average diameter of the protein dots created for each bead size with three different proteins. Dot diameters of protein patterns were measured from fluorescent images using MetaMorph Image Analysis software. SEM imaging was performed to measure the diameters of the dot patterns of FNG. For each condition, a total of three different slides and 80 – 340 dots were measured. A line to guide the eye is shown.

technique.

It should be noted that the fluorescent dot measurements (450 nm) measured for the 2 μm beads were near the resolution limit of standard fluorescent microscopes (200–500 nm). When objects with dimensions smaller than the resolution limit are imaged, they will project with dimensions of the resolution limit. Thus, to confirm that the fluorescent measurements of the protein dots were accurate, we patterned FNG on substrates made with 2, 5, and 10 μm diameter beads and then imaged the samples using SEM.

FNG is composed of an antibody Fab' fragment covalently bound to a 1.4 nm gold

particle, which is smaller than the resolution limit (~50 nm) of the SEM we used. To make the patterned FNG visible by SEM imaging, we used GE EM to increase the size of the gold particles. To prevent the substrates from charging in the SEM, we coated them with a thin (5 nm) layer of carbon. The final result was patterned dots of gold particles on a carbon background. The large atomic number difference between the gold particles and the carbon background allowed us to use BSE imaging to view the FNG dots. Figure 2.5 shows BSE images of substrates that were patterned with FNG via 10, 5, and 2 μm diameter beads. The diameters of the dots on substrates made with 10, 5, and 2 μm beads were 1200 ± 300, 640 ± 60, and 450 ± 50 nm, respectively. These measurements agree quite well with those made by fluorescent microscopy (Figure 2.4). In addition, the absence of gold particles between the dots provides additional evidence of the ability of the PEG regions of the substrate to prevent protein adsorption.

To corroborate that the protein selectively adsorbed in the patterned PEG holes and not in the PEG background, we exposed fluorescent fibrinogen dots formed using 10 μm beads to fluorescent light until they were completely photobleached. Figure 2.6 shows the fluorescent intensity (arbitrary units) of a linescan across three dots with time. Although the fluorescent intensity inside of the dots decreases to zero in about 10 min, the baseline intensity between the dots remains constant. This confirms the protein resistant-properties of the PEG grafted between the protein dots.

Effect of Bead Monolayer Cleaning. In the course of our study, we found that cleaning the bead monolayer in DI water was essential for the formation of consistent

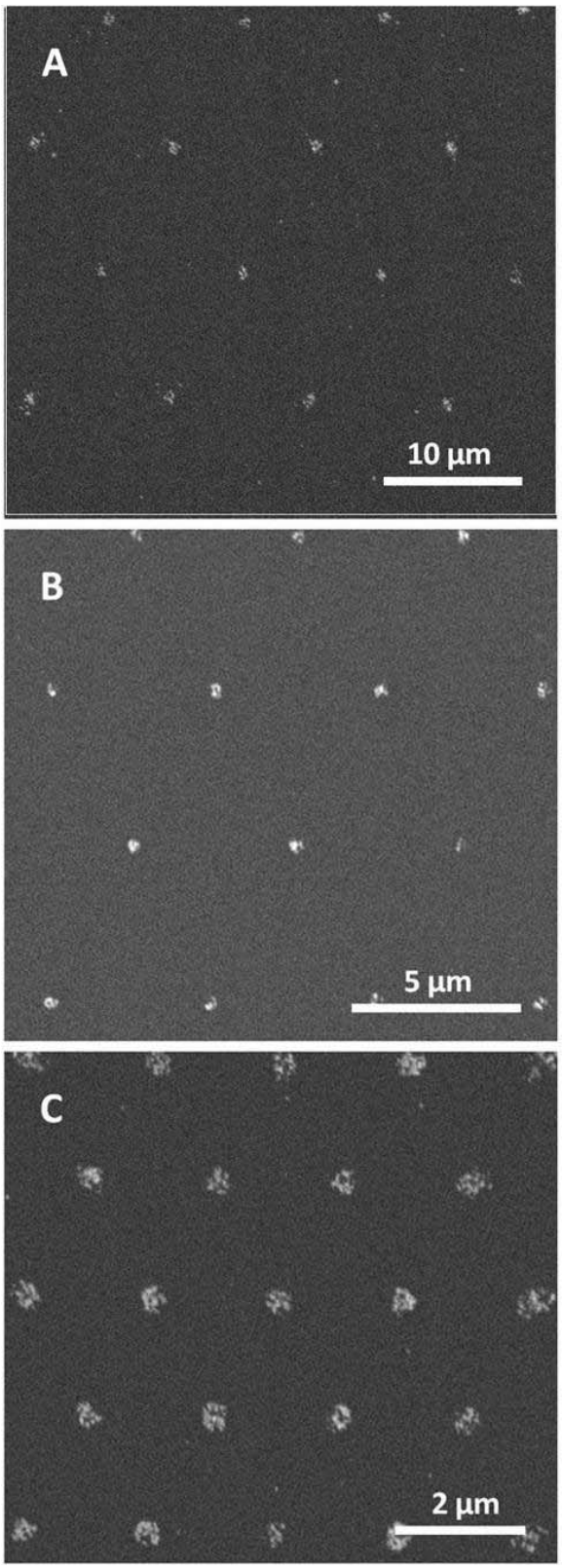

Figure 2.5: Arrays of FNG Particles Fabricated Via Particle Lithography. SEM images of surfaces patterned with FNG particles by particle lithography with (A) 10 µm spheres, (B) 5 µm spheres, and (C) 2 µm spheres.

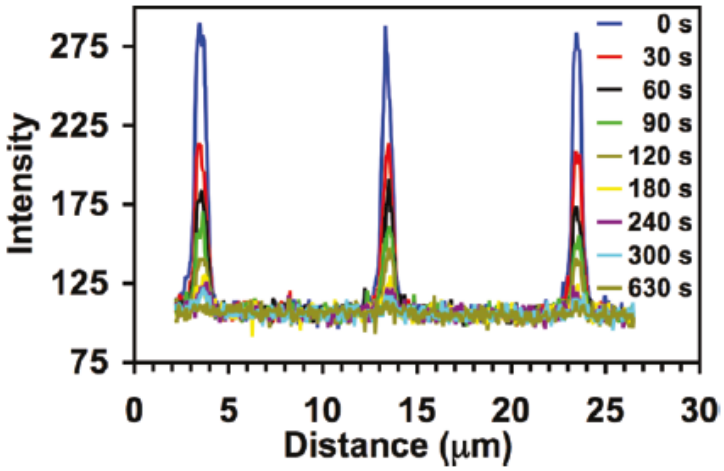

Figure 2.6: Photobleaching of Protein Patterns. Line scans of the fluorescent intensity of three protein dots fabricated via 10 μm beads were measured as a function of time.

protein dots. Figure 2.7A–D shows representative fluorescent images of protein patterns formed on substrates that were not thoroughly cleaned prior to PEG grafting. At the periphery (Figure 2.7E, Region A) of bead monolayer patterns that were not cleaned prior to mPEG-sil grafting, dot patterns with interconnecting lines (Figure 2.7A) were frequently observed. In addition, a 2-fold variation in the protein dot diameters was often observed, with the dot size gradually decreasing and becoming uniform as one moves from the periphery towards the center of the pattern (Figure 2.7B). Towards the center of the pattern (Figure 2.7E, Region B), we observed a haze of protein (Figure 2.7C), and in the center of the pattern (Figure 2.7E, Region C), we observed smaller dots with uniform diameters (Figure 2.7D).

The presence of the interconnecting fluorescent lines suggested that something on the surface was preventing complete grafting of the PEG layer around the beads. We hypothesized that the most likely cause was residual surfactant from the bead

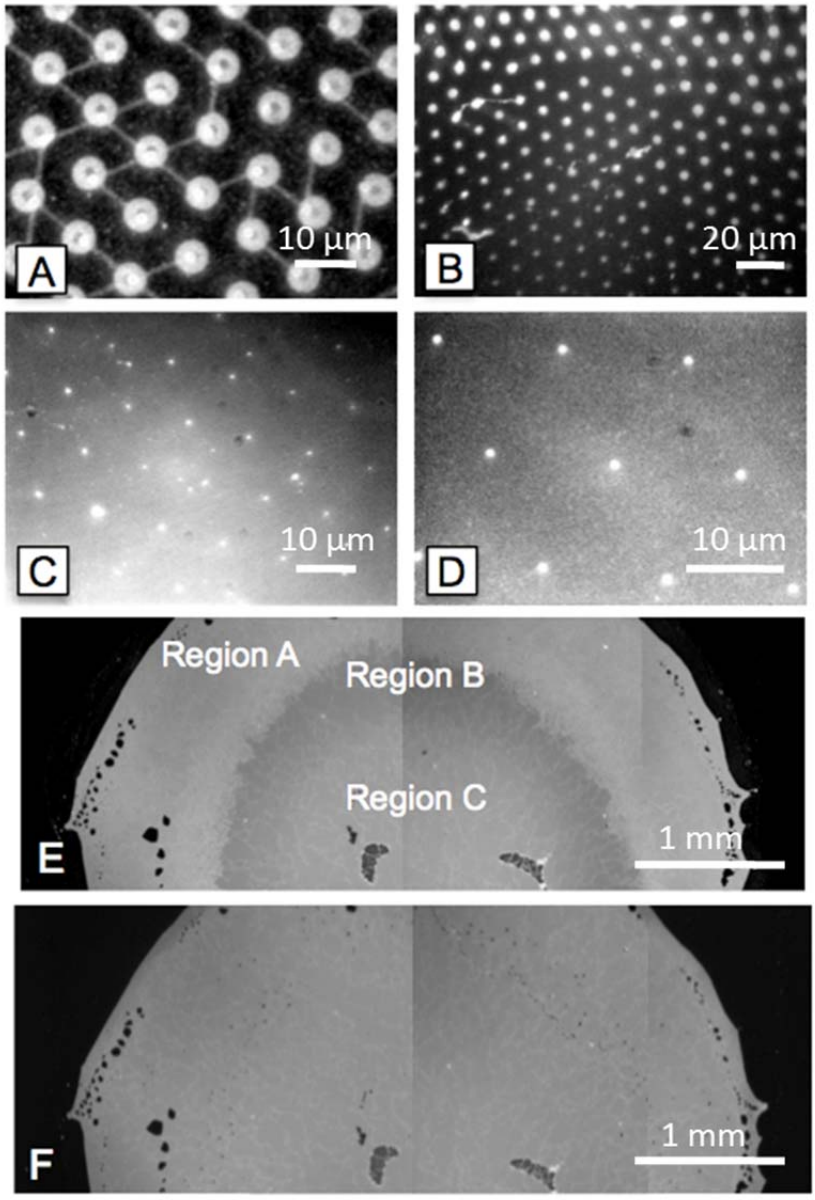

Figure 2.7: Effect of Latex Sphere Monolayer Washing. (A – D) Fluorescent images of unwashed substrates patterned with fluorescent fibrinogen via 10 µm beads. Phase contrast image of a 10 µm bead monolayer (E) prior to cleaning and (F) after cleaning with a 5 min soak in DI water.

suspension being deposited on the surface during evaporation of the liquid.[70,71] To test this hypothesis, we performed phase contrast imaging of the bead monolayers formed after water evaporation and prior to cleaning (Figure 2.7C). The different shading in region A compared to regions B and C appeared to support our hypothesis.

Furthermore, subsequent cleaning of the same bead monolayer by soaking in DI water for 5 min and then allowing the bead monolayer to air-dry for at least 1 hr resulted in the removal of this ring (Figure 2.7D) and produced the uniform dot patterns observed in Figure 2.3.

Conclusions

A simple method for fabricating protein-patterned substrates with nanometer to micrometer scale dimensions was developed. The method includes selectively grafting a protein-repellant layer of PEG in the holes of a SAM of latex spheres, removal of the spheres, and selective adsorption of the protein. The size of the protein dots formed ranged from 450 nm to 1.1 μm, and was dependent upon the size of the spheres utilized. The versatility of this technique was demonstrated by patterning surfaces with three different proteins (fibrinogen, P-selectin, and albumin) as well as with antibody-coated FNG. These results suggest that this is a generic patterning technique that could be extended to a number of proteins. We anticipate that smaller diameter dots (~50 nm) of protein can be created via this technique by using commercially available latex spheres with diameters of 100 nm.

Acknowledgments

We thank Dr. Hendra Setiadi of the Oklahoma Medical Research Foundation for help in fluorescently labeling the P-selectin, and Dr. Preston Larsen for help with the SEM imaging. This work was supported by a National Institutes of Health Grant (P20 RR 018758), an American Heart Association Grant (0230139N), a National Science

Foundation (NSF) Graduate Research Fellowship to Z.R.T., the Center for Semiconductor Physics in Nanostructures (C-SPIN), an OU/UA NSF-funded MRSEC (DMR-0520550), and by OK-NanoNet an NSF EPSCoR supported RII program (EPS-0132534).

References

1. Mrksich, M.; Chen, C. S.; Xia, Y. N.; Dike, L. E.; Ingber, D. E.; Whitesides, G. M. Controlling cell attachment on contoured surfaces with self-assembled monolayers of alkanethiolates on gold. *P. Natl. Acad. Sci. USA.* **1996**, *93*, 10775-10778.

2. Jeon, N. L.; Baskaran, H.; Dertinger, S. K. W.; Whitesides, G. M.; Water, L. V. D.; Toner, M. Neutrophil chemotaxis in linear and complex gradients of interleukin-8 formed in a microfabricated device. *Nat. Biotechnol.* **2002**, *20*, 826-830.

3. Nelson, C. M.; Chen, C. S. Cell-cell signalling by direct contact increases cell proliferation via a PI3K-dependent signal. *FEBS Lett.* **2002**, *514*, 238-242.

4. Chen, C. S.; Mrksich, M.; Huang, S.; Whitesides, G. M.; Ingber, D. E. Micropatterned Surfaces for Control of Cell Shape, Position, and Function. *Biotechnol. Prog.* **1998**, *14*, 356-363.

5. Inerowicz, H. D.; Howell, S.; Regnier, F. E.; Reifenberger, R. Multiprotein immunoassay arrays fabricated by microcontact printing. *Langmuir.* **2002**, *18*, 5263-5268.

6. Howell, S. W.; Inerowicz, H. D.; Regnier, F. E.; Reifenberger, R. Patterned Protein Microarrays for Bacterial Detection. *Langmuir.* **2003**, *19*, 436-439.

7. Thibault, C.; Le Berre, V.; S., C.; Trévisiol, E.; François, J.; Vieu, C. Direct microcontact printing of oligonucleotides for biochip applications. *J. Nanobiotechnol.* **2005**, *3*, 7.

8. Lange, S. A.; Benes, V.; Kern, D. P.; Horber, J. K. H.; Bernard, A. Microcontact printing of DNA molecules. *Anal. Chem.* **2004**, *76*, 1641-1647.

9. Lauer, L.; Ingebrandt, S.; Scholl, M.; Offenhausser, A. Aligned microcontact printing of biomolecules on microelectronic device surfaces. *IEEE T. Biomed. Eng.* **2001**, *48*, 838-842.

10. McDevitt, T. C.; Woodhouse, K. A.; Hauschka, S. D.; Murry, C. E.; Stayton, P. S. Spatially organized layers of cardiomyocytes on biodegradable polyurethane films for myocardial repair. *J. Biomed. Mater. Res. A.* **2003**, *66*, 586-595.

11. Ber, S.; Kose, G. T.; Hasirci, V. Bone tissue engineering on patterned collagen films: an in vitro study. *Biomaterials.* **2005**, *26*, 1977-1986.

12. Bhatia, S. N.; Balis, U. J.; Yarmush, M. L.; Toner, M. Microfabrication of Hepatocyte/Fibroblast Co-cultures: Role of Homotypic Cell Interactions. *Biotechnol. Prog.* **1998**, *14*, 378-387.

13. Bernard, A.; Delamarche, E.; Schmid, H.; Michel, B.; Bosshard, H. R.; Biebuyck, H. Printing patterns of proteins. *Langmuir.* **1998**, *14*, 2225-2229.

14. James, C. D.; Davis, R. C.; Kam, L.; Craighead, H. G.; Isaacson, M.; Turner, J. N.; Shain, W. Patterned protein layers on solid substrates by thin stamp microcontact printing. *Langmuir.* **1998**, *14*, 741-744.

15. Chiu, D. T.; Jeon, N. L.; Huang, S.; Kane, R. S.; Wargo, C. J.; Choi, I. S.; Ingber, D. E.; Whitesides, G. M. Patterned deposition of cells and proteins onto surfaces by using three-dimensional microfluidic systems. *P. Natl. Acad. Sci. USA.* **2000**, *97*, 2408-2413.

16. Delamarche, E.; Bernard, A.; Schmid, H.; Michel, B.; Biebuyck, H. Patterned delivery of immunoglobulins to surfaces using microfluidic networks. *Science.* **1997**, *276*, 779-781.

17. Nalayanda, D. D.; Kalukanimuttam, M.; Schmidtke, D. W. Micropatterned surfaces for controlling cell adhesion and rolling under flow. *Biomed. Microdevices.* **2007**, *9*, 207-214.

18. Neeves, K. B.; Maloney, S. F.; Fong, K. P.; Schmaier, A. A.; Kahn, M. L.; Brass, L. F.; Diamond, S. L. Microfluidic focal thrombosis model for measuring murine platelet deposition and stability: PAR4 signaling enhances shear-resistance of platelet aggregates. *J. Thromb. Haemost.* **2008**, *6*, 2193-2201.

19. Falconnet, D.; Koenig, A.; Assi, F.; Textor, M. A Combined Photolithographic and Molecular-Assembly Approach to Produce Functional Micropatterns for Applications in the Biosciences. *Adv. Funct. Mater.* **2004**, *14*, 749-756.

20. Mooney, J. F.; Hunt, A. J.; McIntosh, J. R.; Liberko, C. A.; Walba, D. M.; Rogers, C. T. Patterning of functional antibodies and other proteins by photolithography of silane monolayers. *P. Natl. Acad. Sci. USA.* **1996**, *93*, 12287-12291.

21. Hoff, J. D.; Cheng, L.-J.; Meyhöfer, E.; Guo, L. J.; Hunt, A. J. Nanoscale Protein Patterning by Imprint Lithography. *Nano Lett.* **2004**, *4*, 853-857.

22. Zhang, G. J.; Tanii, T.; Zako, T.; Hosaka, T.; Miyake, T.; Kanari, Y.; Funatsu, T. W.; Ohdomari, I. Nanoscale patterning of protein using electron beam lithography of organosilane self-assembled monolayers. *Small.* **2005**, *1*, 833-837.

23. Lussi, J. W.; Tang, C.; Kuenzi, P.-A.; Staufer, U.; Csucs, G.; Vörös, J.; Gaudenz Danuser; Hubbell, J. A.; Textor, M. Selective molecular assembly patterning at the nanoscale: a novel platform for producing protein patterns by electron-beam lithography on SiO2/indium tin oxide-coated glass substrates. *Nanotechnology.* **2005**, *16*, 1781-1786.

24. Nicolau, D. V.; Taguchi, T.; Taniguchi, H.; Yoshikawa, S. Negative and positive tone protein patterning on e-beam/deep-UV resists. *Langmuir.* **1999**, *15*, 3845-3851.

25. Kumar, N.; Hahm, J.-i. Nanoscale Protein Patterning Using Self-Assembled Diblock Copolymers. *Langmuir.* **2005**, *21*, 6652-6655.

26. Arnold, M.; Cavalcanti-Adam, E. A.; Glass, R.; Blummel, J.; Eck, W.; Kantlehner, M.; Kessler, H.; Spatz, J. P. Activation of integrin function by nanopatterned adhesive interfaces. *ChemPhysChem.* **2004**, *5*, 383-388.

27. Cavalcanti-Adam, E. A.; Micoulet, A.; Blummel, J.; Auernheimer, J.; Kessler, H.; Spatz, J. P. Lateral spacing of integrin ligands influences cell spreading and focal adhesion assembly. *Eur. J. Cell Biol.* **2006**, *85*, 219-224.

28. Garno, J. C.; Amro, N. A.; Wadu-Mesthrige, K.; Liu, G.-Y. Production of Periodic Arrays of Protein Nanostructures Using Particle Lithography. *Langmuir.* **2002**, *18*, 8186-8192.

29. Cai, Y.; Ocko, B. M. Large-Scale Fabrication of Protein Nanoarrays Based on Nanosphere Lithography. *Langmuir.* **2005**, *21*, 9274-9279.

30. Blättler, T. M.; Binkert, A.; Zimmermann, M.; Textor, M.; Vörös, J.; Reimhult, E. From particle self-assembly to functionalized sub-micron protein patterns. *Nanotechnology.* **2008**, *19*, 075301.

31. Vörös, J.; Blättler, T. M.; Textor, M. Bioactive patterns at the 100-nm scale produced using multifunctional physisorbed monolayers. *MRS Bull.* **2005**, *30*, 202-206.

32. Christman, K. L.; Enriquez-Rios, V. D.; Maynard, H. D. Nanopatterning proteins and peptides *Soft Matter.* **2006**, *2*, 928-939.

33. Wang, X. D.; Graugnard, E.; King, J. S.; Zhong, L. W.; Summers, C. J. Large-scale fabrication of ordered nanobowl arrays. *Nano Lett.* **2004**, *4*, 2223-2226.

34. Velev, O. D.; Jede, T. A.; Lobo, R. F.; Lenhoff, A. M. Microstructured porous silica obtained via colloidal crystal templates. *Chem. Mater.* **1998**, *10*, 3597-3602.

35. Hulteen, J. C.; Vanduyne, R. P. Nanosphere Lithography - A Materials General Fabrication Process for Periodic Particle Array Surfaces. *J. Vac. Sci. Technol. A.* **1995**, *13*, 1553-1558.

36. Sun, F. Q.; Cai, W. P.; Li, Y.; Cao, B. Q.; Lu, F.; Duan, G. T.; Zhang, L. D. Morphology control and transferability of ordered through-pore arrays based on electrodeposition and colloidal monolayers. *Adv. Mater.* **2004**, *16*, 1116-1121.

37. Rossi, R. C.; Tan, M. X.; Lewis, N. S. Size-dependent electrical behavior of spatially inhomogeneous barrier height regions on silicon. *Appl. Phys. Lett.* **2000**, *77*, 2698-2700.

38. Frey, W.; Woods, C. K.; Chilkoti, A. Ultraflat nanosphere lithography: A new method to fabricate flat nanostructures *Adv. Mater.* **2000**, *12*, 1515-1519.

39. Zhao, Y.; Li, M.; Lu, Q. H.; Shi, Z. Y. Superhydrophobic Polyimide Films with a Hierarchical Topography: Combined Replica Molding and Layer-by-Layer Assembly. *Langmuir.* **2008**, *24*, 12651-12657.

40. Marquez, M.; Patel, K.; Carswell, A. D. W.; Schmidtke, D. W.; Grady, B. P. Synthesis of Nanometer-Scale Polymeric Structures on Surfaces from Template Assisted Admicellar Polymerization: A Comparative Study with Protein Adsorption. *Langmuir.* **2006**, *22*, 8010-8016.

41. Denis, F. A.; Hanarp, P.; Sutherland, D. S.; Dufrene, Y. F. Fabrication of nanostructured polymer surfaces using colloidal lithography and spin-coating. *Nano Lett.* **2002**, *2*, 1419-1425.

42. Li, J.-R.; Henry, G. C.; Garno, J. C. Fabrication of nanopatterned films of bovine serum albumin and staphylococcal protein A using latex particle lithography. *Analyst.* **2006**, *131*, 244-250.

43. Ngunjiri, J. N.; Daniels, S. L.; Li, J.-R.; Serem, W. K.; Garno, J. C. Controlling the surface coverage and arrangement of proteins using particle lithography. *Nanomedicine.* **2008**, *3*, 529-541.

44. Batra, D.; Vogt, S.; Laible, P. D.; Firestone, M. A. Self-assembled, mesoporous polymeric networks for patterned protein arrays. *Langmuir.* **2005**, *21*, 10301-10306.

45. Agheli, H.; Malmström, J.; Larsson, E. M.; Textor, M.; Sutherland, D. S. Large Area Protein Nanopatterning for Biological Applications. *Nano Lett.* **2006**, *6*, 1165-1171.

46. Valsesia, A.; Mannelli, I.; Colpo, P.; Bretagnol, F.; Rossi, F. Protein Nanopatterns for Improved Immunodetection Sensitivity. *Anal. Chem.* **2008**, *80*, 7336-7340.

47. Jiang, P.; McFarland, M. J. Large-scale fabrication of wafer-size colloidal crystals, macroporous polymers and nanocomposites by spin-coating. *J. Am. Chem. Soc.* **2004**, *126*, 13778-13786.

48. Kim, M. H.; Im, S. H.; Park, O. O. Rapid fabrication of two- and three-dimensional colloidal crystal films via confined convective assembly. *Adv. Funct. Mater.* **2005**, *15*, 1329-1335.

49. Park, S. H.; Xia, Y. N. Assembly of mesoscale particles over large areas and its application in fabricating tunable optical filters. *Langmuir.* **1999**, *15*, 266-273.

50. vanBlaaderen, A.; Ruel, R.; Wiltzius, P. Template-directed colloidal crystallization. *Nature.* **1997**, *385*, 321-324.

51. Liu, S. T.; Maoz, R.; Schmid, G.; Sagiv, J. Template guided self-assembly of [Au_{55}] clusters on nanolithographically defined monolayer patterns. *Nano Lett.* **2002**, *2*, 1055-1060.

52. Fustin, C. A.; Glasser, G.; Spiess, H. W.; Jonas, U. Parameters influencing the templated growth of colloidal crystals on chemically patterned surfaces. *Langmuir.* **2004**, *20*, 9114-9123.

53. Huwiler, C.; Halter, M.; Rezwan, K.; Falconnet, D.; Textor, M.; Voros, J. Self-assembly of functionalized spherical nanoparticles on chemically patterned microstructures. *Nanotechnology.* **2005**, *16*, 3045-3052.

54. Guo, Q.; Arnoux, C.; Palmer, R. E. Guided assembly of colloidal particles on patterned substrates. *Langmuir.* **2001**, *17*, 7150-7155.

55. Fan, F. Q.; Stebe, K. J. Assembly of colloidal particles by evaporation on surfaces with patterned hydrophobicity. *Langmuir.* **2004**, *20*, 3062-3067.

56. Liu, S. H.; Wang, W. M.; Mannsfeld, S. C. B.; Locklin, J.; Erk, P.; Gomez, M.; Richter, F.; Bao, Z. N. Solution-assisted assembly of organic semiconducting single crystals on surfaces with patterned wettability. *Langmuir.* **2007**, *23*, 7428-7432.

57. Du, H.; Bai, Y. B.; Hui, Z.; Li, L. S.; Chen, Y. M.; Tang, X. Y.; Li, T. J. Two-dimensional arrays from polymer spheres in nanoscale prepared by the Langmuir-Blodgett method. *Langmuir.* **1997**, *13*, 2538-2540.

58. Marquez, M.; Grady, B. P. The use of surface tension to predict the formation of 2D arrays of latex spheres formed via the Langmuir-Blodgett-like technique. *Langmuir.* **2004**, *20*, 10998-11004.

59. Trau, M.; Saville, D. A.; Aksay, I. A. Field-induced layering of colloidal crystals *Science.* **1996**, *272*, 706-709.

60. Choi, W. M.; Park, O. The fabrication of micropatterns of a 2D colloidal assembly by electrophoretic deposition. *Nanotechnology.* **2006**, *17*, 325-329.

61. Yang, S. M.; Jang, S. G.; Choi, D. G.; Kim, S.; Yu, H. K. Nanomachining by colloidal lithography. *Small.* **Small**, *2*, 458-475.

62. Dziomkina, N. V.; Vancso, G. J. Colloidal crystal assembly on topologically patterned templates. *Soft Matter.* **2005**, *1*, 265-279.

63. Sharma, S.; Johnson, R. W.; Desai, T. A. Evaluation of the stability of nonfouling ultrathin poly(ethylene glycol) films for silicon-based microdevices. *Langmuir.* **2004**, *20*, 348-356.

64. Subramaniam, V.; Bhattacharya, P. K.; Memon, A. A. Chemical Contamination of Thin Oxides and Native Silicon for Use in Modern Device Processing. *Int. J. Electron.* **1995**, *78*, 519-525.

65. Sagiv, J. Organized Monolayers By Adsorption. 1. Formation and Structure of Oleophobic Mixed Monolayers on Solid Surfaces. *J. Am. Chem. Soc.* **1980**, *102*, 92-98.

66. Netzer, L.; Iscovici, R.; Sagiv, J. Adsorbed Monolayeres Versus Langmuir-Blodgett Monolayers Why and How. 1. From Monolayer to Multilayer, By Adsorption. *Thin Solid Films.* **1983**, *99*, 235-241.

67. Onclin, S.; Ravoo, B. J.; Reinhoudt, D. N. Engineering silicon oxide surfaces using self-assembled monolayers. *Angew. Chem. Int. Edit.* **2005**, *44*, 6282-6304.

68. Branch, D. W.; Wheeler, B. C.; Brewer, G. J.; Leckband, D. E. Long-term stability of grafted polyethylene glycol surfaces for use with microstamped substrates in neuronal cell culture. *Biomaterials.* **2001**, *22*, 1035-1047.

69. Messing, R. A. Adsorption of Protein on Glass Surfaces and Pertinent Parameters for the Immobilizatoin of Enzymes in the Pores of Inorganic Carriers. *J. Non-Cryst. Solids*. **1975**, *19*, 277-283.

70. Boneberg, J.; Burmeister, F.; Schafle, C.; Leiderer, P.; Reim, D.; Fery, A.; Herminghaus, S. The formation of nano-dot and nano-ring structures in colloidal monolayer lithography. *Langmuir*. **1997**, *13*, 7080-7084.

71. Winzer, M.; Kleiber, M.; Dix, N.; Wiesendanger, R. Fabrication of nano-dot- and nano-ring-arrays by nanosphere lithography. *Appl. Phys. A-Mater.* **1996**, *63*, 617-619.

Chapter 3: Patterning of Quantum Dot Bioconjugates via Particle Lithography

This chapter was reproduced in part with permission from:

Taylor, Z. R.; Sanchez, E. S.; Keay, J. C.; Johnson, M. B.; Schmidtke, D. W. Patterning of Quantum Dot Bioconjugates via Particle Lithography. *Langmuir*. **2010**, *26*, 18938-18944.

Copyright 2010 American Chemical Society.

Introduction

Due to their unique fluorescent properties, semiconductor quantum dots (QDs) have been utilized in the development of novel light emitting devices,[1] solar cells,[2] biological imaging schemes,[3-7] and biosensors for the detection of proteins,[8-11] nucleic acids,[12-16] bacteria,[17,18] and other chemical species.[19-27] Compared to organic fluorophores, QDs exhibit both higher quantum efficiency and greater photostability. Furthermore, since their fluorescent properties are size-dependent, QDs with identical chemical compositions but different diameters can be used when multiple fluorophores are desired. For biological applications, QDs can be conjugated to a number of biomolecules including nucleic acids and proteins.[28-30] These characteristics make QDs an important resource in a number of scientific fields.

Recently, there has been a great deal of interest in patterning surfaces with QDs in sub-micrometer domains (Table 3.1). QD-patterned surfaces have potential applications in electronics, computing, data storage, molecular interaction studies, and biosensors.[31] In biosensing applications, patterned surfaces present increased densification of surface recognition elements,[32] availability of binding sites,[33] and immobilization

Table 3.1: Comparison of Quantum Dot Sub-Micrometer Patterning Methods[a]

Pattern Type	Method of Pattern Formation	Pattern Size	Quantum Dot Bioconjugate(s) Patterned	Ref
Dots	Dip-pen Nanolithography (DPN)	500 – 900 nm	QD-IgG	35
Dots (Single QDs)	S-layer Protein Scaffolding	7 – 22 nm (spacing)		36
Dots Lines	Dip-pen Nanolithography (DPN)	230 nm / 90 – 400 nm	QD-SA QD-IFNα2	37
Dots	Particle Lithography	500 – 600 nm	QD-SA QD-B QD-IgG	This Work
Lines	Microcontact Molding	160 – 510 nm		38
Lines	Electron-beam Lithography	200 nm	QD-IgG	39
Lines Wells	Surface Reconstructed Block Copolymers	<10 – 24 nm		40
Lines Squares Cylinders	Pattern Replication in Nonwetting Templates (PRINT) Process	~50 nm – 3 μm		41
Rings	Evaporative Templating (Particle Lithography)	86 – 266 nm		42
Rings Pores	"Two-particle" Lithography (Particle Lithography)	140 – 210 nm	QD-Cys	43[b]
Squares	Microcontact Printing	500 – 800 nm		44
Squares	Electron-beam Lithography	100 nm – 4 μm	QD-SA	45

[a] SA = streptavidin; Cys = cysteine; IFNα2 = interferon- α2; B = Biotin
[b] CdS QDs; all other references in table use CdSe QDs

efficiency[34] over homogeneously coated surfaces. Ultimately, these advantages lead to lower detection limits.[32-34]

Of the methods used to pattern QDs, particle lithography is an attractive option because it relies on simple, relatively inexpensive techniques and can be used to process several samples simultaneously. Particle lithography has previously been used to create periodic arrays of QD rings and QD films with periodic porelike structures.[42,43] In a study by Lewandowski et al.,[43] particle lithography was used to pattern cysteine-coated QDs, which can be categorized as a type of QD bioconjugate (QDBC). We define QDBCs as QDs that have been conjugated to biological molecules, such as amino acids and proteins. QDBCs have also been patterned in "dot" domains via dip-pen nanolithography (DPN)[35,37] and electron-beam lithography (EBL),[39,45] both of which require specialized equipment and training and have restricted throughput.

Previously, we developed a particle lithography technique to fabricate both honeycomb patterns[46] and dot patterns of proteins.[47] Here we extend particle lithography to pattern sub-micrometer holes in a methoxy-poly(ethylene glycol)-silane (mPEG-sil) layer filled with QDBCs. To our knowledge, this is the first study where QDBCs have been patterned in dot domains by particle lithography. We demonstrate the potential for these patterns to be used in biosensing applications by designing a QD-based fluorescent binding assay with a subpicomolar detection limit.

Experimental Section

Chemicals and Materials. Polystyrene latex spheres (5 μm mean diameter) were purchased from Duke Scientific (Fremont, CA) and washed once in DI water by centrifugation before use. Poly(dimethylsiloxane) (PDMS; Sylgard-184, Dow-Corning)

was purchased from Krayden (Marlborough, MA). Human serum albumin (HSA; Albuminar-25, CSL Behring) was purchased from National Hospital Specialties (Hackensack, NJ). Qdot 655 biotin, Qdot 655 goat F(ab')$_2$ anti-mouse IgG, Qdot 525 streptavidin, Qdot 525 goat F(ab')$_2$ anti-mouse IgG, Alexa Fluor 488 avidin, Alexa Fluor 488 fibrinogen, Alexa Fluor 488 goat anti-chicken IgG, and Qdot incubation buffer (2% BSA in 50 mM borate buffer, pH 8.3, with 0.05% sodium azide) were purchased from Invitrogen (Carlsbad, CA). Monoclonal mouse anti-human IgG-biotin was purchased from Sigma-Aldrich (St. Louis, MO). Finally, methoxy-poly(ethylene glycol)-silane (mPEG-sil; MW=5000) was purchased from Laysan Bio (Arab, AL).

Substrate Preparation. Periodic holes in a protein-repellant layer of mPEG-sil were formed as previously described[47] (Figure 3.1). Briefly, glass slides were cleaned in trichloroethylene, acetone, methanol, and DI water in sequential, 2 minute cycles in an ultrasonic cleaner. Next, a PDMS mold with a 4.5 mm diameter circular hole cut from the center was placed on the surface of each slide. The substrates were then exposed to

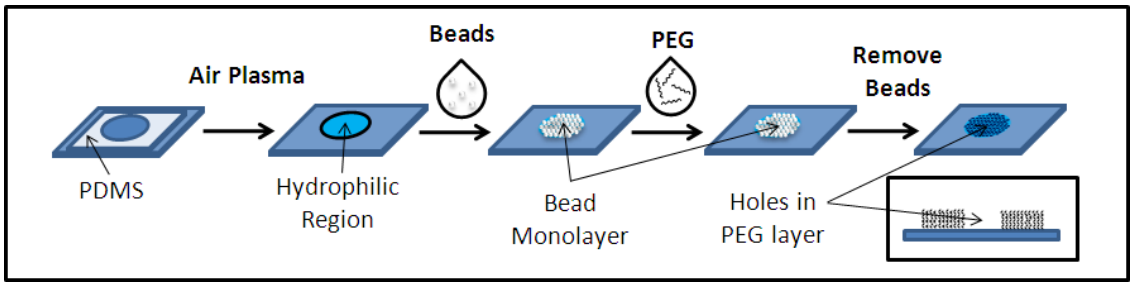

Figure 3.1: Schematic of the mPEG-sil Patterning Procedure. A pattern of periodic holes in a mPEG-sil layer is formed with the following sequence. A PDMS stamp is applied to a substrate before treatment in an air-plasma in order to create a relatively hydrophilic region. A suspension of polystyrene spheres is deposited in the hydrophilic region to create a sphere monolayer. Next, a layer of mPEG-sil is grafted to the substrate around the spheres. Finally, the spheres are removed to reveal areas of bare substrate that serve as adsorption sites.

an air-plasma (Harrick Scientific Corp, model PDC-32G, Ithaca, NY) at 400 mTorr and "low" power (0.010 W/cm^3) for 30 s to create a relatively hydrophilic region in the circular areas of the glass not covered by the PDMS molds. After plasma treatment, the PDMS molds were removed, and the substrates were left untouched for approximately 30 min. To form sphere monolayers, 5.06 μL of 0.075% wt 5 μm sphere suspension was deposited on the circular hydrophilic region of each substrate and was allowed to dry overnight at 4 °C. After monolayer formation, the substrates were heated at 80 °C for 1 h to promote firm adhesion of the spheres to the surface. Next, the substrates were soaked for 5 min in DI water to remove residue from the sphere suspension and then allowed to dry for 1 h in ambient conditions. After drying, mPEG-sil was grafted to the substrates around the spheres by first exposing the substrates to an air-plasma at 400 mTorr and "high" power (0.027 W/cm^3) for 1 min before immediately applying 375 μL of 4 mM mPEG-sil in anhydrous acetonitrile to the substrates. The grafting was allowed to proceed overnight at room temperature. Next, ungrafted mPEG-sil was removed by soaking the substrates in three consecutive Petri dishes full of anhydrous acetonitrile for 5 min each. Finally, the substrates were washed with approximately 50 mL DI water using a wash bottle to remove the spheres and reveal the hexagonal pattern of holes in the mPEG-sil layer. These holes then served as adsorption sites for QDBCs or fluorescent protein.

Single QDBC Patterns. QDBC solutions were centrifuged for 5 min at 6600 rpm (Fisher Scientific, model 05-090-128) to remove any QDBC aggregates that may have formed during storage. Next the supernatant was removed and diluted to a concentration

of 50 nM with phosphate buffered saline (PBS), pH 7.4. Solutions of 655 biotin- and 655 goat anti-mouse IgG-conjugated QD (QD-B and QD-IgG, respectively) solutions were used without further modification. During dilution, HSA was added to 525 streptavidin-conjugated QD (QD-SA) solutions to a final concentration of 3.4 μg/mL to prevent aggregation. After the addition of HSA, QD-SA solutions were allowed to sit for 30 min prior to use. After preparation, 75 μL of QDBC solution was dispensed onto the mPEG-sil-patterned surface and incubated for 2 h at room temperature to allow QDBCs to adsorb in the mPEG-sil holes. Finally, substrates were washed with 25 mL PBS using a transfer pipette and 50 mL DI water using a wash bottle to remove any unbound QDBCs.

Colocalized Dual-QDBC Patterns. Single QD-B patterns were produced as described in the "Single QDBC patterns" section above. After incubating with QD-B and washing, about 1 mL of 5 mg/mL HSA in PBS was dispensed on the substrate for 30 min to block any remaining adsorption sites. The substrates were then washed with 25 mL of PBS using a transfer pipette. A QD-SA solution was mixed as described in the "Single QDBC patterns" section above but with a final HSA concentration of 10 mg/mL to prevent aggregation and nonspecific adsorption. Next, 75 μL of the QD-SA solution was dispensed and allowed to incubate on the substrate for 30 min. Finally, the substrate was washed with 25 mL of 5 mg/mL HSA in PBS using a transfer pipette and 50 mL DI water using a wash bottle.

IgG-biotin Binding Assay Substrates. mPEG-sil surfaces patterned with periodic holes were produced as described in the "Substrate Preparation" section above. Next, 75 μL of 20 μg/mL Alexa Fluor 488 avidin diluted in PBS was dispensed onto the surface for 2 h to allow the protein to adsorb in the mPEG-sil holes. After incubation, substrates were washed with 50 mL of PBS using a wash bottle. The substrates were then held vertically and gently shaken to remove excess liquid from the surface. Next, 75 μL of mouse anti-human IgG-biotin diluted in PBS to a final concentration between 500 fM and 50 nM was distributed onto the surface and incubated for 1 h. The substrates were washed with PBS using a wash bottle and excess liquid was removed before a final incubation with 75 μL of 50 nM QD-IgG for 30 min. Lastly, the substrates were sequentially washed with 25 mL of PBS and 50 mL of DI water using wash bottles.

Substrate Characterization. Fluorescent images of QDBC patterns were acquired with a Zeiss Axiovert 200 inverted microscope equipped with a 100x objective (NA = 1.3) and a CoolSnap cf digital camera. The image acquisition time was adjusted between 0.5 and 10 s depending on the type of sample. Atomic force microscopy (AFM) images were obtained with a Topometrix Explorer SPM instrument operating in noncontact mode.

Image Analysis. Image analysis was performed with the open source software packages ImageJ (version 1.40 g) and Gwyddion (version 2.19). To determine QDBC dot sizes, images were first thresholded to create a binary image of black QDBC dots and white background. The thresholding criteria were optimized and remained constant for each

image analyzed. Next, the areas of each QDBC dot were measured. Finally, the area measurements were used to calculate the diameters of the QDBC dots with the assumption they were circular.

For the dose-response and binding assay experiments, the peak fluorescent intensity within each QDBC dot was measured. Next, the intensities were reduced by the value of the background which was determined by taking an image with the camera completely blocked. This correction assigns a value of zero to all protein dots that did not contain a QD fluorescent signal. The background-corrected QDBC intensities were then averaged for each concentration.

Calculations and Statistics. Values are presented as means ± standard deviation of the mean unless otherwise specified, and statistical significance was assessed when appropriate by Student's *t* test, with $P < 0.05$ considered as statistically significant. Outliers were identified as measurements outside of three standard deviations of the mean and were eliminated. All experiments except AFM measurements were performed on at least three different samples each made on different days.

Results and Discussion

QDBC Patterning Process. QDBC patterns were formed via particle lithography by a three-step process: (1) formation of a polystyrene sphere monolayer, (2) grafting of a protein-repellant methoxy-poly(ethylene glycol)-silane (mPEG-sil) layer, and (3) selective adsorption of the QDBC into the resulting mPEG-sil holes.

QDs Conjugated to Biologically Important Small Molecules, Proteins, or Antibodies Can Be Patterned in Sub-micrometer Domains. Figure 3.2 shows

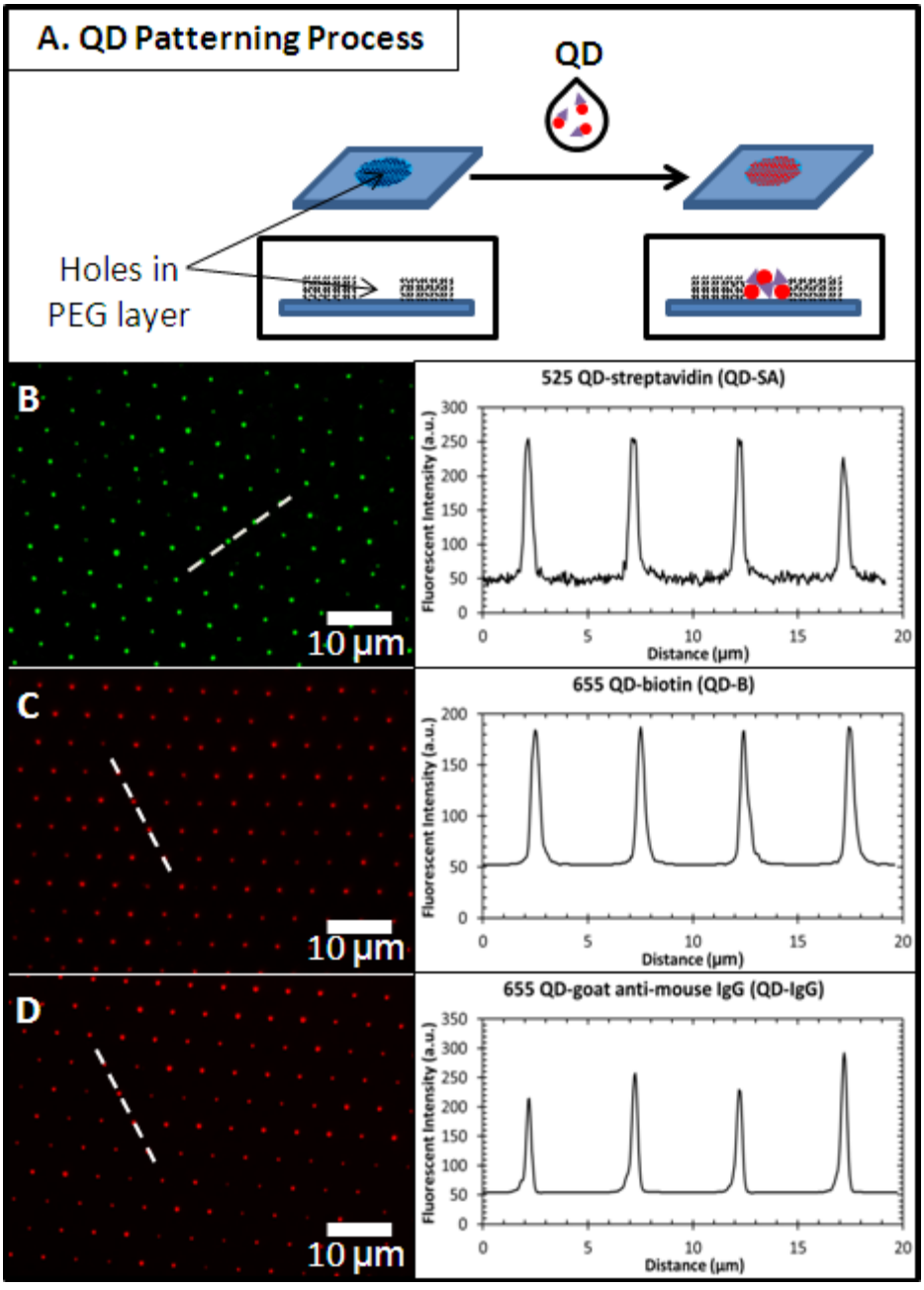

Figure 3.2: Fluorescent Images of Single-QDBC Patterns. (A) Schematic of the final step to make a single-QDBC pattern. Fluorescent images (pseudocolored post-acquisition) of patterns made with 525 QD-streptavidin (B), 655 QD-biotin (C), and 655 QD-goat-anti-mouse IgG (D). The fluorescent line intensity (arbitrary units) graphs to the right of each image correspond to the dashed lines in each image.

representative fluorescent images of QDBC-filled holes formed with QDs conjugated **to** streptavidin (QD-SA), biotin (QD-B), and goat anti-mouse IgG (QD-IgG). The mean diameters of the fluorescing regions (dots) were determined to be 570 nm ± 110 nm, 570 ± 90 nm, and 530 ± 90 nm for QD-SA, QD-B, and QD-IgG, respectively. The similar values obtained for all three species indicate that the size of the dots is independent of the QDBC patterned. To verify the fluorescent dot size measurements, we also obtained images using AFM of these QDBC arrays. Figure 3.3A shows a representative AFM image of a substrate patterned with QD-IgG. Applying the same analysis procedure used to determine the fluorescent dot sizes, we found the mean diameter of the QD-IgG dots to be 500 ± 70 nm, corroborating the fluorescent measurements. Figure 3C shows a representative line-cut through three QD-IgG dots. The average peak height within the QD-IgG dots was 9-10 nm, which agrees well with the approximate size of a single QDBC, suggesting that QDBCs do not form multiple layers in our patterns. Furthermore, these data demonstrate that our technique is versatile and can be used to pattern QDs conjugated to several different classes of biologically important molecules.

QDBCs Exhibit High Photostability. To assess the photostability of the patterned QDBCs, we exposed QD-B patterns to continual fluorescent light and obtained images every 5 min for 30 min. For comparison with a typical fluorescent dye, we performed the same experiment with patterns of Alexa Fluor 488 fibrinogen (AF-Fib) but acquired images every 30 s for 10 min. Three representative dots were chosen from each substrate's set of images, and their peak fluorescent intensities were measured over

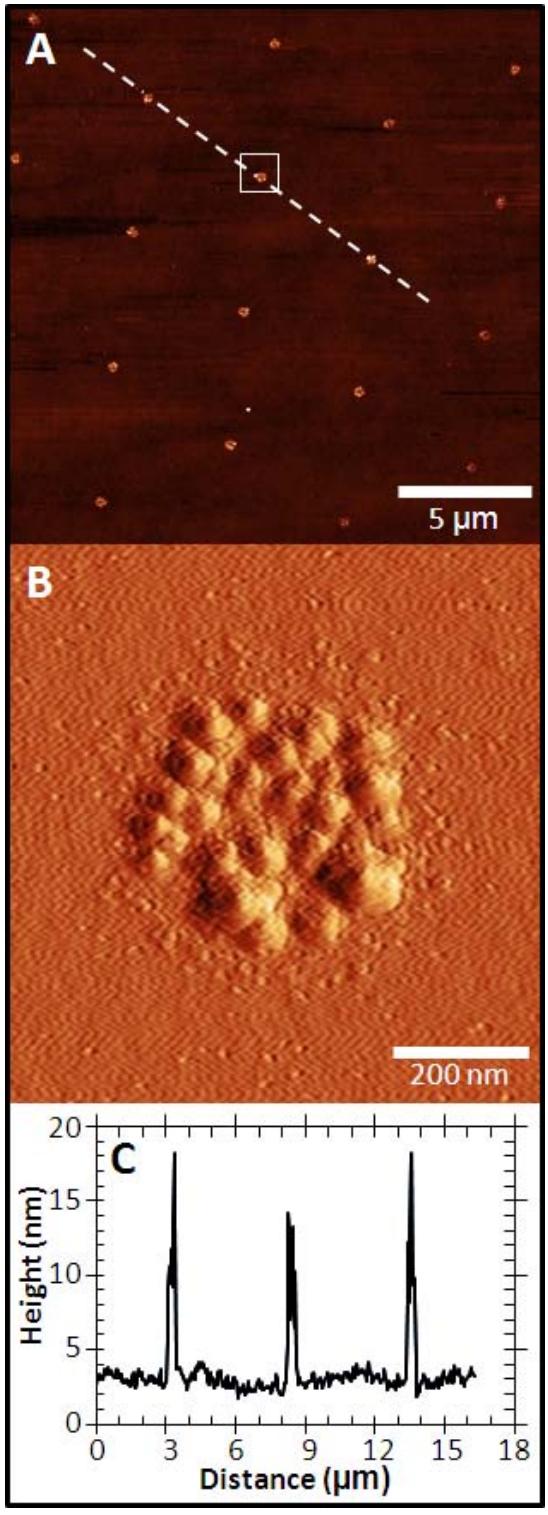

Figure 3.3: AFM Images of a Single-QDBC Pattern. (A) A 20 µm x 20 µm AFM image of a QD-IgG pattern. (B) A differentiated image of the single dot outlined by the box in (A). The color scale for (A) and the height scale for (B) are 25 nm. The height profile graph (C) corresponds to the dashed line in (A).

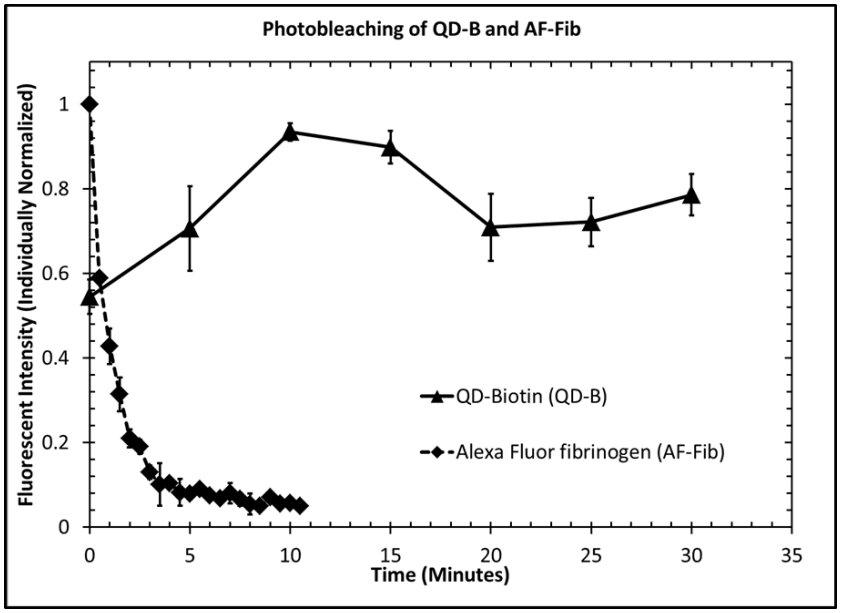

Figure 3.4: Comparison of the Photobleaching of a QDBC and a Common Fluorescent Dye. The intensities for each fluorescent species were normalized individually to show the percent change in intensity over time. Data are shown as mean ± standard error of the mean.

time. Figure 3.4 shows the average peak fluorescent intensities of the QD-B and AF-Fib dots during photobleaching. After 10 min, the AF-Fib dots were nearly completely photobleached while the intensities of the QD- B dots remained relatively constant.

Although there is fluctuation in the average intensities of the QD-B dots over time, the difference between the initial and final data points is not statistically significant. We hypothesize that these fluctuations are due to the phenomenon of quantum dot blinking.[28] Our results compare favorably with previous studies documenting the photostability of QDBCs.[48,49] These data demonstrate the high photostability of QDs, especially compared to common fluorescent dyes.

The Site Density of QDBCs Can Be Manipulated By Varying the Coating Concentration. Since QDBCs adsorb in the unfilled holes of the mPEG-sil-patterned substrates nonspecifically, the number of QDs that adsorb to the surface should be dependent on the coating concentration of the QDBC solution. To verify that the site density of QDBC patterns is dependent on the coating concentration of the QDBC solution, we made QD-IgG patterns using solutions between 500 pM and 50 nM. Figure 3.5A shows the fluorescent intensity of the QD-IgG that adsorbed to the glass substrate as a function of the solution coating concentration. The average intensities for the

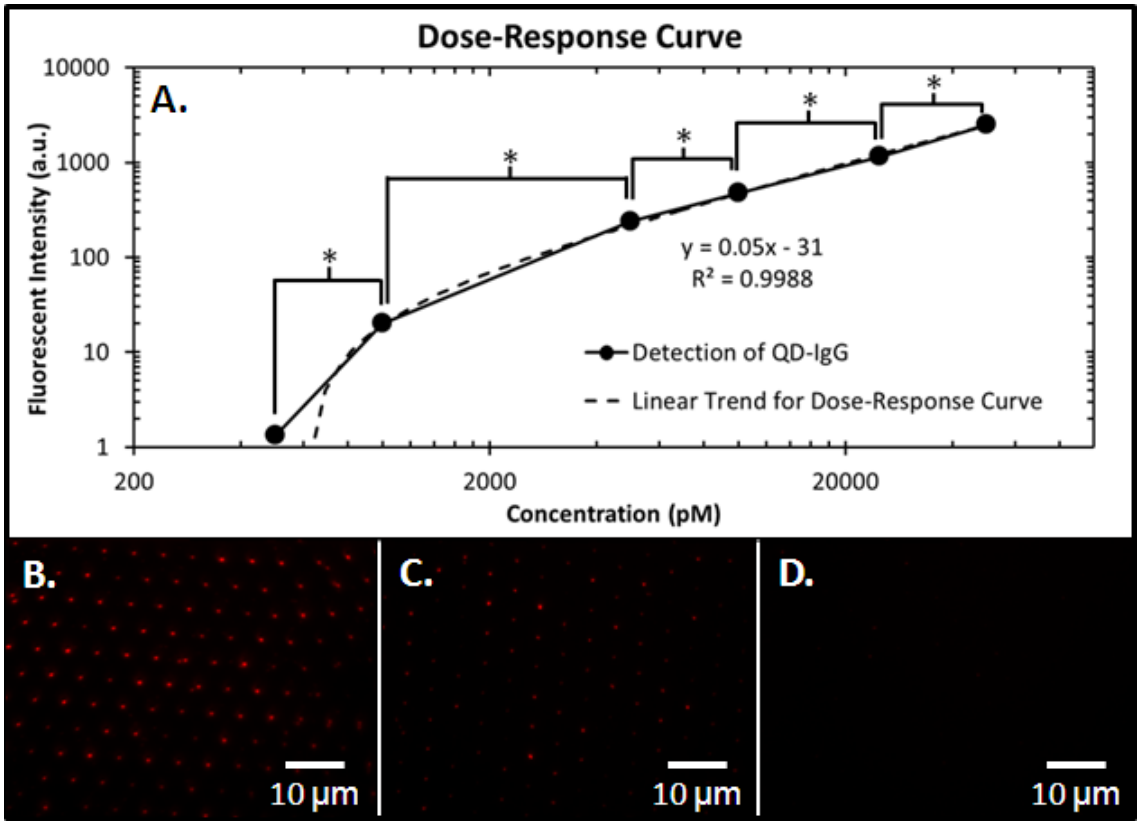

Figure 3.5: Dose-Response Curve of the Single-QDBC Patterning Technique. (A) Fluorescent intensity versus concentration graph for patterns made with various concentrations of QD-IgG (500 pM to 50 nM). (B—D) Representative fluorescent images (pseudocolored post-acquisition) of patterns made with 50 nM (B), 10 nM (C), and 1 nM (D) QD-IgG. Data are shown as mean ± standard error of the mean (* $P <$ 0.001).

concentrations investigated were each statistically significant from the intensities for the nearest higher and lower concentrations. The linear trend observed suggests that the solution concentration tested is below the critical amount required for saturation of the surface and demonstrates that the site density of QDBCs may be controlled by the coating concentration of the QDBC solution.

QDBC Patterns Retain Biological Functionality and Can Be Used to Create Dual-QDBC Patterns. Figure 3.6A shows a schematic of the process to fabricate colocalized QDBC patterns. To create dual-QDBC patterns, we first made QD-B patterns. The patterns were then incubated with HSA to fill any remaining adsorption sites. Finally, the patterns were incubated with QD-SA and imaged. Figure 3.6B—D shows representative fluorescent images of the individual and colocalized QD-B and QD-SA signals. Overall, 99% ± 2% of the QD-B dots were colocalized with QD-SA. To verify the specificity of the binding between QD-B and QD-SA, positive control samples were made with QD-B and Alexa Fluor 488 avidin. Two sets of negative control samples were also made with QD-B and either Alexa Fluor 488 goat anti-chicken IgG or 525 QD-IgG. Images from the positive control samples were similar to those from samples made with QD-B and QD-SA, while images from the negative controls had no signal from the 488 goat anti-chicken IgG or the 525 QD-IgG (data not shown). The results from the controls indicate that QD-SA binding to QD-B is a result of the specific interaction of the biotin and streptavidin moieties and not due to the QDs interacting with each other or with the protein portions of the QDBCs. These data demonstrate that dual-QDBC patterns can be created with high specificity.

QDBCs Can Be Used to Create Sensitive Binding Assays. In order to demonstrate one application of our patterning technique, we designed a QD-based fluorescent binding assay (Figure 3.7A). Surface-based binding assays typically include a capture molecule adsorbed or covalently bound to a substrate that specifically binds an analyte of interest. After the substrate is exposed to a solution containing an unknown that also specifically binds the analyte of interest and can be directly or indirectly detected. The signal from the reporter molecule can then be quantified and related to the concentration of the analyte. In the construction of our binding assay, we used avidin as our capture molecule, biotinylated mouse IgG as our analyte of interest, and goat QD-IgG as our reporter molecule. First, Alexa Fluor 488 avidin was dispensed on a mPEG-sil-patterned surface where it nonspecifically adsorbed in the mPEG-sil holes. Next, biotinylated mouse anti-human IgG (IgG-biotin) was distributed on the surface, and the

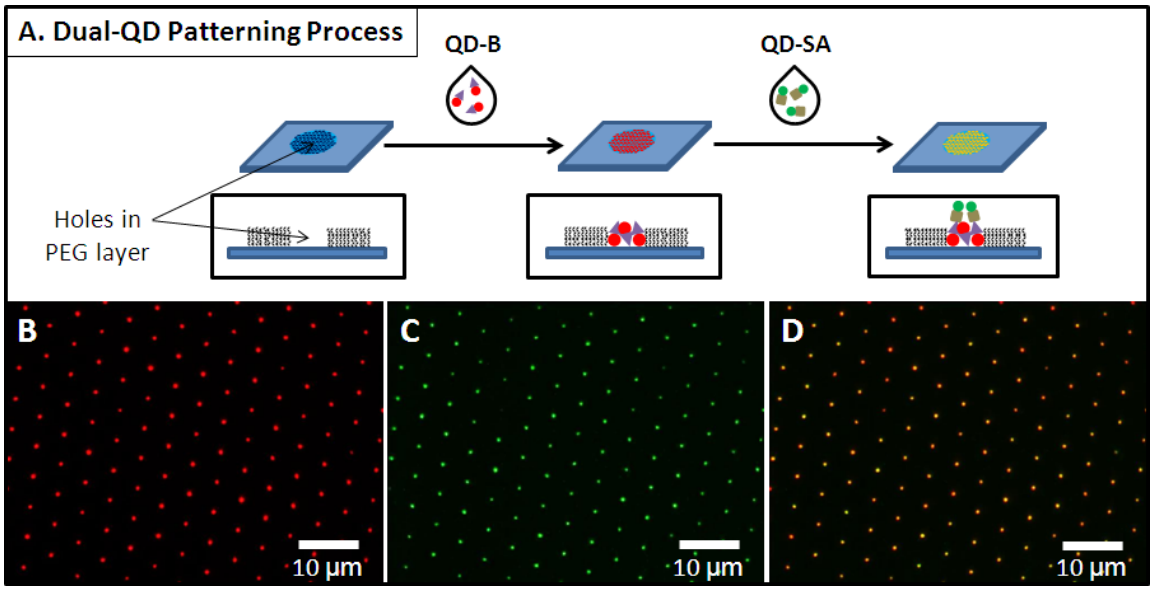

Figure 3.6: Fluorescent Images of a Colocalized Dual-QD Pattern. (A) Schematic of the formation of a dual-QDBC pattern of QD-SA colocalized with QD-B. (B, C) Images (pseudocolored post-acquisition) of the fluorescent signal from QD-B (B) and QD-SA (C) from the same area of a single substrate obtained by switching fluorescent filters.(D) Resulting image when (B) and (C) are combined.

biotin moieties of the biotin-IgG were specifically bound by the avidin. The QD-goat anti-mouse IgG was then deposited on the surface and specifically bound to sites on the protein portion of the IgG-biotin. Finally, the fluorescent intensity of the QDs was quantified. By using the same concentration of avidin and QD-IgG but varying the concentration of IgG-biotin for each sample, the amount of IgG-biotin that was bound

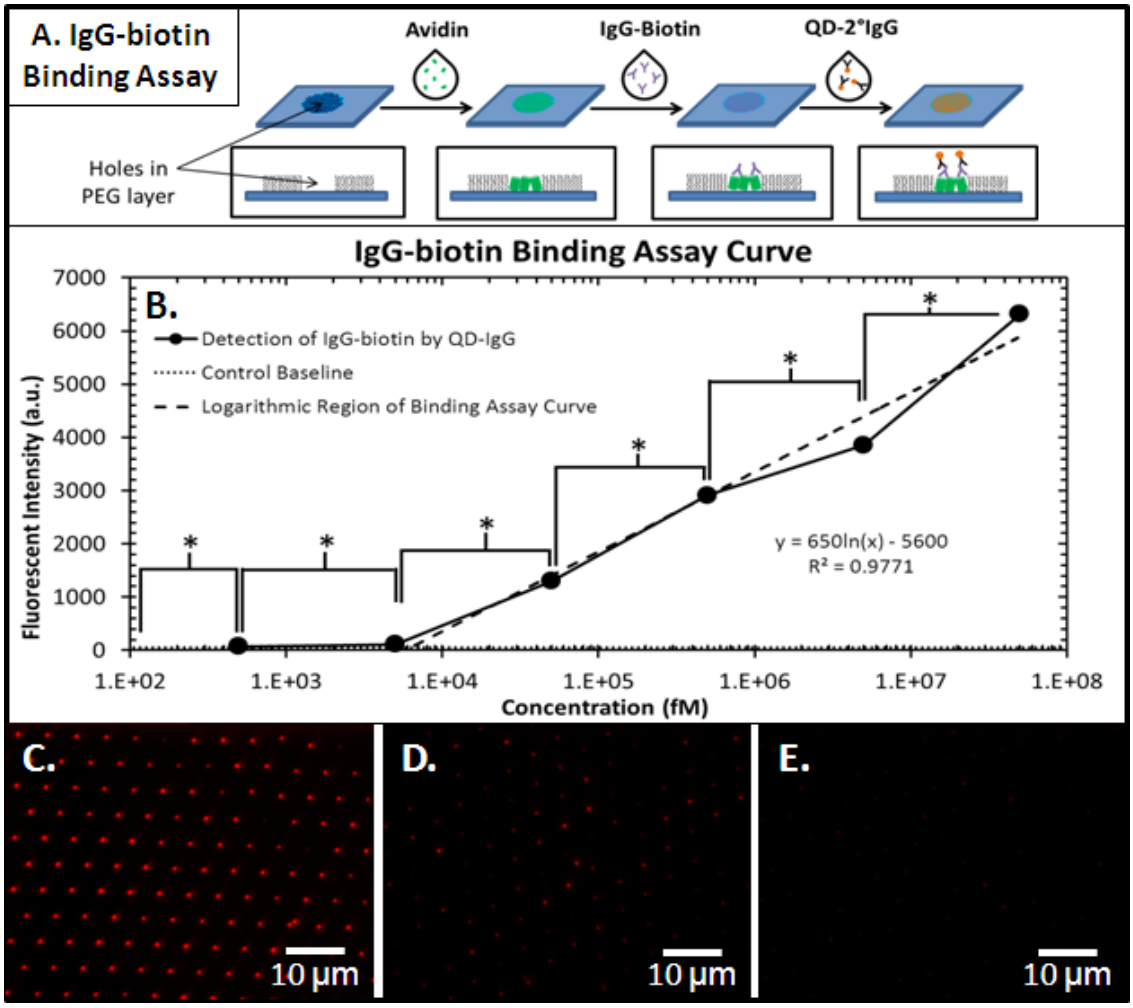

Figure 3.7: IgG-biotin Binding Assay Curve. (A) Schematic of the binding assay procedure. (B) Fluorescent intensity versus concentration graph for patterns made with various concentrations of IgG-biotin (500 fM to 50 nM). (C—E) Representative fluorescent images (pseudocolored post-acquisition) of patterns with 50 nM (C), 500 pM (D), and 5 pM (E) IgG-biotin. Data are shown as mean ± standard error of the mean (* $P < 0.001$).

to each sample was only dependent on the concentration of IgG-biotin used for each sample. Consequently, the amount of QD-IgG bound to each sample, and the intensity of the resulting fluorescent signal, also varied with IgG-biotin concentration.

We measured the fluorescent intensities of dot patterns made with IgG-biotin concentrations of 50 nM and 10-fold dilutions to 500 fM (Figure 3.7B). Between 50 nM and 5 pM, the curve follows a logarithmic trend with a coefficient of determination of $R^2 = 0.9771$. The average intensities for the concentrations investigated were each statistically significant from the intensities for the nearest higher and lower concentrations. Below 50 pM, the fluorescent intensities were relatively low. However, because this patterning technique allows for hundreds of redundant samples on a single substrate, the differences in intensities were statistically significant. Since only 75 µL of IgG-biotin solution is required per binding assay substrate (see Experimental Section), the mass of IgG-biotin detected was between 560 pg and 5.6 fg for 50 nM and 500 fM substrates, respectively. These data show that our QDBC patterning technique can be used to detect biological species over a concentration range of several orders of magnitude.

Conclusions

A simple, high throughput method of patterning QDBCs in sub-micrometer domains was developed. Substrates were patterned by forming a self-assembled monolayer of polystyrene spheres, grafting mPEG-sil to the substrate around the spheres, and then removing the spheres and adsorbing QDBCs into the sites previously occupied by the

spheres. To exhibit the versatility of this technique, we patterned QDs conjugated to biologically important small molecules, proteins, and antibodies. The diameters of the dots formed were 500-600 nm and independent of the QDBC adsorbed. Dual-QDBC patterns were created through specific interactions between biotin- and avidin-conjugated QDs. The applicability of this method was also demonstrated by designing a QD-based immunoassay with a detection limit in the femtomolar range. Based on these results we anticipate that this platform may be extended to a wide range of immunoassays. In addition, by changing the diameters of the spheres during monolayer formation, the spacing between and diameters of the resulting QDBC dots can be varied from the nanometer to micrometer scale, and be applied to a variety of cell adhesion and molecular interaction studies where patterns of fluorescent bioconjugates are required.

Acknowledgements

This work was supported by a National Science Foundation (NSF) Graduate Research Fellowship to Z.R.T, the Center for Semiconductor Physics in Nanostructures (C-SPIN), an OU/UA NSF-funded MRSEC (DMR-0520550), and by a grant from the Oklahoma Center for the Advancement of Science and Technology (HR06-102).

References

1. Gopal, A.; Hoshino, K.; Kim, S.; Zhang, X. Multi-color colloidal quantum dot based light emitting diodes micropatterned on silicon hole transporting layers. *Nanotechnology.* **2009**, *20*, 235201.

2. Robel, I.; Subramanian, V.; Kuno, M.; Kamat, P. V. Quantum Dot Solar Cells. Harvesting Light Energy with CdSe Nanocrystals Molecularly Linked to Mesoscopic TiO_2 Films. *J. Am. Chem. Soc.* **2006**, *128*, 2385-2393.

3. Clarke, S.; Pinaud, F.; Beutel, O.; You, C.; Piehler, J.; Dahan, M. Covalent Monofunctionalization of Peptide-Coated Quantum Dots for Single-Molecule Assays. *Nano Lett.* **2010**, *10*, 2147-2154.

4. Delehanty, J. B.; Medintz, I. L.; Pons, T.; Brunel, F. M.; Dawson, P. E.; Mattoussi, H. Self-Assembled Quantum Dot-Peptide Bioconjugates for Selective Intracellular Delivery. *Bioconjugate Chem.* **2006**, *17*, 920-927.

5. Liu, J.; Lau, S. K.; Varma, V. A.; Moffitt, R. A.; Caldwell, M.; Liu, T.; Young, A. N.; Petros, J. A.; Osunkoya, A. O.; Krogstad, T.; Leyland-Jones, B.; Wang, M. D.; Nie, S. Heterogeneity on Clinical Tissue Specimens with Multiplexed Quantum Dots. *ACS Nano.* **2010**, *4*, 2755-2765.

6. Nurunnabi, M.; Cho, K. J.; Choi, J. S.; Huh, K. M.; Lee, Y.-k. Targeted near-IR QDs-loaded micelles for cancer therapy and imaging. *Biomaterials.* **2010**, *31*, 5436-5444.

7. Park, J. W.; Park, A.-Y.; Lee, S.; Yu, N.-K.; Lee, S.-H.; Kaang, B.-K. Detection of TrkB Receptors Distributed in Cultured Hippocampal Neurons through Bioconjugation between Highly Luminescent (Quantum Dot-Neutravidin) and (Biotinylated Anti-TrkB Antibody) on Neurons by Combined Atomic Force Microscope and Confocal Laser Scanning Microscope. *Bioconjugate Chem.* **2010**, *21*, 597-603.

8. Jokerst, J. V.; Raamanathan, A.; Christodoulides, N.; Floriano, P. N.; Pollard, A. A.; Simmons, G. W.; Wong, J.; Gage, C.; Furmaga, W. B.; Redding, S. W.; McDevitt, J. T. Nano-bio-chips for high performance multiplexed protein detection: Determinations of cancer biomarkers in serum and saliva using quantum dot bioconjugate labels. *Biosens. Bioelectron.* **2009**, *24*, 3622-3629.

9. Kerman, K.; Endo, T.; Tsukamoto, M.; Chikae, M.; Takamura, Y.; Tamiya, E. Quantum dot-based immunosensor for the detection of prostate-specific antigen using fluorescence microscopy. *Talanta.* **2007**, *71*, 1494-1499.

10. Lee, M.-H.; Chen, Y.-C.; Ho, M.-H.; Lin, H.-Y. Optical recognition of salivary proteins by use of molecularly imprinted poly(ethylene-co-vinyl alcohol)/quantum dot composite nanoparticles. *Anal. Bioanal. Chem.* **2010**, *397*, 1457-1466.

11. Rauf, S.; Glidle, A.; Cooper, J. M. Application of quantum dot barcodes prepared using biological self-assembly to multiplexed immunoassays. *Chem. Commun.* **2010**, *46*, 2814-2816.

12. Eastman, P. S.; Ruan, W.; Doctolero, M.; Nuttall, R.; Feo, G. d.; Park, J. S.; Chu, J. S. F.; Cooke, P.; Gray, J. W.; Li, S.; Chen, F. F. Qdot Nanobarcodes for Multiplexed Gene Expression Analysis. *Nano Lett.* **2006**, *6*, 1059-1064.

13. Jiang, J.; Peng, Z.; Deng, L.; Li, G.; Chen, L. Detection of Bifidobacterium Species-specific 16S rDNA Based on QD FRET Bioprobe. *J. Fluoresc.* **2010**, *20*, 365-369.

14. Lee, J.; Kim, I. S.; Yu, H.-W. Flow Cytometric Detection of Bacillus spoOA Gene in Biofilm Using Quantum Dot Labeling. *Anal. Chem.* **2010**, *82*, 2836-2843.

15. Wang, X.; Lou, X.; Wang, Y.; Guo, Q.; Fang, Z.; Zhong, X.; Mao, H.; Jin, Q.; Wu, L.; Zhao, H.; Zhao, J. QDs-DNA nanosensor for the detection of hepatitis B virus DNA and the single-base mutants. *Biosens. Bioelectron.* **2010**, *25*, 1934-1940.

16. Zhang, H.; Xu, T.; Li, C.-W.; Yang, M. A microfluidic device with microbead array for sensitive virus detection and genotyping using quantum dots as fluorescence labels. *Biosens. Bioelectron.* **2010**, *25*, 2402-2407.

17. Bae, P. K.; So, H.-M.; Kim, K. N.; You, H. S.; Choi, K. S.; Kim, C. H.; Park, J.-K.; Lee, J.-O. Simple route for the detection of *Escherichia coli* using quantum dots *BioChip J.* **2010**, *4*, 129-133.

18. Su, X.-L.; Li, Y. Quantum Dot Biolabeling Coupled with Immunomagnetic Separation for Detection of Escherichia coli O157:H7. *Anal. Chem.* **2004**, *76*, 4806-4810.

19. Chen, H.; Li, R.; Lin, L.; Guo, G.; Lin, J.-M. Determination of l-ascorbic acid in human serum by chemiluminescence based on hydrogen peroxide–sodium hydrogen carbonate–CdSe/CdS quantum dots system. *Talanta.* **2010**, *81*, 1688-1696.

20. Chen, Y. P.; Ning, B.; Liu, N.; Feng, Y.; Liu, Z.; Liu, X.; Gao, Z. X. A rapid and sensitive fluoroimmunoassay based on quantum dot for the detection of chlorpyrifos residue in drinking water. *J. Environ. Sci. Health B.* **2010**, *45*, 508-515.

21. Chouhan, R. S.; Vinayaka, A. C.; Thakur, M. S. Thiol-stabilized luminescent CdTe quantum dot as biological fluorescent probe for sensitive detection of methyl parathion by a fluoroimmunochromatographic technique. *Anal. Bioanal. Chem.* **2010**, *397*, 1467-1475.

22. Frasco, M. F.; Vamvakaki, V.; Chaniotakis, N. Porphyrin decorated CdSe quantum dots for direct fluorescent sensing of metal ions. *J. Nanopart. Res.* **2010**, *12*, 1449-1458.

23. Ge, S.; Zhang, C.; Zhu, Y.; Yu, J.; Zhang, S. BSA activated CdTe quantum dot nanosensor for antimony ion detection. *Analyst.* **2009**, *135*, 111-115.

24. Hu, X.; Han, H.; Hua, L.; Sheng, Z. Electrogenerated chemiluminescence of blue emitting ZnSe quantum dots and its biosensing for hydrogen peroxide. *Biosens. Bioelectron.* **2010**, *25*, 1843-1846.

25. Liu, J.; Bao, C.; Zhong, X.; Zhao, C.; Zhu, L. Highly selective detection of glutathione using a quantum-dot-based OFF–ON fluorescent probe. *Chem. Commun.* **2010**, *46*, 2971-2973.

26. Peng, C.; Li, Z.; Zhu, Y.; Chen, W.; Yuan, Y.; Liu, L.; Li, Q.; Xu, D.; Qiao, R.; Wang, L.; Zhu, S.; Jin, Z.; Xu, C. Simultaneous and sensitive determination of multiplex chemical residues based on multicolor quantum dot probes. *Biosens. Bioelectron.* **2009**, *24*, 3657-3662.

27. Zou, Z.; Du, D.; Wang, J.; Smith, J. N.; Timchalk, C.; Li, Y.; Lin, Y. Quantum Dot-Based Immunochromatographic Fluorescent Biosensor for Biomonitoring Trichloropyridinol, a Biomarker of Exposure to Chlorpyrifos. *Anal. Chem.* **2010**, *82*, 5125-5133.

28. Biju, V.; Itoh, T.; Anas, A.; Sujith, A.; Ishikawa, M. Semiconductor quantum dots and metal nanoparticles: syntheses, optical properties, and biological applications. *Anal. Bioanal. Chem.* **2008**, *391*, 2469-2495.

29. Han, C.; Li, H. Host-molecule-coated quantum dots as fluorescent sensors. *Anal. Bioanal. Chem.* **2010**, *397*, 1437-144.

30. Yu, W. W.; Chang, E.; Drezek, R.; Colvin, V. L. Water-soluble quantum dots for biomedical applications. *Biochem. Biophys. Res. Commun.* **2006**, *348*, 781-786.

31. Yoffe, A. D. Semiconductor quantum dots and related systems: electronic, optical, luminescence and related properties of low dimensional systems. *Adv. Phys.* **2001**, *50*, 1-208.

32. Valsesia, A.; Colpo, P.; Manneill, I.; Mornet, S.; Bretagnol, F.; Ceccone, G.; Rossi, F. Use of nanopatterned surfaces to enhance immunoreaction efficiency. *Anal. Chem.* **2008**, *80*, 1418-1424.

33. Agheli, H.; Malmström, J.; Larsson, E. M.; Textor, M.; Sutherland, D. S. Large Area Protein Nanopatterning for Biological Applications. *Nano Lett.* **2006**, *6*, 1165-1171.

34. Lisboa, P.; Valsesia, A.; Mannelli, I.; Mornet, S.; Colpo, P.; Rossi, F. Sensitivity enhancement of surface-plasmon resonance imaging by nanoarrayed organothiols. *Adv. Mater.* **2008**, *20*, 2352-2358.

35. Gokarna, A.; Jin, L.-H.; Hwang, J. S.; Cho, Y.-H.; Lim, Y. T.; Chung, B. H.; Youn, S. H.; Choi, D. S.; Lim, J. H. Quantum dot-based protein micro- and nanoarrays for detection of prostate cancer biomarkers. *Proteomics.* **2008**, *8*, 1809-1818.

36. Mark, S. S.; Bergkvist, M.; Yang, X.; Teixeira, L. M.; Bhatnagar, P.; Angert, E. R.; Batt, C. A. Bionanofabrication of Metallic and Semiconductor Nanoparticle Arrays Using S-Layer Protein Lattices with Different Lateral Spacings and Geometries. *Langmuir.* **2006**, *22*, 3763-3774.

37. Rakickas, T.; Gavutis, M.; Reichel, A.; Piehler, J.; Liedberg, B.; Valiokas, R. Protein-Protein Interactions in Reversibly Assembled Nanopatterns. *Nano Lett.* **2008**, *8*, 3369-3375.

38. Shallcross, R. C.; Chawla, G. S.; Marikkar, F. S.; Tolbert, S.; Pyun, J.; Armstrong, N. R. Efficient CdSe Nanocrystal Diffraction Gratings Prepared by Microcontact Molding. *ACS Nano.* **2009**, *3*, 3629-3637.

39. Hoa, X. D.; Martinb, M.; Jimenezb, A.; Beauvais, J.; Charetteb, P.; Kirk, A.; Tabriziana, M. Fabrication and characterization of patterned immobilization of quantum dots on metallic nano-gratings. *Biosens. Bioelectron.* **2008**, *24*, 970-975.

40. Son, J. G.; Bae, W. K.; Kang, H.; Nealey, P. F.; Char, K. Placement Control of Nanomaterial Arrays on the Surface-Reconstructed Block Copolymer Thin Films. *ACS Nano.* **2009**, *3*, 3927-3934.

41. Hampton, M. J.; Templeton, J. L.; DeSimone, J. M. Direct Patterning of CdSe Quantum Dots into Sub-100 nm Structures. *Langmuir.* **2010**, *26*, 3012-3015.

42. Chen, J.; Liao, W.-S.; Chen, X.; Yang, T.; Wark, S. E.; Son, D. H.; Batteas, J. D.; Cremer, P. S. Evaporation-Induced Assembly of Quantum Dots into Nanorings. *ACS Nano.* **2009**, *3*, 173-180.

43. Lewandowski, B. R.; Kelley, A. T.; Singleton, R.; Li, J.-R.; Lowry, M.; Warner, I. M.; Garno, J. C. Nanostructures of Cysteine-Coated CdS Nanoparticles Produced with "Two-Particle" Lithography. *J. Phys. Chem. C.* **2009**, *113*, 5933-5940.

44. Gopal, A.; Hoshino, K.; Zhang, X. Photolithographic patterning of subwavelength top emitting colloidal quantum dot based inorganic light emitting diodes on silicon. *Appl. Phys. Lett.* **2010**, *96*, 131109.

45. Kramer, R. K.; Pholchai, N.; Sorger, V. J.; Yim, T. J.; Oulton, R.; Zhang, X. Positioning of quantum dots on metallic nanostructures. *Nanotechnology.* **2010**, *21*, 145307.

46. Marquez, M.; Patel, K.; Carswell, A. D. W.; Schmidtke, D. W.; Grady, B. P. Synthesis of Nanometer-Scale Polymeric Structures on Surfaces from Template Assisted Admicellar Polymerization: A Comparative Study with Protein Adsorption. *Langmuir.* **2006**, *22*, 8010-8016.

47. Taylor, Z. R.; Patel, K.; Spain, T. G.; Keay, J. C.; Jernigen, J. D.; Sanchez, E. S.; Grady, B. P.; Johnson, M. B.; Schmidtke, D. W. Fabrication of Protein Dot Arrays via Particle Lithography. *Langmuir.* **2009**, *25*, 10932-10938.

48. Kaul, Z.; Yaguchi, T.; Kaul, S. C.; Hirano, T.; Wadhwa, R.; Taira, K. Mortalin imaging in normal and cancer cells with quantum dot immuno-conjugates. *Cell Res.* **2003**, *13*, 503-507.

49. Pattani, V. P.; Li, C.; Desai, T. A.; Vu, T. Q. Microcontact printing of quantum dot bioconjugate arrays for localized capture and detection of biomolecules. *Biomed. Microdevices.* **2008**, *10*, 367-374.

Chapter 4: Independently Controlling Protein Dot Size and Spacing in Particle Lithography

This chapter was reproduced in part with permission from *Langmuir*, submitted for publication.

Unpublished work copyright 2012 American Chemical Society.

Introduction

Protein patterns with micro- and nanometer scale features have been fabricated by a number of different techniques, including microfluidic patterning,[1-3] photolithography,[4-6] electron-beam lithography (EBL),[7,8] microcontact printing (μCP),[9-11] dip-pen nanolithography (DPN),[12,13] and particle lithography.[14-19] There are several factors to consider when choosing a technique for a specific application, including desired feature size and geometry, cost, processing time, and accessibility. Particle lithography is an attractive option to pattern protein because it relies on low cost, bench-top technology with the ability to produce nano-structured samples in parallel.

Although particle lithography has several advantages, the process is not without limitations. The area of the contact point between a spherical particle and the underlying substrate, which eventually defines each protein-attractive or repellant region, is determined by the diameter of the sphere. For close-packed colloidal masks, the diameter of the spheres also fixes the center-to-center distance between the contact points. Consequently, the area of protein-attractive or repellant regions and the center-

to-center distance between those regions change simultaneously when the diameter of the spheres is altered.

In order to independently control the size and center-to-center spacing of protein pattern features, colloidal masks have been altered by etching and heat treatment techniques. To reduce feature size, reactive ion etching (RIE) has been utilized to shrink spheres before using them as a lithographic mask.[16,20,21] Alternatively, to increase feature size, Agheli et al. used a modification of the heat treatment procedure developed by Hanarp et al.[22,23] After deposition, spheres were heated above their glass transition temperature (approximately 100 °C)[24] to produce deformation and thus increase their contact area with the underlying substrate. However, neither group investigated the increase in feature size as a function of temperature. Furthermore, the colloidal masks used were dispersed rather than close-packed, which eliminated the effects of sphere to sphere contact during deformation.

In this work, we present a new heating technique to independently control the size and center-to-center spacing of features produced with close-packed colloidal masks. Monolayers of 10 μm spheres were heated at various temperatures to create protein dots with uniform diameters of approximately 2 – 8 μm. Using differential heating, protein patterns were made with a continuous gradient of dot sizes of approximately 1 – 9 μm. Finally, we demonstrate the utility of these protein patterns by observing the effect of protein patch geometry on the spreading of human neutrophils.

Experimental Section

Chemicals and Materials. Polystyrene latex spheres (10 μm mean diameter) were purchased from Duke Scientific (Fremont, CA) and washed once in DI water by centrifugation before use. Poly(dimethylsiloxane) (PDMS; Sylgard-184, Dow-Corning) was purchased from Krayden (Marlborough, MA). Alexa Fluor 488 fibrinogen and Qdot 655 goat $F(ab')_2$ anti-mouse IgG (QD-IgG) were purchased from Invitrogen (Carlsbad, CA). Human serum albumin (HSA) was purchased from Gemini Bio-Products (West Sacramento, CA). Methoxy-poly(ethylene glycol)-silane (mPEG-sil; MW=5000) was purchased from Laysan Bio (Arab, AL). Finally, mouse anti-human P-selectin glycoprotein ligand-1 (PSGL-1) (PL1 antibody), mouse anti-human CD3, the Src tyrosine kinase inhibitor PP2, and its inactive analogue PP3, were generously provided by Dr. Rodger P. McEver's group at the Oklahoma Medical Research Foundation.

Single Protein Dot Size Substrate Preparation. Periodic patterns of protein dots were formed using a modified version of our previously described protocols (Figure 4.1).[18,19] Briefly, glass slides were cleaned in trichloroethylene, acetone, methanol, and DI water in sequential, two-minute cycles in an ultrasonic cleaner. After drying the slides under a stream of nitrogen, a PDMS mold with a 4.5 mm diameter circular hole cut from the center was placed on the surface of each slide. The substrates were then exposed to an air-plasma (Harrick Scientific Corp, model PDC-32G, Ithaca, NY) at 400 mTorr and "low" power (0.010 W/cm^3) for 30 s. After plasma treatment, the PDMS molds were removed, and the substrates were left untouched for approximately 30 min.

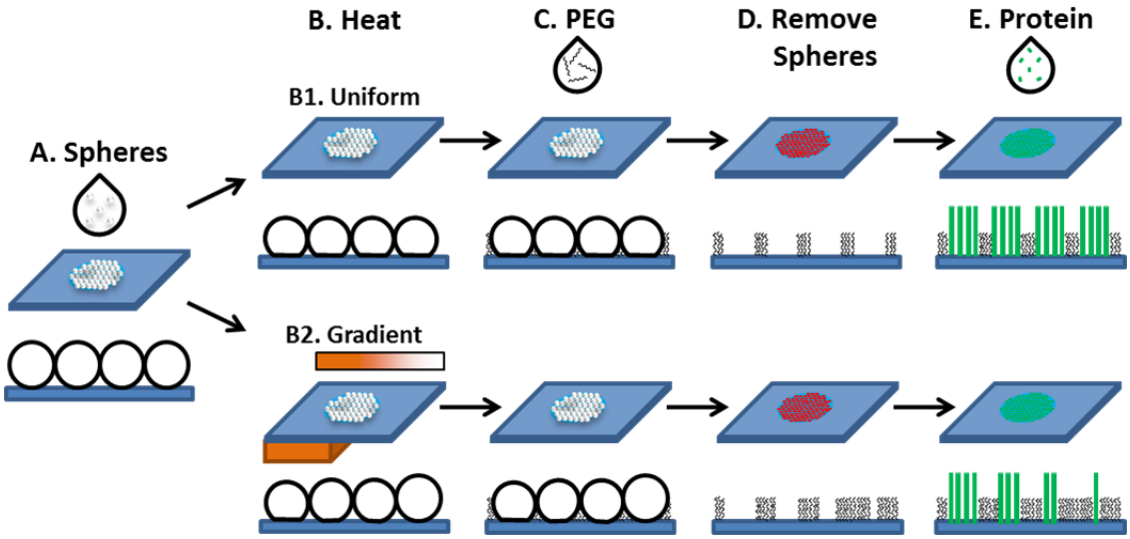

Figure 4.1: Schematic of the Protein Patterning Procedure. A periodic pattern of protein dots is formed using a modified version of our previously described protocols.[18,19] (A) A drop of polystyrene sphere suspension is deposited on a glass slide. As the solvent evaporates, a sphere monolayer is formed. (B) The spheres are deformed by exposing the monolayer to either a uniform temperature (B1) or a temperature gradient (B2). (C) A protein-repellant mPEG-sil is covalently grafted to the glass surface around the spheres. (D) The spheres are removed to reveal protein adsorption sites in an mPEG-sil background. (E) A protein solution is deposited on the mPEG-sil patterned surface, and the protein selectively adsorbs to the bare glass in the PEG holes.

To form sphere monolayers, 12.7 µL of 0.67% wt 10 µm sphere suspension was deposited on the patterned region of each substrate and was allowed to dry in ambient conditions overnight. After monolayer formation, the substrates were heated at 80 °C for 30 min to promote firm adhesion of the spheres to the surface. Next, the substrates were soaked for 5 min in DI water to remove residue from the sphere suspension and then allowed to dry for 1 hr in ambient conditions. After drying, the substrates were placed in a laboratory oven (Shel Lab, model 1415M, Cornelius, OR) at 105, 115, 125, or 135 °C for 60 min. After heating, mPEG-sil was grafted to the substrates around the spheres by first exposing the substrates to an air-plasma at 400 mTorr and "high" power (0.027 W/cm^3) for 1 min and then immediately applying 375 µL of 4 mM mPEG-sil in

anhydrous acetonitrile to the substrates. The grafting was allowed to proceed overnight at room temperature. Next, ungrafted PEG was removed by soaking the substrates in three consecutive Petri dishes full of anhydrous acetonitrile for 5 min each. The substrates were then washed with approximately 50 mL DI water using a wash bottle to remove the spheres and reveal the hexagonal pattern of holes in the PEG layer. These holes then served as adsorption sites for fluorescent protein. Alexa Fluor 488 fibrinogen was dissolved in HBSS at a concentration of 20 μg/mL and was dispensed on the PEG-patterned surfaces for 2 hr. Following incubation, the substrates were first rinsed with 25 mL HBSS using a transfer pipette and then with 50 mL of DI water using a wash bottle to remove any unbound protein.

Gradient Protein Dot Size Substrate Preparation. Substrates with a gradient of protein dot sizes were made using the same procedure for single protein dot size substrates but with a custom differential heating setup instead of a laboratory oven (Figure 4.1B2). After the DI water soak and dry, the substrates were held on a ¾" x ¾" stainless steel vacuum chuck using vacuum and two stainless steel wire clips (0.030" diameter). The chuck was heated using a cartridge heater controlled by a variac and the chuck temperature measured using a type-K thermocouple spot welded to the vacuum chuck sidewall. Differential heating of samples was achieved by placing a sample with the patterned region half on the heated surface and the other half free standing in air. Substrates were heated for 30 min at a chuck temperature of 150 °C. After the substrates cooled, the PEG-grafting and protein adsorption steps were completed as described for substrates with single protein dot sizes.

Human Neutrophil Isolation. Peripheral whole blood was obtained by venipuncture from donors via a syringe containing heparin (20 USP units / mL blood to be collected). Collected blood was layered on top of an equal volume of Lympholyte-poly Cell Separation Media (Cedarlane Labs, Burlington, NC) and was centrifuged for 30 min at 650 x g. After centrifugation, the polymorphonuclear cell band was transferred to a new centrifuge tube, diluted with an equal volume of 0.4% sodium chloride, and further diluted with two volumes of HBSS to restore normal osmolarity. The resulting cell suspension was centrifuged for 10 min at 650 x g. After discarding the supernatant, remaining red blood cells were lysed by adding 10 mL 0.2% sodium chloride, quickly inverting to mix, and then adding 10 mL 1.6% sodium chloride. The suspension was centrifuged for 5 min at 650 x g, the supernatant was discarded, and the cells were resuspended in 5 mL 0.5% HSA in HBSS. The cells were washed three times by centrifugation (5 min at 650 x g in 5 mL 0.5% HSA in HBSS), counted, and resuspended at 10^6 cells / mL in 0.5% HSA in HBSS. For experiments involving an inhibitor, PP2 or PP3 was added to the isolated cells to a final concentration of 10 μM, and the cells were allowed to incubate with the inhibitor at least 30 min before use. The blood collection protocol was approved by the Institutional Review Board of the University of Oklahoma, and informed consent was obtained from all donors.

Neutrophil Spreading Experiments. Single dot size PEG-patterned substrates were created as described above using spheres heated to 135 °C for 60 min. Next, QD-IgG stock solution was centrifuged for 5 min at 2200 x g to remove any aggregates formed during storage. The supernatant was removed, diluted to 50 nM in PBS, and dispensed

on the PEG-patterned surfaces. After incubating 3 hr at room temperature, the substrates were washed with approximately 50 mL PBS using a laboratory wash bottle to remove any unbound QD-IgG. Next, 20 μg/mL PL1 antibody in PBS was dispensed on the patterned surfaces. After incubating 1 hr at room temperature, the slides were washed with 25 mL PBS using a transfer pipette to remove any unbound antibody. Finally, the slides were coated with 0.5% HSA for at least 1 hr to block any remaining adsorption sites. A parallel plate flow chamber (GlycoTech, Gaithersburg, MD) was attached by vacuum to a spreading experiment substrate. Isolated neutrophils were pulled into the chamber at a shear rate of 500 s^{-1} and were allowed to settle onto the patterned surface under static conditions. Cellular interactions were recorded directly to video in real time for up to 30 min.

Substrate Characterization. Fluorescent and differential interference contrast (DIC) images and video of spreading cells and protein dot patterns were acquired with a Zeiss Axiovert 200 inverted microscope equipped with a 100X objective (NA = 1.3) as previously described.[19,25] In cell spreading experiments, the same setup was used to perform interference reflection microscopy (IRM) to visualize the dynamic adhesive interactions of neutrophils with the protein-coated substrates. Interference reflection microscopy is a well-established technique used to image close apposition (< 100 nm) between cells and surfaces.[26,27] IRM is based upon the destructive and constructive interference patterns that are generated from light reflected from the substrate-buffer interface with light reflected from the buffer-cell interface. In regions where the cell adheres to the substrate or is in close contact (~10-15 nm), the light waves reflected

from the substrate buffer and buffer-cell interfaces cancel each other out, which produces the darkest (black) regions in the image. As the distance between the cell membrane and the substrate increases, the interference effect becomes attenuated with more distant regions appearing dark grey (~30-40 nm) or white (~100 nm).[28,29] Consequently, IRM can be used to visualize the adhesion patterns or "footprint" of cells with substrates. A CoolSnap cf digital camera was used to capture still images, and a Dage-MTI CCD-300T-RC camera was used to capture video**.**

Image Analysis. Image analysis was performed with the open source software package ImageJ (version 1.40g), and video was analyzed using MetaMorph Imaging Software. To determine fluorescent protein dot sizes, images were first thresholded to create a binary image of black fluorescent protein dots and white background. The thresholding criteria were optimized and remained constant for each image analyzed. Next, the areas of each fluorescent protein dot were measured. Finally, the area measurements were used to calculate the diameters of the fluorescent protein dots with the assumption they were circular.

Calculations and Statistics. Values are presented as means ± standard deviation of the mean unless otherwise specified. All experiments except the protein dot gradient patterning were performed on at least three different samples each made on different days.

Results and Discussion

Protein dot patterns with independently controlled dot diameters and center-to-center spacing were formed via particle lithography by a five-step process (Figure 4.1): (1) formation of a polystyrene sphere monolayer, (2) deformation heating of the sphere

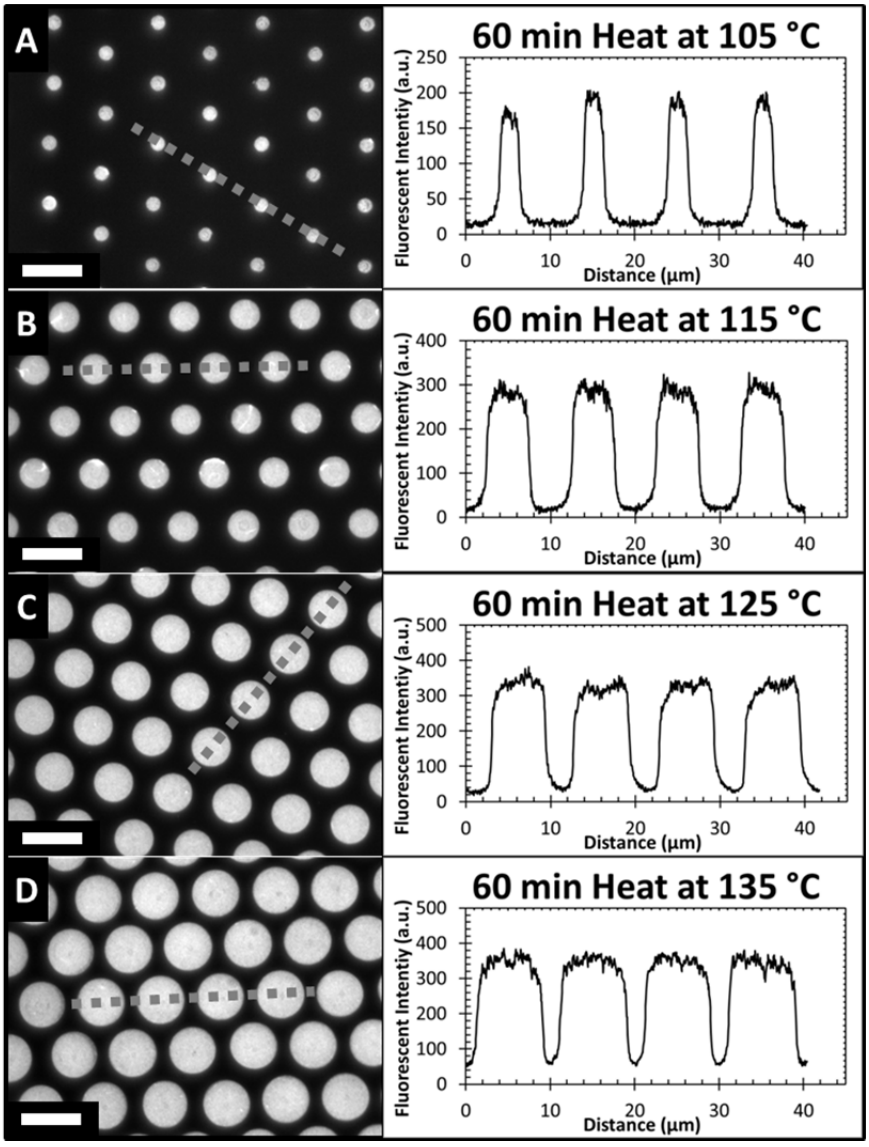

Figure 4.2: Fluorescent Images of Protein Dot Patterns. Fluorescent fibrinogen patterns made via particle lithography using 10 μm spheres heated to (A) 105 °C, (B) 115 °C, (C) 125 °C, and (D) 135 °C. The fluorescent line intensity (arbitrary units) graphs to the right of each image correspond to the dashed lines in each image. All scale bars are 10 μm.

monolayer, (3) grafting of a protein-repellant methoxy-poly(ethylene glycol)-silane (mPEG-sil) layer, (4) removal of the sphere monolayer, and (5) selective adsorption of protein into the resulting mPEG-sil holes.

Protein Dot Diameters Are Dependent On Deformation Heating Temperature. Figure 4.2 shows representative images of protein dots formed with fluorescent fibrinogen. The sharp transitions between fluorescing and non-fluorescing regions in the accompanying fluorescent line intensity graphs suggest that the protein selectively adsorbs into the holes in the PEG layer. The diameters of the protein dots varied approximately linearly with the deformation heating temperature for sphere monolayers heated for 60 min (Figure 4.3). Initially, other heating times were also attempted, but shorter heating times generated larger variations in protein dot diameters, while longer heating times did not produce a significant improvement in dot size variation (data not shown). We hypothesize that relatively long deformation heating times yield smaller variations in protein dot diameter by minimizing the effects of fluctuations in temperature and slight differences in sample loading and unloading times. The data from the optimized heating time demonstrate the reproducibility of the patterning procedure.

Deformation Heating Can Be Used to Create Uniform or Gradient Protein Dot Patterns. Figure 4.4 shows representative fluorescent images and the relationship between protein dot diameters and monolayer position for a sample differentially heated at 150 °C for 30 min. The differential heating produced three distinct regions of protein dot diameters. The spheres on the left side of the sample, which were in direct contact

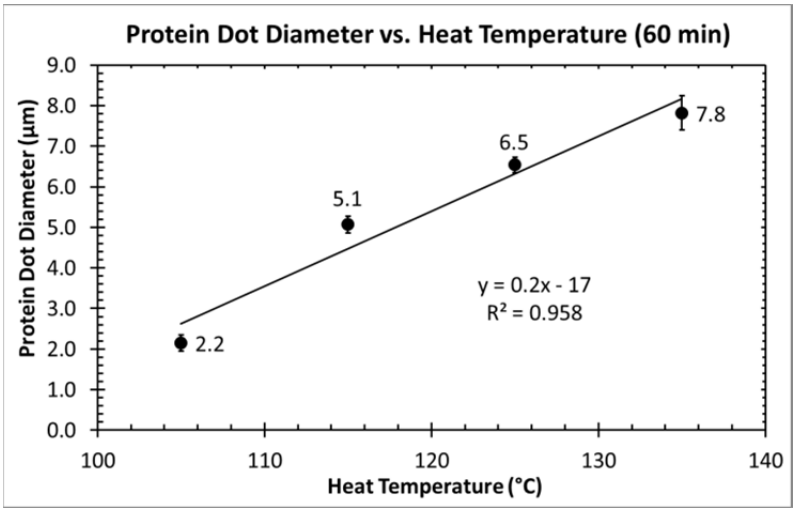

Figure 4.3: Relationship Between Protein Dot Diameter and Heat Temperature. Fluorescent protein dots created using 10 µm spheres heated for 60 min at 105 – 135 °C were measured using ImageJ software. Data is shown as mean ± standard error of the mean.

with the heat source, deformed enough to completely cover the substrate. Consequently, the PEG could not graft to the underlying glass, and protein was allowed to adsorb homogenously across the surface. This is represented in the graph as protein dots with diameters equivalent to their center-to-center spacing of 10 µm. At approximately 1.8 mm from the monolayer's left edge, sphere deformation decreased to a threshold that allowed individual dots to be resolved, and their diameters decreased linearly with increasing distance from the heat source. Finally, at the far right of the sample, the protein dot diameters stabilized at approximately 1.2 µm, which agrees well with our previous measurements of protein dots made using unheated 10 µm sphere monolayers. The data demonstrate the ability of the patterning technique to produce samples with single or multiple protein dot diameters.

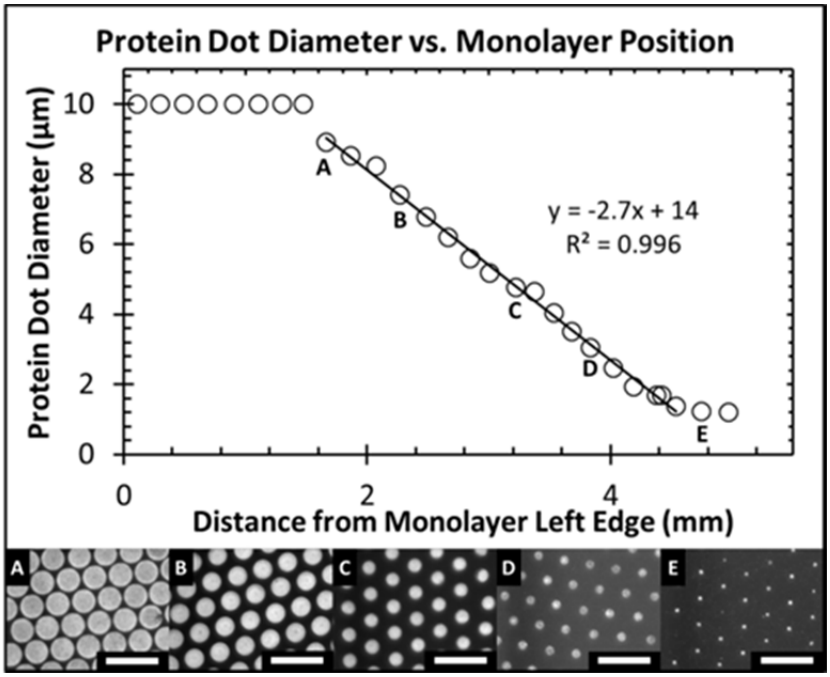

Figure 4.4: Diameter Measurements and Fluorescent Images of Protein Dots Formed Using Gradient Heating. Fluorescent fibrinogen dots formed using 10 μm spheres exposed to a temperature gradient were measured using ImageJ software. The thermal gradient was created by attaching the left half of the sample to a heated microscope stage at 150 °C, while the right half was freestanding in air (Figure 1B2). The labeled data points on the graph correspond to the fluorescent images of areas with dot diameters of approximately (A) 9 μm, (B) 7 μm, (C) 5 μm, (D) 3 μm, and (E) 1 μm. Data points with a value of 10 μm indicate areas of continuous protein coverage. All scale bars are 20 μm.

Neutrophils Spread on Immobilized PL1 Under Static Conditions. Although particle lithography has previously been used to generate protein patterns, to our knowledge, those patterns have not been used to investigate cell adhesion. We used our particle lithography technique to produce neutrophil adhesion substrates by capturing mouse anti-human monoclonal antibody (PL1) to P-selectin glycoprotein ligand-1 (PSGL-1) with adsorbed quantum dots conjugated to goat anti-mouse IgG (QD-IgG). Neutrophil adhesive interactions with QD-IgG/PL1 coated substrates were monitored by nearly-simultaneous (switching time of ~ 1 s) IRM and DIC imaging (Figure 4.5). When isolated neutrophils were allowed to settle on substrates coated with unpatterned

QD-IgG/PL1, the PSGL-1 constitutively expressed on the neutrophil cell membranes was bound by the PL1, and neutrophil spreading was observed (Figure 4.5A). Since the substrate was homogenously coated with ligand, the neutrophil spread relatively evenly in all directions. After five minutes, the neutrophil had spread completely, which is evidenced by its flat appearance in the final DIC image and the lack of bright areas in the final IRM image. To our knowledge, neutrophil spreading on immobilized PL1 has not previously been documented, but this response is not surprising since the role of PSGL-1 as a signaling molecule has been well established. PSGL-1 mediated signaling during rolling interactions with either P-selectin or E-selectin has been reported to induce integrin activation and slow rolling.[30-33] Similarly, several groups have observed that cross-linking PSGL-1 to antibodies induces activation.[34-36]

Neutrophil spreading on PL1 is Src-dependent. In order to determine the mechanism of neutrophil spreading on immobilized PL1, several control experiments were performed. Neutrophils were allowed to settle on surfaces coated with QD-IgG but without any bound PL1 or other primary antibody. No spreading was observed, which indicates that spreading on QD-IgG/PL1 coated surfaces was not due to the QDs or their conjugated $F(ab')_2$ fragments. Likewise, neutrophils also did not spread on surfaces coated with QD-IgG with bound mouse anti-human CD3. Since neutrophils do not express CD3, these results indicate that neutrophil spreading on QD-IgG/PL1 was not due to the presence of a primary antibody in general but required the specific interaction between PSGL-1 and PL1. PSGL-1 engagement to E-selectin has previously been shown to induce signaling through the Src-family kinases.[37] To investigate whether the

Src-family kinases are involved in neutrophil spreading on PL1, neutrophils were pretreated with PP2 or PP3 before exposure to QD-IgG/PL1 coated surfaces. PP2 is a selective Src-family kinase inhibitor, and PP3 is a nonfunctional molecule structurally similar to PP2 that is used as a PP2 negative control. The addition of PP2 abolished neutrophil spreading while the addition of PP3 did not affect neutrophil spreading. These results indicate neutrophil spreading on immobilized PL1 is induced by Src-dependent signaling through the interaction of PSGL-1 and PL1.

Neutrophil Adhesion is Limited to Protein Dots on Patterned Substrates. To investigate whether neutrophil spreading would be affected by the spatial presentation of PL1, we performed similar experiments with neutrophils on dot patterns of QD-IgG/PL1. Figure 4.5B and Figure 4.5C show representative images of neutrophils spreading on QD-IgG dots with and without bound PL1, respectively. The diameters of the dots in both patterns are approximately 8 μm with a center-to-center spacing of 10 μm. After 10 min, the neutrophil settled on the substrate without PL1 (Figure 5C) showed no spreading, which indicates that PL1 and not the QD-IgG was responsible for neutrophil spreading as previously discussed. The neutrophil that settled on the QD-IgG pattern with PL1 (Figure 4.5B) spread asymmetrically with adhesion initially limited to four protein dots immediately accessible to the cell. After fully covering the four dots by t = 5 min, the neutrophil began probing the surrounding area by repeatedly extending and retracting areas of the neutrophil membrane. Through this process, the neutrophil eventually made contact with a fifth protein dot. The neutrophil only spread thinly enough to partially cover the final dot, and there was no observable change after t = 20

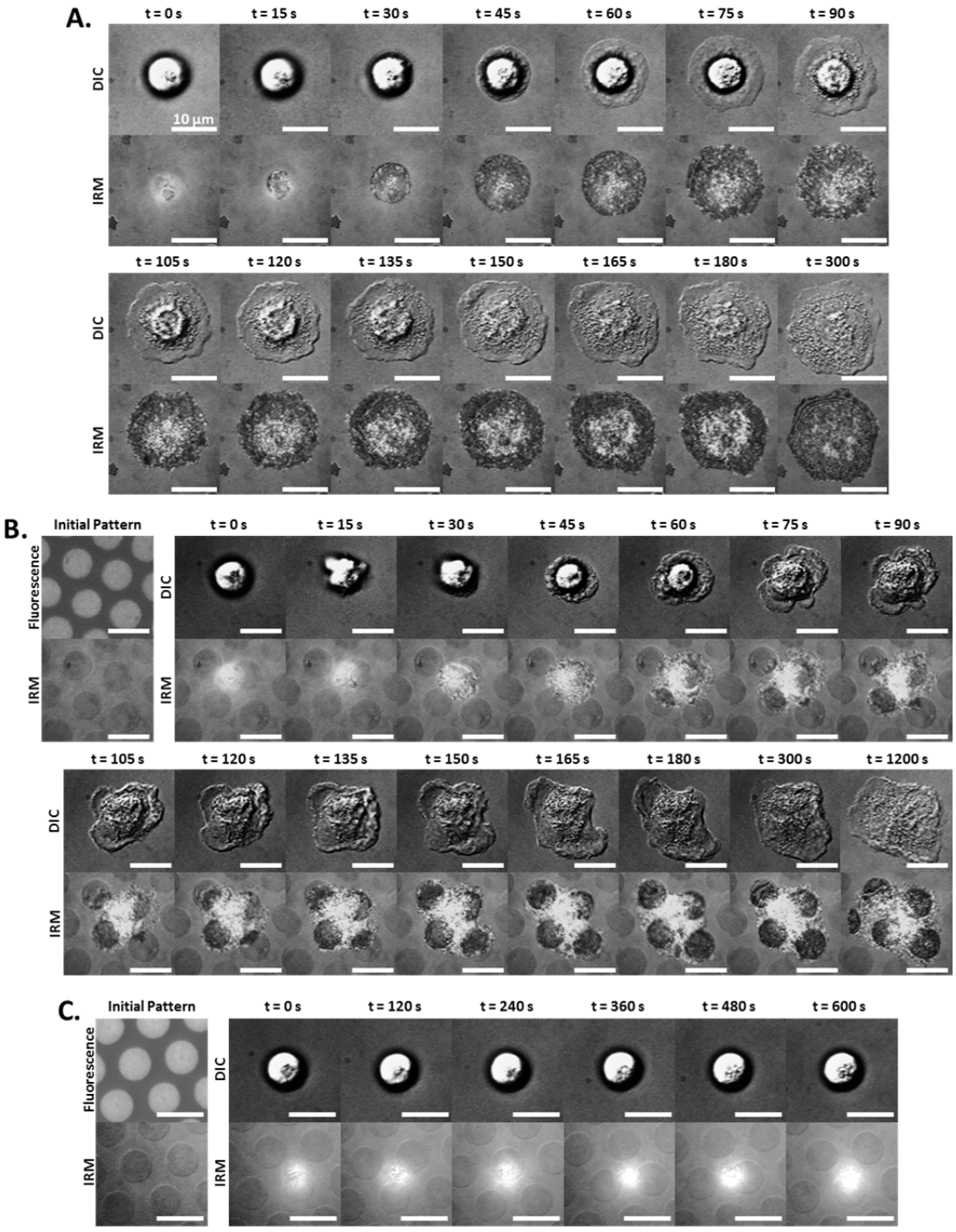

Figure 4.5: Neutrophil Spreading on PL1. Isolated neutrophils were allowed to settle on cell adhesion substrates coated with QD-IgG and PL1 (A – homogeneously coated, B – patterned) or QD-IgG only (C – patterned). Protein patterns and cellular interactions were recorded to video using IRM, DIC microscopy, and fluorescent microscopy, and still images were captured from the video using MetaMorph Imaging Software. Patterned substrates (B,C) were created with 10 µm spheres heated to 135 °C for 60 min. All scale bars are 10 µm.

min. Throughout the spreading experiment, IRM imaging showed the neutrophil was only in close contact with the substrate in the QD-IgG/PL1 coated areas. These results indicate that neutrophil adhesion to a substrate can be controlled using our protein patterning technique.

Areas of Continuous Neutrophil Coverage Can Be Created with Multiple Cell Perfusions. When only a single perfusion of neutrophils was used for adhesion experiments, only part of the patterned area was eventually covered by spread neutrophils. However, when multiple cycles of perfusing new neutrophils and pausing the flow to let them settle were used on a single substrate, areas of continuous spread-neutrophil coverage could be created. Figure 6 shows a set of representative DIC, IRM, and fluorescent images of an area almost completely covered by spread neutrophils. The dashed circle in each image emphasizes the only full-dot break in the coverage. The uncovered dot is visible in the IRM image and has the highest intensity in the fluorescent image, which is likely because it is not covered by a spread neutrophil.

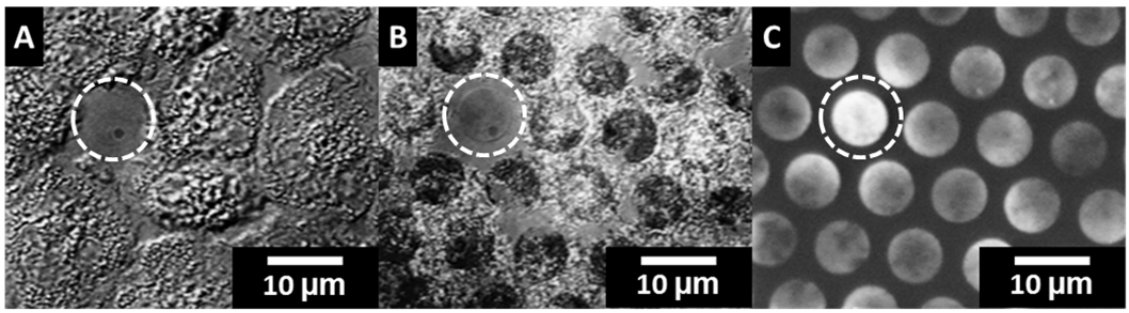

Figure 4.6: Continuous Layer of Neutrophils on QD-IgG/PL1 Dots. (A) DIC, (B) IRM, and (C) fluorescent images of neutrophils spreading on patterned QD-IgG and PL1. The circle in each image outlines the only dot that is not covered by spread neutrophil. The substrate was created by infusing cells several times over a patterned substrate fabricated using 10 µm spheres heated to 135 °C for 60 min

These results show the capability of our technique to vary the density of spread neutrophils on patterned substrates.

Conclusions

A simple method to independently control protein dot diameters and center-to-center spacing in protein patterns fabricated via particle lithography was developed. The patterns were made by forming a monolayer of polystyrene spheres, heating the spheres to various levels of deformation, grafting a layer of protein-repellant mPEG-sil around the spheres, and then adsorbing protein into the holes created by sphere removal. The versatility of our technique was demonstrated by using 10 μm spheres to create single-diameter dot patterns of approximately 2 – 8 μm and gradient dot patterns with a continuum of dot diameters between those produced by an unheated sphere monolayer (approximately 1 μm) and a melted sphere monolayer (homogenous protein coverage). We demonstrated one application of our patterning method by controlling the adhesion of human neutrophils in a static spreading assay. We anticipate this technique could be extended to include more protein dot diameters and center-to-center spacings as well as new cell lines and adhesion types (i.e., rolling under shear).

Acknowledgements

This work was supported by a National Science Foundation (NSF) Graduate Research Fellowship to Z.R.T, the Center for Semiconductor Physics in Nanostructures (C-SPIN), and an OU/UA NSF-funded MRSEC (DMR-0520550). We would like to thank Dr. Rodger P. McEver and Dr. Tadayuki Yago at the Oklahoma Medical Research

Foundation for assisting in the spreading assay design and for kindly supplying PL1 antibody, anti-CD3 antibody, PP2, and PP3.

References

1. Neeves, K. B.; Maloney, S. F.; Fong, K. P.; Schmaier, A. A.; Kahn, M. L.; Brass, L. F.; Diamond, S. L. Microfluidic focal thrombosis model for measuring murine platelet deposition and stability: PAR4 signaling enhances shear-resistance of platelet aggregates. *J. Thromb. Haemost.* **2008**, *6*, 2193-2201.

2. Fosser, K. A.; Nuzzo, R. G. Fabrication of Patterned Multicomponent Protein Gradients and Gradient Arrays Using Microfluidic Depletion. *Anal. Chem.* **2003**, *75*, 5775-5782.

3. Nalayanda, D. D.; Kalukanimuttam, M.; Schmidtke, D. W. Micropatterned surfaces for controlling cell adhesion and rolling under flow. *Biomed. Microdevices.* **2007**, *9*, 207-214.

4. Tuleuova, N.; Revzin, A. Micropatterning of Aptamer Beacons to Create Cytokine-Sensing Surfaces. *Cell. Mol. Bioeng.* **2010**, *3*, 337-344.

5. Kim, M.; Choi, J.-C.; Jung, H.-R.; Katz, J. S.; Kim, M.-G.; Doh, J. Addressable Micropatterning of Multiple Proteins and Cells by Microscope Projection Photolithography Based on a Protein Friendly Photoresist. *Langmuir.* **2010**, *26*, 12112-12118.

6. Falconnet, D.; Koenig, A.; Assi, F.; Textor, M. A Combined Photolithographic and Molecular-Assembly Approach to Produce Functional Micropatterns for Applications in the Biosciences. *Adv. Funct. Mater.* **2004**, *14*, 749-756.

7. Zhang, G. J.; Tanii, T.; Zako, T.; Hosaka, T.; Miyake, T.; Kanari, Y.; Funatsu, T. W.; Ohdomari, I. Nanoscale patterning of protein using electron beam lithography of organosilane self-assembled monolayers. *Small.* **2005**, *1*, 833-837.

8. Christman, K. L.; Schopf, E.; Broyer, R. M.; Li, R. C.; Chen, Y.; Maynard, H. D. Positioning Multiple Proteins at the Nanoscale with Electron Beam Cross-Linked Functional Polymers. *J. Am. Chem. Soc.* **2009**, *131*, 521-527.

9. Bernard, A.; Renault, J. P.; Michel, B.; Bosshard, H. R.; Delamarche, E. Microcontact Printing of Proteins. *Adv. Mater.* **2000**, *12*, 1067-1070.

10. Renault, J. P.; Bernard, A.; Bietsch, A.; Michel, B.; Bosshard, H. R.; Delamarche, E. Fabricating Arrays of Single Protein Molecules on Glass Using Microcontact Printing. *J. Phys. Chem. B.* **2003**, *107*, 703-711.

11. Graber, D. J.; Zieziulewicz, T. J.; Lawrence, D. A.; Shain, W.; Turner, J. N. Antigen Binding Specificity of Antibodies Patterned by Microcontact Printing. *Langmuir.* **2003**, *19*, 5431-5434.

12. Lee, K.-B.; Park, S.-J.; Mirkin, C. A.; Smith, J. C.; Mrksich, M. Protein Nanoarrays Generated By Dip-Pen Nanolithography. *Science.* **2002**, *295*, 1702-1705.

13. Lee, S. W.; Oh, B.-K.; Sanedrin, R. G.; Salaita, K.; Fujigaya, T.; Mirkin, C. A. Biologically Active Protein Nanoarrays Generated Using Parallel Dip-Pen Nanolithography. *Adv. Mater.* **2006**, *18*, 1133-1136.

14. Garno, J. C.; Amro, N. A.; Wadu-Mesthrige, K.; Liu, G.-Y. Production of Periodic Arrays of Protein Nanostructures Using Particle Lithography. *Langmuir.* **2002**, *18*, 8186-8192.

15. Ngunjiri, J. N.; Daniels, S. L.; Li, J.-R.; Serem, W. K.; Garno, J. C. Controlling the surface coverage and arrangement of proteins using particle lithography. *Nanomedicine.* **2008**, *3*, 529-541.

16. Blättler, T. M.; Binkert, A.; Zimmermann, M.; Textor, M.; Vörös, J.; Reimhult, E. From particle self-assembly to functionalized sub-micron protein patterns. *Nanotechnology.* **2008**, *19*, 075301.

17. Cai, Y.; Ocko, B. M. Large-Scale Fabrication of Protein Nanoarrays Based on Nanosphere Lithography. *Langmuir.* **2005**, *21*, 9274-9279.

18. Taylor, Z. R.; Patel, K.; Spain, T. G.; Keay, J. C.; Jernigen, J. D.; Sanchez, E. S.; Grady, B. P.; Johnson, M. B.; Schmidtke, D. W. Fabrication of Protein Dot Arrays via Particle Lithography. *Langmuir.* **2009**, *25*, 10932-10938.

19. Taylor, Z. R.; Sanchez, E. S.; Keay, J. C.; Johnson, M. B.; Schmidtke, D. W. Patterning of Quantum Dot Bioconjugates via Particle Lithography. *Langmuir.* **2010**, *26*, 18938-18944.

20. Valsesia, A.; Colpo, P.; Meziani, T.; Lisboa, P.; Lejeune, M.; Rossi, F. Immobilization of Antibodies on Biosensing Devices by Nanoarrayed Self-Assembled Monolayers. *Langmuir.* **2006**, *22*, 1763-1767.

21. Valsesia, A.; Mannelli, I.; Colpo, P.; Bretagnol, F.; Rossi, F. Protein Nanopatterns for Improved Immunodetection Sensitivity. *Anal. Chem.* **2008**, *80*, 7336-7340.

22. Agheli, H.; Malmström, J.; Larsson, E. M.; Textor, M.; Sutherland, D. S. Large Area Protein Nanopatterning for Biological Applications. *Nano Lett.* **2006**, *6*, 1165-1171.

23. Hanarp, P.; Käll, M.; Sutherland, D. S. Optical Properties of Short Range Ordered Arrays of Nanometer Gold Disks Prepared by Colloidal Lithography. *J. Phys. Chem. B.* **2003**, *107*, 5768-5772.

24. Rieger, J. The glass transition temperature of polystyrene. *J. Therm. Anal.* **1996**, *46*, 965-972.

25. Ramachandran, V.; Williams, M.; Yago, T.; Schmidtke, D. W.; McEver, R. P. Dynamic alterations of membrane tethers stabilize leukocyte rolling on P-selectin *P. Natl. Acad. Sci. USA.* **2004**, *101*, 13519-13524.

26. Verschueren, H. Interference reflection microscopy in cell biology: methodology and applications. *J. Cell Sci.* **1985**, *75*, 279-301.

27. Sengupta, K.; Aranda-Espinoza, H.; Smith, L.; Janmey, P.; Hammer, D. Spreading of Neutrophils: From Activation to Migration. *Biophys. J.* **2006**, *91*, 4638-4648.

28. Roberts, T. M.; Streitmatter, G. Membrane-substrate contact under the spermatozoon of Caenorhabditis elegans, a crawling cell that lacks filamentous actin. *J. Cell Sci.* **1984**, *69*, 117-126.

29. Schurch, S.; Gehr, P.; Green, F.; Wallace, J. A.; McIver, D. J. L. Cell-substrate adhesion affects intracellular motility of pulmonary macrophages. *Colloid. Surface.* **1989**, *42*, 271-288.

30. Miner, J. J.; Xia, L.; Yago, T.; Kappelmayer, J.; Liu, Z.; Klopocki, A. G.; Shao, B.; McDaniel, J. M.; Setiadi, H.; Schmidtke, D. W.; McEver, R. P. Separable requirements for cytoplasmic domain of PSGL-1 in leukocyte rolling and signaling under flow. *Blood.* **2008**, *1112*, 2035-2045.

31. Yago, T.; Shao, B. J.; Miner, J. J.; Yao, L. B.; Klopocki, A. G.; Maeda, K.; Coggeshall, K. M.; McEver, R. P. E-selectin engages PSGL-1 and CD44 through a common signaling pathway to induce integrin $\alpha_L\beta_2$-mediated slow leukocyte rolling *Blood.* **2010**, *116*, 485-494.

32. Zarbock, A.; Lowell, C. A.; Ley, K. Spleen tyrosine kinase syk is necessary for E-Selectin-induced $\alpha_L\beta_2$ integrin-mediated rolling on intercellular adhesion molecule-1 *Immunity.* **2007**, *26*, 773-783.

33. Green, C. E.; Pearson, D. N.; Camphausen, R. T.; Staunton, D. E.; Simon, S. I. Shear-dependent capping of L-selectin and P-selectin glycoprotein ligand 1 by E-selectin signals activation of high-avidity beta 2-integrin on neutrophils *J. Immunol.* **2004**, *172*, 7780-7790.

34. Hidari, K. I.-P. J.; Weyrich, A. S.; Zimmerman, G. A.; McEver, R. P. Engagement of P-selectin Glycoprotein Ligand-1 Enhances Tyrosine Phosphorylation and Activates Mitogen-activated Protein Kinases in Human Neutrophils. *J. Biol. Chem.* **1997**, *272*, 28750–28756.

35. Evangelista, V.; Manarini, S.; Sideri, R.; Rotondo, S.; Martelli, N.; Piccoli, A.; Totani, L.; Piccardoni, P.; Vestweber, D.; Gaetano, G. d.; Cerletti, C. Platelet/Polymorphonuclear Leukocyte Interaction: P-Selectin Triggers Protein-Tyrosine Phosphorylation -Dependent CD11b/CD18 Adhesion: Role of PSGL-1 as a Signaling Molecule. *Blood.* **1999**, *93*, 876-885.

36. Atarashi, K.; Hirata, T.; Matsumoto, M.; Kanemitsu, N.; Miyasaka, M. Rolling of Th1 Cells via P-Selectin Glycoprotein Ligand-1 Stimulates LFA-1-Mediated Cell Binding to ICAM-1. *J. Immunol.* **2005**, *174*, 1424-1432.

37. Zarbock, A.; Abram, C. L.; Hundt, M.; Altman, A.; Lowell, C. A.; Ley, K. PSGL-1 engagement by E-selectin signals through Src kinase Fgr and ITAM adapters DAP12 and FcRg to induce slow leukocyte rolling. *J. Exp. Med.* **2008**, *205*, 2339-2347.

Chapter 5: Suggestions for Future Directions

After our basic protein patterning method was established, our work was directed towards overcoming limitations of the technique (i.e. long-term visualization of protein patterns and independent control of protein dot size and center-to-center spacing) and applying the technique to new investigations and technologies (i.e. neutrophil spreading on patterned PL1 and the design of a fluorescent immunoassay). To maximize the versatility and impact of the patterning process, further work should be performed in both of these areas.

Multi-protein Patterns

As previously discussed, particle lithography has not yet been used to create multi-protein patterns despite their utility in heterogeneous cell co-cultures,[1] multi-analyte biosensors,[2] and the examination of the cellular response to multiple ligands that are spatially segregated.[3] We are currently investigating extensions of our particle lithography technique to pattern multiple proteins. In keeping with our original design principles, the new modifications are relatively inexpensive and simple to employ.

Filled-Honeycomb Patterns were created by substituting a protein-adherent silane for the protein-repellant mPEG-sil typically used in our patterning technique (Figure 5.1). The filled-honeycomb patterning procedure is identical to the process outlined in Chapter 4 through the deformation heating step. After heating, trimethoxyoctadecyl-silane (Aquasil; Thermo Fisher Scientific, Waltham, MA) was grafted to the substrates around the spheres by first exposing the substrates to an air-plasma at 400 mTorr and

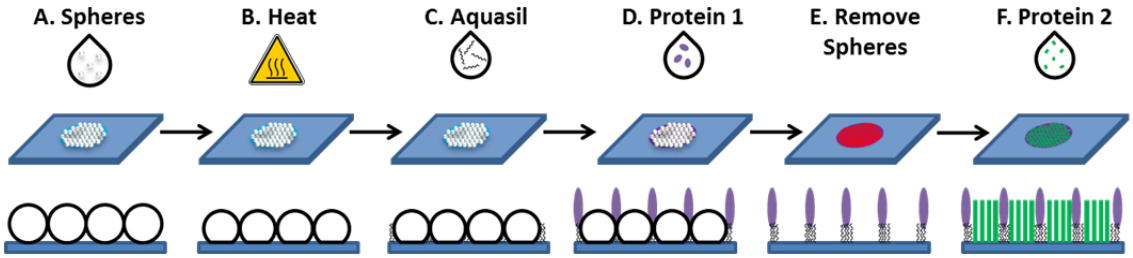

Figure 5.1: Filled-Honeycomb Patterning Schematic.

"high" power (0.027 W/cm^3) for 1 min and then immediately applying 500 µL of 1% Aqausil in DI water to the substrates. The grafting was allowed to proceed for 10 s before the excess liquid was aspirated from the surface and the substrates were soaked in DI water for 5 min to remove any unbound Aquasil. The substrates were then dried under a stream of nitrogen. Alexa Fluor 488 BSA was dissolved in HBSS at a concentration of 20 µg/mL and was dispensed on the Aquasil-patterned surfaces for up to 2 hr. It is important to note that the Aquasil treatment, DI water washing, nitrogen drying, and protein incubation did not remove the spherical particles from the substrates under the conditions studied. Following protein incubation, the substrates were rinsed with 25 mL HBSS using a transfer pipette to remove the spheres and any unbound protein. If the rinsing did not remove the spheres, the substrates were sonicated in HBSS in 2 min intervals until the spheres were removed. Alexa Fluor 647 fibrinogen was dissolved in HBSS at a concentration of 20 µg/mL and was dispensed on the BSA-patterned surfaces for up to 2 hr. Finally, the substrates were rinsed with 25 mL HBSS using a transfer pipette and 50 mL of DI water using a wash bottle to remove any unbound protein.

Figure 5.2 shows images from a filled-honeycomb pattern that was created with 10 μm spheres heated to 125 °C for 60 min and thus had similar dimensions to the single protein pattern in Figure 4.2C. The boundaries between the BSA and fibrinogen coated honeycomb background and dots, respectively, were well defined. In addition, there was no signal from the fibrinogen in the pattern background and no signal from the BSA in the pattern dots, which indicates that the protein adsorbed only in the desired areas.

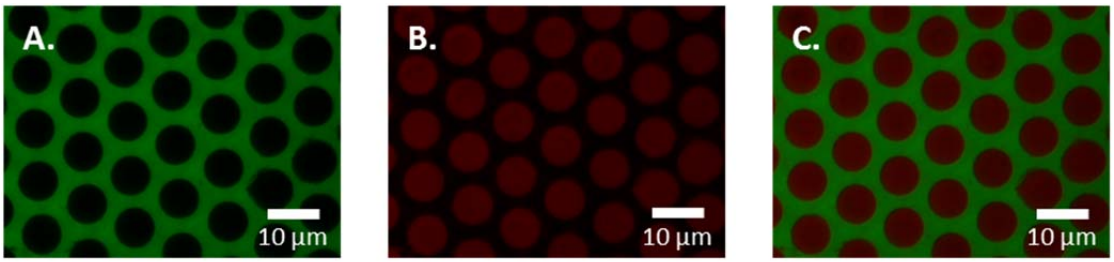

Figure 5.2: Fluorescent Images of a Filled-Honeycomb Pattern. (A, B) Images (pseudocolored post-acquisition) of the fluorescent signal from Alexa Fluor 488 BSA (A) and Alexa Fluor 647 fibrinogen (B) from the same area of a single substrate obtained by switching fluorescent filters. (C) Resulting image when (A) and (B) are combined.

This technique should be further validated by determining the reproducibility of the patterns, the activity of the protein adsorbed in the background, the activity of the protein adsorbed in the dots, and the amount of protein (if any) that adsorbs in undesired locations. Since this technique relies on the sphere mask (1) to stay attached to the substrate during the first protein incubation and (2) to detach from the surface without contact to the surface (i.e. removal by scratching), the feasibility of using this process with different sphere sizes and deformation heating conditions should also be investigated.

Dual-Protein Dot Patterns were created with a different modification to our patterning technique (Figure 5.3). One side of Alexa Fluor 488 fibrinogen patterns (20 µg/mL coating concentration) produced by the process outlined in Chapter 4 were simply "wiped" with a sharp edge of a rectangular piece of Teflon sheet. This procedure was performed with the samples covered with HBSS to prevent protein drying and inactivation. Although the wiping action can be performed by hand, the Teflon was secured to a linear translation stage (Newport Corporation, North Billerica, MA) to provide even pressure to the substrates' surfaces along the straightest paths possible. After wiping, the samples were rinsed with 25 mL of HBSS using a transfer pipette to prevent any detached protein from readsorbing. Next, an Alexa Fluor 647 fibrinogen solution (20 µg/mL) was dispensed on the substrates for 2 hr. Finally, the substrates were rinsed with 25 mL of HBSS using a transfer pipette and 50 mL of DI water using a wash bottle to remove any unbound protein.

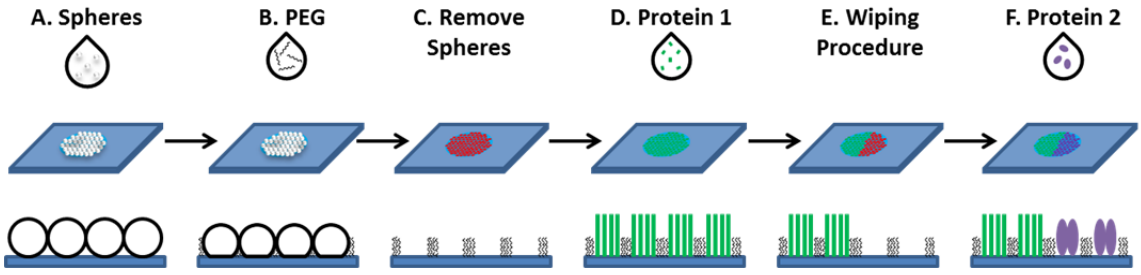

Figure 5.3: Dual-Protein Dot Patterning Procedure.

Figure 5.4 shows images from a two-protein dot pattern that was created with 10 µm spheres heated to 135 °C for 60 min and thus had similar dimensions to the single protein pattern in Figure 4.2D. The boundary between the wiped and unaltered sides of the pattern is sharp and even divides individual dots. Although the wiped and unaltered sides of the pattern appear to only have Alexa Fluor 647 fibrinogen and Alexa Fluor

488 fibrinogen signals, respectively, each side showed some (approximately 15x less signal) undesirable adsorption of fibrinogen labeled with the opposite fluorophore. The contamination on the wiped side of the pattern may be due to incomplete removal of the protein that was initially adsorbed or readsorption of protein detached during the wiping process. The contamination on the unaltered side of the pattern may be due to the second protein filling unoccupied adsorption sites in the dot domains or the formation of fibrinogen multilayers, which has been previously documented.[4]

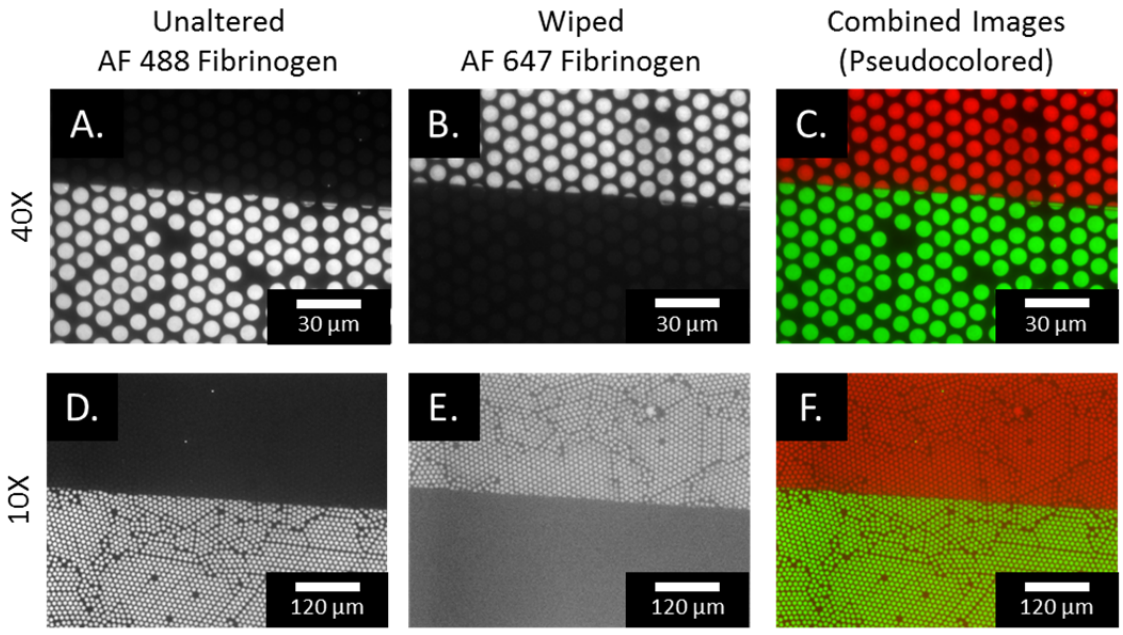

Figure 5.4: Fluorescent Images of a Dual-Protein Dot Pattern. (A, B, D, E) Images of the fluorescent signal from Alexa Fluor 488 fibrinogen (A, D) and Alexa Fluor 647 fibrinogen (B, E) from the same area of a single substrate obtained by switching fluorescent filters and magnifications (40X and 10X). (C) Resulting image when (A) and (B) are pseudocolored and combined. (F) Resulting image when (D) and (E) are pseudocolored and combined.

Further experiments with this technique should be performed to determine the reproducibility of the patterns, the activity of the protein adsorbed in the dots on the wiped side, the activity of the protein adsorbed in the dots on the unaltered side, and the

amount of protein that adsorbs in undesired locations. Although some applications may not be affected by a small amount of the opposite protein contaminating each side of the dual-protein dot patterns, methods to reduce or eliminate contamination should be investigated. To exclude the possibility that single-protein multilayers are forming, two different proteins (e.g. BSA and fibrinogen, as in the filled-honeycomb patterns) should be used to create patterns instead of the same protein with different fluorophores. Contamination may be reduced on the unaltered side by blocking unoccupied adsorption sites before the wiping procedure. Contamination on the wiped side may be reduced by performing the wiping procedure in the presence of the second protein to be patterned so that it can compete with the detached protein for recently-vacated adsorption sites. In addition, multiple wiping steps may be employed with intermediate rinses to more thoroughly remove the originally adsorbed protein.

If the contamination can be reduced to an acceptable level, the dual-protein dot patterning procedure could be extended to pattern protein dots in more complicated geometries and/or to pattern more than two proteins on a single substrate. Using a wiping tool with single or multiple points, adsorbed protein could be removed from smaller areas of patterned substrates with each wiping procedure. This would allow lines or even more complicated designs to be "drawn" in an originally adsorbed protein before adsorbing a second protein. If multiple wiping procedures were used, each followed by the adsorption of a different protein, complex designs of several proteins could be created on a single substrate.

Cell Adhesion Studies

As discussed in Chapter 1, one of the initial motivations for our protein patterning technique was to investigate the relationship between neutrophil adhesion and protein spatial arrangement. Under different physiological conditions, neutrophils can adhere transiently (i.e. rolling) or firmly (i.e. spreading) to physiological surfaces. Chapter 4 includes a proof of concept neutrophil spreading study, but there are a number of neutrophil adhesion experiments that remain to be completed.

Neutrophil Spreading Experiments. To better understand the effects of ligand spatial arrangement on neutrophil spreading, the study performed in Chapter 4 should be extended. The neutrophil spreading response to other protein dot sizes and center-to-center spacings should be examined to determine the minimum feature size necessary to induce spreading and the relationship between experimental conditions and the rate and extent of spreading. By varying protein dot dimensions, contact between spreading cells could be encouraged or restricted to determine whether cell-to-cell communication affects spreading. In addition to varying protein dot dimensions, neutrophil spreading characteristics could also be compared for different ligands and in the presence of different inhibitors, which has been studied for homogeneously coated substrates but not for patterned substrates.[5]

Neutrophil Rolling Experiments. During the inflammatory response, neutrophils roll on activated endothelial cells that express P-selectin in a punctated fashion.[6-8] P-selectin patterned substrates could be used to determine the minimum dimensions

required to support rolling on individual features, the effects of patch size and spacing on rolling characteristics (e.g. velocity and fluidity), and the prevalence of different rolling behaviors (e.g. smooth rolling, skipping, and pausing) on patterns with various geometries.

Other Recommended Studies

Although there are numerous applications of protein patterns with the dimensions that have already been fabricated, the particle lithography technique should be extended to other sphere sizes to produce larger and smaller protein dot diameters and center-to-center spacings. In addition, the knowledge gained from the suggested cell adhesion studies could be applied to similar studies of other cell types. For example, the information from neutrophil rolling experiments could be useful to investigations of platelet rolling in thrombosis,[9] infected red blood cell rolling in malaria,[10] and cancer cell rolling in metastasis.[11]

References

1. Collins, J. M.; Nettikadan, S. Subcellular scaled multiplexed protein patterns for single cell cocultures. *Anal. Biochem.* **2011**, *419*, 339-341.

2. Inerowicz, H. D.; Howell, S.; Regnier, F. E.; Reifenberger, R. Multiprotein immunoassay arrays fabricated by microcontact printing. *Langmuir.* **2002**, *18*, 5263-5268.

3. Shen, K.; Thomas, V. K.; Dustin, M. L.; Kam, L. C. Micropatterning of costimulatory ligands enhances CD4+ T cell function. *P. Natl. Acad. Sci. USA.* **2008**, *105*, 7791-7796.

4. Bai, Z.; Filiaggi, M. J.; Dahn, J. R. Fibrinogen adsorption onto 316L stainless steel, Nitinol and titanium. *Surf. Sci.* **2009**, *603*, 839-846.

5. Galkina, S. I.; Sud'ina, G. F.; Klein, T. Metabolic regulation of neutrophil spreading, membrane tubulovesicular extensions (cytonemes) formation and intracellular pH upon adhesion to fibronectin. *Experimental Cell Research.* **2006**, *312*, 2568-2579.

6. McEver, R. P.; Beckstead, J. H.; Moore, K. L.; Marshall-Carlson, L.; Bainton, D. F. GMP-140, a Platelet a-Granule Membrane Protein, Is Also Synthesized by Vascular Endothelial Cells and Is Localized in Weibel-Palade Bodies. *J. Clin. Invest.* **1989**, 92-99.

7. Moore, K. L.; Patel, K. D.; Bruehl, R. E.; Fugang, L.; Johnson, D. A.; Lichenstein, H. S.; Cummings, R. D.; Bainton, D. F.; McEver, R. P. P-Selectin Glycoprotein Ligand-1 Mediates Rolling of Human Neutrophils on P-Selectin. *J. Cell Biol.* **1995**, *128*, 661-671.

8. Setiadi, H.; Disdier, M.; Green, S. A.; Canfield, W. M.; McEver, R. P. Residues Throughout the Cytoplasmic Domain Affect the Internalization Efficiency of P-selectin. *J. Biol. Chem.* **1995**, *45*, 26818-26826.

9. Frenette, P. S.; Johnson, R. C.; Hynes, R. O.; Wagner, D. D. Platelets roll on stimulated endothelium *in vivo*: An interaction mediated by endothelial P-selectin. *P. Natl. Acad. Sci. USA.* **1995**, *92*, 7450-7454.

10. Ho, M.; Schollaardt, T.; Niu, X.; Looareesuwan, S.; Patel, K. D.; Kubes, P. Characterization of *Plasmodium falciparum*-Infected Erythrocyte and P-Selectin Interaction Under Flow Conditions. *Blood.* **1998**, *91*, 4803-4809.

11. Aigner, S.; Ramos, C. L.; Hafezi-Moghadam, A.; Lawrence, M. B.; Friederichs, J.; Altevogt, P.; Ley, K. CD24 mediates rolling of breast carcinoma cells on P-selectin. *FASEB J.* **1998**, *12*, 1241-1251.

Chapter 6: Conclusions

The major conclusions from this dissertation are as follows:

- The development of a novel protein patterning method based on particle lithography was described.
- The patterning technique relies on inexpensive, "bench-top" processes and equipment and was used to produce samples with millions of protein-coated "dot" features in parallel.
- By changing the diameters of the spherical particles used as the lithographic mask, the diameters and center-to-center spacing of the resulting protein dots were varied simultaneously between 450 – 1050 nm and 2 – 10 μm, respectively.
- Sphere monolayer washing was critical to PEG-layer integrity and pattern uniformity.
- Patters were created with multiple proteins and biomolecule-coated particles (i.e. CdSe quantum dots, nanogold). The pattern dimensions were independent of the protein or biomolecule-coated particle used during patterning.
- Quantum dot bioconjugates (QDBCs) were used to construct a fluorescent-based immunoassay that was well-characterized by a logarithmic function over four orders of magnitude of analyte concentration. The assay had a subpicomolar concentration detection limit, which, when combined with the low sample volume required for the assay, corresponds to a mass detection limit of only several femtograms.

- Protein dot diameters and center-to-center spacing were controlled independently with the addition of a simple heating process. Using the patterning procedure with the heating modification, protein dots with diameters of 1.1 – 9 μm were created with a center-to-center distance of 10 μm.
- Protein dot patterns with single diameters could be created using uniform heat or a continuous gradient of diameters using differential heating.
- PEG-patterned substrates coated with anti-PSGL-1 (PL1) were used to study neutrophil spreading. Neutrophils adhered only to antibody-coated regions of the patterns.
- Multiple infusions of neutrophils were used to form a continuous layer of spread neutrophils over a PL1-patterned surface.

Bibliography

Agheli, H.; Malmström, J.; Larsson, E. M.; Textor, M.; Sutherland, D. S. Large Area Protein Nanopatterning for Biological Applications. *Nano Lett.* **2006**, *6*, 1165-1171.

Aigner, S.; Ramos, C. L.; Hafezi-Moghadam, A.; Lawrence, M. B.; Friederichs, J.; Altevogt, P.; Ley, K. CD24 mediates rolling of breast carcinoma cells on P-selectin. *FASEB J.* **1998**, *12*, 1241-1251.

Andruzzi, L.; Senaratne, W.; Hexemer, A.; Sheets, E. D.; Ilic, B.; Kramer, E. J.; Baird, B.; Ober, C. K. Oligo(ethylene glycol) Containing Polymer Brushes as Bioselective Surfaces. *Langmuir.* **2005**, *21*, 2495-2504.

Arnold, M.; Cavalcanti-Adam, E. A.; Glass, R.; Blummel, J.; Eck, W.; Kantlehner, M.; Kessler, H.; Spatz, J. P. Activation of integrin function by nanopatterned adhesive interfaces. *ChemPhysChem.* **2004**, *5*, 383-388.

Atarashi, K.; Hirata, T.; Matsumoto, M.; Kanemitsu, N.; Miyasaka, M. Rolling of Th1 Cells via P-Selectin Glycoprotein Ligand-1 Stimulates LFA-1-Mediated Cell Binding to ICAM-1. *J. Immunol.* **2005**, *174*, 1424-1432.

Aydin, D.; Schwieder, M.; Louban, I.; Knoppe, S.; Ulmer, J.; Haas, T. L.; Walczak, H.; Spatz, J. P. Micro-Nanostructured Protein Arrays: A Tool for Geometrically Controlled Ligand Presentation**. *Small.* **2009**, *5*, 1014-1018.

Bae, P. K.; So, H.-M.; Kim, K. N.; You, H. S.; Choi, K. S.; Kim, C. H.; Park, J.-K.; Lee, J.-O. Simple route for the detection of *Escherichia coli* using quantum dots *BioChip J.* **2010**, *4*, 129-133.

Bai, Z.; Filiaggi, M. J.; Dahn, J. R. Fibrinogen adsorption onto 316L stainless steel, Nitinol and titanium. *Surf. Sci.* **2009**, *603*, 839-846.

Ballav, N.; Thomas, H.; Winkler, T.; Terfort, A.; Zharnikov, M. Making Protein Patterns by Writing in a Protein-Repelling Matrix. *Angew. Chem. Int. Edit.* **2009**, *48*, 5833-5836.

Batra, D.; Vogt, S.; Laible, P. D.; Firestone, M. A. Self-assembled, mesoporous polymeric networks for patterned protein arrays. *Langmuir.* **2005**, *21*, 10301-10306.

Bellido, E.; Miguel, R. d.; Ruiz-Molina, D.; Lostao, A.; Maspoch, D. Controlling the Number of Proteins with Dip-Pen Nanolithography. *Adv. Mater.* **2010**, *22*, 352-355.

Ber, S.; Kose, G. T.; Hasirci, V. Bone tissue engineering on patterned collagen films: an in vitro study. *Biomaterials.* **2005**, *26*, 1977-1986.

Bernard, A.; Delamarche, E.; Schmid, H.; Michel, B.; Bosshard, H. R.; Biebuyck, H. Printing patterns of proteins. *Langmuir.* **1998**, *14*, 2225-2229.

Bernard, A.; Renault, J. P.; Michel, B.; Bosshard, H. R.; Delamarche, E. Microcontact Printing of Proteins. *Adv. Mater.* **2000**, *12*, 1067-1070.

Bhatia, S. N.; Balis, U. J.; Yarmush, M. L.; Toner, M. Microfabrication of Hepatocyte/Fibroblast Co-cultures: Role of Homotypic Cell Interactions. *Biotechnol. Prog.* **1998**, *14*, 378-387.

Bhatnagar, P.; Malliaras, G. G.; Kim, I.; Batt, C. A. Multiplexed Protein Patterns on a Photosensitive Hydrophilic Polymer Matrix. *Adv. Mater.* **2009**, *22*, 1242-1246.

Bietsch, A.; Michel, B. Conformal contact and pattern stability of stamps used for soft lithography. *J. Appl. Phys.* **2000**, *88*, 4310-4318.

Biju, V.; Itoh, T.; Anas, A.; Sujith, A.; Ishikawa, M. Semiconductor quantum dots and metal nanoparticles: syntheses, optical properties, and biological applications. *Anal. Bioanal. Chem.* **2008**, *391*, 2469-2495.

Blättler, T. M.; Binkert, A.; Zimmermann, M.; Textor, M.; Vörös, J.; Reimhult, E. From particle self-assembly to functionalized sub-micron protein patterns. *Nanotechnology.* **2008**, *19*, 075301.

Boneberg, J.; Burmeister, F.; Schafle, C.; Leiderer, P.; Reim, D.; Fery, A.; Herminghaus, S. The formation of nano-dot and nano-ring structures in colloidal monolayer lithography. *Langmuir.* **1997**, *13*, 7080-7084.

Branch, D. W.; Wheeler, B. C.; Brewer, G. J.; Leckband, D. E. Long-term stability of grafted polyethylene glycol surfaces for use with microstamped substrates in neuronal cell culture. *Biomaterials.* **2001**, *22*, 1035-1047.

Braunschweig, A. B.; Senesi, A. J.; Mirkin, C. A. Redox-Activating Dip-Pen Nanolithography (RA-DPN). *J. Am. Chem. Soc.* **2009**, *131*, 922-923.

Brétagnol, F.; Ceriotti, L.; Valsesia, A.; Sasak, T.; Ceccone, G.; Gilliland, D.; Colpo, P.; Rossi, F. Fabrication of functional nano-patterned surfaces by a combination of plasma processes and electron-beam lithography. *Nanotechnology.* **2007**, *18*, 135303.

Brétagnol, F.; Sirghi, L.; Mornet, S.; Sasaki, T.; Gilliland, D.; Colpo, P.; Rossi, F. Direct fabrication of nanoscale bio-adhesive patterns by electron beam surface modification of plasma polymerized poly ethylene oxide-like coatings. *Nanotechnology.* **2008**, *19*, 125306.

Cai, Y.; Ocko, B. M. Large-Scale Fabrication of Protein Nanoarrays Based on Nanosphere Lithography. *Langmuir.* **2005**, *21*, 9274-9279.

Cavalcanti-Adam, E. A.; Micoulet, A.; Blummel, J.; Auernheimer, J.; Kessler, H.; Spatz, J. P. Lateral spacing of integrin ligands influences cell spreading and focal adhesion assembly. *Eur. J. Cell Biol.* **2006**, *85*, 219-224.

Ceccone, G.; Leung, B. O.; Perez-Roldan, M. J.; Valsesia, A.; Colpo, P.; Rossi, F.; Hitchcock, A. P.; Scholl, A. X-ray spectromicroscopy study of ubiquitin adsorption to plasma polymerized microstructures. *Surf. Interface Anal.* **2010**, *42*, 830-834.

Chai, J.; Wong, L. S.; Giam, L.; Mirkin, C. A. Single-molecule protein arrays enabled by scannin probe block copolymer lithography. *P. Natl. Acad. Sci. USA.* **2011**, *108*, 19521-19525.

Chalmeau, J.; Thibault, C.; Carcenac, F.; Vieu, C. Micro-Contact Printing of Two Different Biomolecules in One Step Using Deformable Poly(dimethylsiloxane)-Based Stamp. *Jpn. J. Appl. Phys.* **2008**, *47*, 5221-5225.

Chen, C. S.; Mrksich, M.; Huang, S.; Whitesides, G. M.; Ingber, D. E. Geometric Control of Cell Life and Death. *Science.* **1997**, *276*, 1425-1428.

Chen, C. S.; Mrksich, M.; Huang, S.; Whitesides, G. M.; Ingber, D. E. Micropatterned Surfaces for Control of Cell Shape, Position, and Function. *Biotechnol. Prog.* **1998**, *14*, 356-363.

Chen, H.; Li, R.; Lin, L.; Guo, G.; Lin, J.-M. Determination of l-ascorbic acid in human serum by chemiluminescence based on hydrogen peroxide–sodium hydrogen carbonate–CdSe/CdS quantum dots system. *Talanta.* **2010**, *81*, 1688-1696.

Chen, J.; Liao, W.-S.; Chen, X.; Yang, T.; Wark, S. E.; Son, D. H.; Batteas, J. D.; Cremer, P. S. Evaporation-Induced Assembly of Quantum Dots into Nanorings. *ACS Nano.* **2009**, *3*, 173-180.

Chen, Y. P.; Ning, B.; Liu, N.; Feng, Y.; Liu, Z.; Liu, X.; Gao, Z. X. A rapid and sensitive fluoroimmunoassay based on quantum dot for the detection of chlorpyrifos residue in drinking water. *J. Environ. Sci. Health B.* **2010**, *45*, 508-515.

Chiu, D. T.; Jeon, N. L.; Huang, S.; Kane, R. S.; Wargo, C. J.; Choi, I. S.; Ingber, D. E.; Whitesides, G. M. Patterned deposition of cells and proteins onto surfaces by using three-dimensional microfluidic systems. *P. Natl. Acad. Sci. USA.* **2000**, *97*, 2408-2413.

Choi, W. M.; Park, O. The fabrication of micropatterns of a 2D colloidal assembly by electrophoretic deposition. *Nanotechnology.* **2006**, *17*, 325-329.

Chouhan, R. S.; Vinayaka, A. C.; Thakur, M. S. Thiol-stabilized luminescent CdTe quantum dot as biological fluorescent probe for sensitive detection of methyl parathion by a fluoroimmunochromatographic technique. *Anal. Bioanal. Chem.* **2010**, *397*, 1467-1475.

Christman, K. L.; Broyer, R. M.; Schopf, E.; Kolodziej, C. M.; Chen, Y.; Maynard, H. D. Protein Nanopatterns by Oxime Bond Formation. *Langmuir.* **2011**, *27*, 1415-1418.

Christman, K. L.; Enriquez-Rios, V. D.; Maynard, H. D. Nanopatterning proteins and peptides *Soft Matter.* **2006**, *2*, 928-939.

Christman, K. L.; Requa, M. V.; Enriquez-Rios, V. D.; Ward, S. C.; Bradley, K. A.; Turner, K. L.; Maynard, H. D. Submicron Streptavidin Patterns for Protein Assembly. *Langmuir.* **2006**, *22*, 7444-7450.

Christman, K. L.; Schopf, E.; Broyer, R. M.; Li, R. C.; Chen, Y.; Maynard, H. D. Positioning Multiple Proteins at the Nanoscale with Electron Beam Cross-Linked Functional Polymers. *J. Am. Chem. Soc.* **2009**, *131*, 521-527.

Chuang, Y.-H.; Chang, Y.-T.; Liu, K.-L.; Chang, H.-Y.; Yew, T.-R. Electrical impedimetric biosensors for liver function detection. *Biosens. Bioelectron.* **2011**, *28*, 368-372.

Clarke, S.; Pinaud, F.; Beutel, O.; You, C.; Piehler, J.; Dahan, M. Covalent Monofunctionalization of Peptide-Coated Quantum Dots for Single-Molecule Assays. *Nano Lett.* **2010**, *10*, 2147-2154.

Collins, J. M.; Nettikadan, S. Subcellular scaled multiplexed protein patterns for single cell cocultures. *Anal. Biochem.* **2011**, *419*, 339-341.

Cong, C.; Junus, W. C.; Shen, Z.; Yu, T. New Colloidal Lithographic Nanopatterns Fabricated by Combining Pre-Heating and Reactive Ion Etching. *Nanoscale Res. Lett.* **2009**, *4*, 1324-1328.

Cuvelier, D.; Rossier, O.; Bassereau, P.; Nassoy, P. Micropatterned ‘‘adherent /repellent’’ glass surfaces for studying the spreading kinetics of individual red blood cells onto protein-decorated substrates. *Eur. Biophys. J.* **2003**, *32*, 342-354.

Daniels, S. L.; Ngunjiri, J. N.; Garno, J. C. Investigation of the magnetic properties of ferritin by AFM imaging with magnetic sample modulation. *Anal. Bioanal. Chem.* **2009**, *394*, 215-223.

Delamarche, E.; Bernard, A.; Schmid, H.; Michel, B.; Biebuyck, H. Patterned delivery of immunoglobulins to surfaces using microfluidic networks. *Science.* **1997**, *276*, 779-781.

Delamarche, E.; Schmid, H.; Michel, B.; Biebuyck, H. Stability of Molded Polydimethylsiloxane Microstructures. *Adv. Mater.* **1997**, *9*, 741-746.

Delehanty, J. B.; Ligler, F. S. A Microarray Immunoassay for Simultaneous Detection of Proteins and Bacteria. *Anal. Chem.* **2002**, *74*, 5681-5687.

Delehanty, J. B.; Medintz, I. L.; Pons, T.; Brunel, F. M.; Dawson, P. E.; Mattoussi, H. Self-Assembled Quantum Dot-Peptide Bioconjugates for Selective Intracellular Delivery. *Bioconjugate Chem.* **2006**, *17*, 920-927.

DeMond, A. L.; Mossman, K. D.; Starr, T.; Michael L. Dustin; Groves, J. T.; Yager, P. T Cell Receptor Microcluster Transport through Molecular Mazes Reveals Mechanism of Translocation. *Biophys. J.* **2008**, *94*, 3286-3292.

Denis, F. A.; Hanarp, P.; Sutherland, D. S.; Dufrene, Y. F. Fabrication of nanostructured polymer surfaces using colloidal lithography and spin-coating. *Nano Lett.* **2002**, *2*, 1419-1425.

Denis, F. A.; Pallandre, A.; Nysten, B.; Jonas, A. M.; Dupont-Gillain, C. C. Alignment and Assembly of Adsorbed Collagen Molecules Induced by Anisotropic Chemical Nanopatterns. *Small.* **2005**, *1*, 984-991.

Dike, L. E.; Chen, C. S.; Mrksich, M.; Tien, J.; Whitesides, G. M.; Ingber, D. E. Geometric control of switching between growth, apoptosis, and differentiation during angiogenesis using micropatterned substrates. *In Vitro Cell Dev.-An.* **1999**, *35*, 441-448.

Dmitriev, A.; Hägglund, C.; Chen, S.; Fredriksson, H.; Pakizeh, T.; Käll, M.; Sutherland, D. S. Enhanced Nanoplasmonic Optical Sensors with Reduced Substrate Effect. *Nano Lett.* **2008**, *8*, 3893-3898.

Doh, J.; Irvine, D. J. Immunological synapse arrays: Patterned protein surfaces that modulate immunological synapse structure formation in T cells. *P. Natl. Acad. Sci. USA.* **2006**, *103*, 5700-5705.

Doyle, A. D.; Wang, F. W.; Matsumoto, K.; Yamada, K. M. One-dimensional topography underlies three-dimensional fibrillar cell migration. *J. Cell Biol.* **2009**, *184*, 481-490.

Du, H.; Bai, Y. B.; Hui, Z.; Li, L. S.; Chen, Y. M.; Tang, X. Y.; Li, T. J. Two-dimensional arrays from polymer spheres in nanoscale prepared by the Langmuir-Blodgett method. *Langmuir.* **1997**, *13*, 2538-2540.

Duan, X.; Zhao, Y.; Berenschot, E.; Tas, N. R.; Reinhoudt, D. N.; Huskens, J. Large-Area Nanoscale Patterning of Functional Materials by Nanomolding in Capillaries. *Adv. Funct. Mater.* **2010**, *20*, 2519-2526.

Dyer, P. E.; Maswadi, S. M.; Walton, C. D.; Ersoz, M.; Fletcher, P. D. I.; Paunov, V. N. 157-nm laser micromachining of N-BK7 glass and replication for microcontact printing. *Appl. Phys. A-Mater.* **2003**, *77*, 391-394.

Dziomkina, N. V.; Vancso, G. J. Colloidal crystal assembly on topologically patterned templates. *Soft Matter.* **2005**, *1*, 265-279.

Eastman, P. S.; Ruan, W.; Doctolero, M.; Nuttall, R.; Feo, G. d.; Park, J. S.; Chu, J. S. F.; Cooke, P.; Gray, J. W.; Li, S.; Chen, F. F. Qdot Nanobarcodes for Multiplexed Gene Expression Analysis. *Nano Lett.* **2006**, *6*, 1059-1064.

Escalante, M.; Maury, P.; Bruinink, C. M.; Werf, K. v. d.; Olsen, J. D.; Timney, J. A.; Huskens, J.; Hunter, C. N.; Subramaniam, V.; Otto, C. Directed assembly of functional light harvesting antenna complexes onto chemically patterned surfaces. *Nanotechnology.* **2008**, *19*, 025101.

Evangelista, V.; Manarini, S.; Sideri, R.; Rotondo, S.; Martelli, N.; Piccoli, A.; Totani, L.; Piccardoni, P.; Vestweber, D.; Gaetano, G. d.; Cerletti, C. Platelet/Polymorphonuclear Leukocyte Interaction: P-Selectin Triggers Protein-Tyrosine Phosphorylation -Dependent CD11b/CD18 Adhesion: Role of PSGL-1 as a Signaling Molecule. *Blood.* **1999**, *93*, 876-885.

Falconnet, D.; Koenig, A.; Assi, F.; Textor, M. A Combined Photolithographic and Molecular-Assembly Approach to Produce Functional Micropatterns for Applications in the Biosciences. *Adv. Funct. Mater.* **2004**, *14*, 749-756.

Falconnet, D.; Pasqui, D.; Park, S.; Eckert, R.; Schift, H.; Gobrecht, J.; Barbucci, R.; Textor, M. A Novel Approach to Produce Protein Nanopatterns by Combining Nanoimprint Lithography and Molecular Self-Assembly. *Nano Lett.* **2004**, *4*, 1909-1914.

Fan, F. Q.; Stebe, K. J. Assembly of colloidal particles by evaporation on surfaces with patterned hydrophobicity. *Langmuir.* **2004**, *20*, 3062-3067.

Folch, A.; Toner, M. Cellular Micropatterns on Biocompatible Materials. *Biotechnol. Prog.* **1998**, *14*, 388-392.

Folch, A.; Toner, M. Microengineering of Cellular Interactions. *Annu. Rev. Biomed. Eng.* **2000**, *2*, 227-256.

Foley, J. O.; Fu, E.; Gamble, L. J.; Yager, P. Microcontact Printed Antibodies on Gold Surfaces: Function, Uniformity, and Silicone Contamination. *Langmuir.* **2008**, *24*, 3628-3635.

Fosser, K. A.; Nuzzo, R. G. Fabrication of Patterned Multicomponent Protein Gradients and Gradient Arrays Using Microfluidic Depletion. *Anal. Chem.* **2003**, *75*, 5775-5782.

Frasco, M. F.; Vamvakaki, V.; Chaniotakis, N. Porphyrin decorated CdSe quantum dots for direct fluorescent sensing of metal ions. *J. Nanopart. Res.* **2010**, *12*, 1449-1458.

Frenette, P. S.; Johnson, R. C.; Hynes, R. O.; Wagner, D. D. Platelets roll on stimulated endothelium *in vivo*: An interaction mediated by endothelial P-selectin. *P. Natl. Acad. Sci. USA.* **1995**, *92*, 7450-7454.

Frey, W.; Woods, C. K.; Chilkoti, A. Ultraflat nanosphere lithography: A new method to fabricate flat nanostructures *Adv. Mater.* **2000**, *12*, 1515-1519.

Fustin, C. A.; Glasser, G.; Spiess, H. W.; Jonas, U. Parameters influencing the templated growth of colloidal crystals on chemically patterned surfaces. *Langmuir.* **2004**, *20*, 9114-9123.

Galkina, S. I.; Sud'ina, G. F.; Klein, T. Metabolic regulation of neutrophil spreading, membrane tubulovesicular extensions (cytonemes) formation and intracellular pH upon adhesion to fibronectin. *Experimental Cell Research.* **2006**, *312*, 2568-2579.

Gao, B.; Bernstein, G. H.; Lieberman, M. Self-assembled monolayers of poly(ethylene glycol) siloxane as a resist for ultrahigh-resolution electron beam lithography on silicon oxide. *J. Vac. Sci. Technol. B.* **2009**, *27*, 2292-2300.

Gao, P.; Cai, Y. The Boundary Molecules in a Lysozyme Pattern Exhibit Preferential Antibody Binding. *Langmuir.* **2008**, *24*, 10334-10339.

Gao, X.; Zhu, S.; Sheardown, H.; Brash, J. L. Nanoscale patterning through self-assembly of hydrophilic block copolymers with one chain end constrained to surface. *Polymer.* **2010**, *51*, 1771-1778.

Garno, J. C.; Amro, N. A.; Wadu-Mesthrige, K.; Liu, G.-Y. Production of Periodic Arrays of Protein Nanostructures Using Particle Lithography. *Langmuir.* **2002**, *18*, 8186-8192.

Ge, S.; Zhang, C.; Zhu, Y.; Yu, J.; Zhang, S. BSA activated CdTe quantum dot nanosensor for antimony ion detection. *Analyst.* **2009**, *135*, 111-115.

Geng, D. L.; Miao, Y. H.; Helseth, L. E. Influence of Salt on Colloidal Lithography of Albumin. *Langmuir.* **2007**, *23*, 8480-8484.

Glass, R.; Möller, M.; Spatz, J. P. Block copolymer micelle nanolithography. *Nanotechnology.* **2003**, *14*, 1153-1160.

Gokarna, A.; Jin, L.-H.; Hwang, J. S.; Cho, Y.-H.; Lim, Y. T.; Chung, B. H.; Youn, S. H.; Choi, D. S.; Lim, J. H. Quantum dot-based protein micro- and nanoarrays for detection of prostate cancer biomarkers. *Proteomics.* **2008**, *8*, 1809-1818.

Gopal, A.; Hoshino, K.; Kim, S.; Zhang, X. Multi-color colloidal quantum dot based light emitting diodes micropatterned on silicon hole transporting layers. *Nanotechnology.* **2009**, *20*, 235201.

Gopal, A.; Hoshino, K.; Zhang, X. Photolithographic patterning of subwavelength top emitting colloidal quantum dot based inorganic light emitting diodes on silicon. *Appl. Phys. Lett.* **2010**, *96*, 131109.

Graber, D. J.; Zieziulewicz, T. J.; Lawrence, D. A.; Shain, W.; Turner, J. N. Antigen Binding Specificity of Antibodies Patterned by Microcontact Printing. *Langmuir.* **2003**, *19*, 5431-5434.

Green, C. E.; Pearson, D. N.; Camphausen, R. T.; Staunton, D. E.; Simon, S. I. Shear-dependent capping of L-selectin and P-selectin glycoprotein ligand 1 by E-selectin signals activation of high-avidity beta 2-integrin on neutrophils *J. Immunol.* **2004**, *172*, 7780-7790.

Guillaume-Gentil, O.; Gabi, M.; Zenobi-Wong, M.; Vörös, J. Electrochemically switchable platform for the micro-patterning and release of heterotypic cell sheets. *Biomed. Microdevices.* **2011**, *13*, 221-230.

Guo, Q.; Arnoux, C.; Palmer, R. E. Guided assembly of colloidal particles on patterned substrates. *Langmuir.* **2001**, *17*, 7150-7155.

Haaheim, J.; Val, V.; Bussan, J.; Rozhok, S.; Jang, J.-W.; Fragala, J.; Nelson, M. Self-Leveling Two-Dimensional Probe Arrays for Dip Pen Nanolithography. *Scanning.* **2010**, *32*, 49-59.

Hale, P. S.; Kappen, P.; Prissanaroon, W.; Brack, N.; Pigram, P. J.; Liesegang, J. Minimizing silicone transfer during micro-contact printing. *Appl. Surf. Sci.* **2007**, *253*, 3746-3750.

Hammond, S.; Wagenknecht-Wiesner, A.; Veatch, S. L.; Holowka, D.; Baird, B. Roles for SH2 and SH3 domains in Lyn kinase association with activated FceRI in RBL mast cells revealed by patterned surface analysis. *J. Struct. Biol. 168*, 161-167.

Hampton, M. J.; Templeton, J. L.; DeSimone, J. M. Direct Patterning of CdSe Quantum Dots into Sub-100 nm Structures. *Langmuir.* **2010**, *26*, 3012-3015.

Han, C.; Li, H. Host-molecule-coated quantum dots as fluorescent sensors. *Anal. Bioanal. Chem.* **2010**, *397*, 1437-144.

Hanarp, P.; Käll, M.; Sutherland, D. S. Optical Properties of Short Range Ordered Arrays of Nanometer Gold Disks Prepared by Colloidal Lithography. *J. Phys. Chem. B.* **2003**, *107*, 5768-5772.

Harris, L. G.; Schofield, W. C. E.; Badyal, J. P. S. MultiFunctional Molecular Scratchcards. *Chem. Mater.* **2007**, *19*, 1546-1551.

Hartman, N. C.; Nye, J. A.; Groves, J. T. Cluster size regulates protein sorting in the immunological synapse. *P. Natl. Acad. Sci. USA.* **2009**, *106*, 12729-12734.

Haynes, C. L.; Duyne, R. P. V. Nanosphere Lithography: A Versatile Nanofabrication Tool for Studies of Size-Dependent Nanoparticle Optics. *J. Phys. Chem. B.* **2001**, *105*, 5599-5611.

Hidari, K. I.-P. J.; Weyrich, A. S.; Zimmerman, G. A.; McEver, R. P. Engagement of P-selectin Glycoprotein Ligand-1 Enhances Tyrosine Phosphorylation and Activates Mitogen-activated Protein Kinases in Human Neutrophils. *J. Biol. Chem.* **1997**, *272*, 28750–28756.

Ho, M.; Schollaardt, T.; Niu, X.; Looareesuwan, S.; Patel, K. D.; Kubes, P. Characterization of *Plasmodium falciparum*-Infected Erythrocyte and P-Selectin Interaction Under Flow Conditions. *Blood.* **1998**, *91*, 4803-4809.

Hoa, X. D.; Martinb, M.; Jimenezb, A.; Beauvais, J.; Charetteb, P.; Kirk, A.; Tabriziana, M. Fabrication and characterization of patterned immobilization of quantum dots on metallic nano-gratings. *Biosens. Bioelectron.* **2008**, *24*, 970-975.

Hoff, J. D.; Cheng, L.-J.; Meyhöfer, E.; Guo, L. J.; Hunt, A. J. Nanoscale Protein Patterning by Imprint Lithography. *Nano Lett.* **2004**, *4*, 853-857.

Hong, J. M.; Ozkeskin, F. M.; Zou, J. A micromachined elastomeric tip array for contact printing with variable dot size and density. *J. Micromech. Microeng.* **2008**, *18*, 015003.

Howell, S. W.; Inerowicz, H. D.; Regnier, F. E.; Reifenberger, R. Patterned Protein Microarrays for Bacterial Detection. *Langmuir.* **2003**, *19*, 436-439.

Hu, X.; Han, H.; Hua, L.; Sheng, Z. Electrogenerated chemiluminescence of blue emitting ZnSe quantum dots and its biosensing for hydrogen peroxide. *Biosens. Bioelectron.* **2010**, *25*, 1843-1846.

Hu, Y.; Chen, D.; Park, S.; Emrick, T.; Russell, T. P. Guided Assemblies of Ferritin Nanocages: Highl Ordered Arrays of Monodisperse Nanoscopic Elements. *Adv. Mater.* **2010**, *22*, 2583-2587.

Hucknall, A.; Simnick, A. J.; Hill, R. T.; Chilkoti, A.; Garcia, A.; Johannes, M. S.; Clark, R. L.; Zauscher, S.; Ratner, B. D. Versatile synthesis and micropatterning of nonfouling polymer brushes on the wafer scale. *Biointerphases.* **2009**, *4*, FA50-FA57.

Hui, C. Y.; Jagota, A.; Lin, Y. Y.; Kramer, E. J. Constraints on Microcontact Printing Imposed by Stamp Deformation. *Langmuir.* **2002**, *18*, 1394-1407.

Hui, E. E.; Bhatia, S. N. Microscale Control of Cell Contact and Spacing via Three-Component Surface Patterning. *Langmuir.* **2007**, *23*, 4103-4107.

Hulteen, J. C.; Vanduyne, R. P. Nanosphere Lithography - A Materials General Fabrication Process for Periodic Particle Array Surfaces. *J. Vac. Sci. Technol. A.* **1995**, *13*, 1553-1558.

Huwiler, C.; Halter, M.; Rezwan, K.; Falconnet, D.; Textor, M.; Voros, J. Self-assembly of functionalized spherical nanoparticles on chemically patterned microstructures. *Nanotechnology.* **2005**, *16*, 3045-3052.

Inerowicz, H. D.; Howell, S.; Regnier, F. E.; Reifenberger, R. Multiprotein immunoassay arrays fabricated by microcontact printing. *Langmuir.* **2002**, *18*, 5263-5268.

Ionov, L.; Diez, S. Environment-Friendly Photolithography Using Poly(N-isopropylacrylamide)-Based Thermoresponsive Photoresists. *J. Am. Chem. Soc.* **2009**, *131*, 13315-13319.

Ito, Y.; Chen, G.; Imanishi, Y. Micropatterned Immobilization of Epidermal Growth Factor To Regulate Cell Function. *Bioconjugate Chem.* **1998**, *9*, 277-282.

Jaehrling, S.; Thelen, K.; Wolfram, T.; Pollerberg, G. E. Nanopatterns Biofunctionalized with Cell Adhesion Molecule DM-GRASP Offered as Cell Substrate: Spacing Determines Attachment and Differentiation of Neurons. *Nano Lett.* **2009**, *9*, 4115-4121.

James, C. D.; Davis, R. C.; Kam, L.; Craighead, H. G.; Isaacson, M.; Turner, J. N.; Shain, W. Patterned protein layers on solid substrates by thin stamp microcontact printing. *Langmuir.* **1998**, *14*, 741-744.

Jeon, N. L.; Baskaran, H.; Dertinger, S. K. W.; Whitesides, G. M.; Water, L. V. D.; Toner, M. Neutrophil chemotaxis in linear and complex gradients of interleukin-8 formed in a microfabricated device. *Nat. Biotechnol.* **2002**, *20*, 826-830.

Jiang, J.; Peng, Z.; Deng, L.; Li, G.; Chen, L. Detection of Bifidobacterium Species-specific 16S rDNA Based on QD FRET Bioprobe. *J. Fluoresc.* **2010**, *20*, 365-369.

Jiang, P.; McFarland, M. J. Large-scale fabrication of wafer-size colloidal crystals, macroporous polymers and nanocomposites by spin-coating. *J. Am. Chem. Soc.* **2004**, *126*, 13778-13786.

Johnson, D. M.; Maurer, J. A. Recycling and reusing patterned self-assembled monolayers for cell culture. *Chem. Commun.* **2011**, *47*, 520-522.

Jokerst, J. V.; Raamanathan, A.; Christodoulides, N.; Floriano, P. N.; Pollard, A. A.; Simmons, G. W.; Wong, J.; Gage, C.; Furmaga, W. B.; Redding, S. W.; McDevitt, J. T. Nano-bio-chips for high performance multiplexed protein detection: Determinations of cancer biomarkers in serum and saliva using quantum dot bioconjugate labels. *Biosens. Bioelectron.* **2009**, *24*, 3622-3629.

Jung, J.-M.; Kwon, K. Y.; Ha, T.-H.; Chung, B. H.; Jung, H.-T. Gold-Conjugated Protein Nanoarrays through Block-Copolymer Lithography: From Fabrication to Biosensor Design. *Small.* **2006**, *2*, 1010-1015.

Kandere-Grzybowska, K.; Campbell, C.; Komarova, Y.; Grzybowski, B. A.; Borisy, G. G. Molecular dynamics imaging in micropatterned living cells. *Nat. Methods.* **2005**, *2*, 739-741.

Kaul, Z.; Yaguchi, T.; Kaul, S. C.; Hirano, T.; Wadhwa, R.; Taira, K. Mortalin imaging in normal and cancer cells with quantum dot immuno-conjugates. *Cell Res.* **2003**, *13*, 503-507.

Kenar, H.; Kocabas, A.; Aydinli, A.; Hasirc, V. Chemical and topographical modification of PHBV surface to promote osteoblast alignment and confinement. *J. Biomed. Mater. Res. A.* **2007**, *85*, 1001-1010.

Kerman, K.; Endo, T.; Tsukamoto, M.; Chikae, M.; Takamura, Y.; Tamiya, E. Quantum dot-based immunosensor for the detection of prostate-specific antigen using fluorescence microscopy. *Talanta.* **2007**, *71*, 1494-1499.

Khanh, N. N.; Yoon, K. B. Facile Organization of Colloidal Particles into Large, Perfect One and Two-Dimensional Arrays by Dry Manual Assembly on Patterned Substrates. *J. Am. Chem. Soc.* **2009**, *131*, 14228-14230.

Kim, H.; Cohen, R. E.; Hammond, P. T.; Irvine, D. J. Live Lymphocyte Arrays for Biosensing. *Adv. Funct. Mater.* **2006**, *16*, 1313-1323.

Kim, H.; Doh, J.; Irvine, D. J.; Cohen, R. E.; Hammond, P. T. Large Area Two-Dimensional B Cell Arrays for Sensing and Cell-Sorting Applications. *Biomacromolecules.* **2004**, *5*, 822-827.

Kim, K. H.; Kim, J. D.; Kim, Y. J.; Kang, S. H.; Jung, S. Y.; Jung, H. Protein Immobilization Without Purification via Dip-Pen Nanolithography. *Small.* **2008**, *4*, 1089-1094.

Kim, M.; Choi, J.-C.; Jung, H.-R.; Katz, J. S.; Kim, M.-G.; Doh, J. Addressable Micropatterning of Multiple Proteins and Cells by Microscope Projection Photolithography Based on a Protein Friendly Photoresist. *Langmuir.* **2010**, *26*, 12112-12118.

Kim, M. B.; Sarelius, I. H. Role of shear forces and adhesion molecule distribution on P-selectin-mediated leukocyte rolling in postcapillary venules. *Am. J. Physiol.-Heart C.* **2004**, *287*, H2705-H2711.

Kim, M. H.; Im, S. H.; Park, O. O. Rapid fabrication of two- and three-dimensional colloidal crystal films via confined convective assembly. *Adv. Funct. Mater.* **2005**, *15*, 1329-1335.

Kita, A.; Sakurai, Y.; Myers, D. R.; Rounsevell, R.; Huang, J. N.; Seok, T. J.; Yu, K.; Wu, M. C.; Fletcher, D. A.; Lam, W. A. Microenvironmental Geometry Guides Platelet Adhesion and Spreading: A Quantitative Analysis at the Single Cell Level. *PLoS ONE.* **2011**, *6*, e26437.

Kosiorek, A.; Kandulski, W.; Glaczynska, H.; Giersig, M. Fabrication of Nanoscale Rings, Dots, and Rods by Combining Shadow Nanosphere Lithography and Annealed Polystyrene Nanosphere Masks. *Small.* **2005**, *1*, 439-444.

Krakert, S.; Ballav, N.; Zharnikov, M.; Terfort, A. Adjustment of the bioresistivity by electron irradiation: self-assembled monolayers of oligo(ethyleneglycol)-terminated alkanethiols with embedded cleavable group. *Phys. Chem. Chem. Phys.* **2010**, *12*, 507-515.

Kramer, M. A.; Park, H. C.; Ivanisevic, A. Dip-Pen Nanolithography on SiOx and Tissue-Derived Substrates: Comparison with Multiple Biological Inks. *Scanning.* **2010**, *32*, 30-34.

Kramer, R. K.; Pholchai, N.; Sorger, V. J.; Yim, T. J.; Oulton, R.; Zhang, X. Positioning of quantum dots on metallic nanostructures. *Nanotechnology.* **2010**, *21*, 145307.

Krämer, S.; Fuierer, R. R.; Gorman, C. B. Scanning Probe Lithography Using Self-Assembled Monolayers. *Chem. Rev.* **2003**, *103*, 4367-4418.

Krsko, P.; Sukhishvili, S.; Mansfield, M.; Clancy, R.; Libera, M. Electron-Beam Surface-Patterned Poly(ethylene glycol) Microhydrogels. *Langmuir.* **2003**, *19*, 5618-5625.

Kumar, N.; Hahm, J.-i. Nanoscale Protein Patterning Using Self-Assembled Diblock Copolymers. *Langmuir.* **2005**, *21*, 6652-6655.

Kumar, N.; Parajuli, O.; Dorfman, A.; Kipp, D.; Hahm, J.-i. Activity Study of Self-Assembled Proteins on Nanoscale Diblock Copolymer Templates. *Langmuir.* **2007**, *23*, 7416-7422.

Kuo, C. W.; Chien, F.-C.; Shiu, J.-Y.; Tsai, S.-M.; Chueh, D.-Y.; Hsiao, Y.-S.; Yang, Z.-H.; Chen, P. Investigation of the growth of focal adhesions using protein nanoarrays fabricated by nanocontact printing using size tunable polymeric nanopillars. *Nanotechnology.* **2011**, *22*, 265302.

Kwon, K. W.; Choi, J.-C.; Suh, K.-Y.; Doh, J. Multiscale Fabrication of Multiple Proteins and Topographical Structures by Combining Capillary Force Lithography and Microscope Projection Photolithography. *Langmuir.* **2011**, *27*, 3238-3243.

Lange, S. A.; Benes, V.; Kern, D. P.; Horber, J. K. H.; Bernard, A. Microcontact printing of DNA molecules. *Anal. Chem.* **2004**, *76*, 1641-1647.

Lau, K. H. A.; Bang, J.; Kim, D. H.; Knoll, W. Self-assembly of Protein Nanoarrays on Block Copolymer Templates. *Adv. Funct. Mater.* **2008**, *18*, 3148-3157.

Lauer, L.; Ingebrandt, S.; Scholl, M.; Offenhausser, A. Aligned microcontact printing of biomolecules on microelectronic device surfaces. *IEEE T. Biomed. Eng.* **2001**, *48*, 838-842.

Lee, D.; King, M. R. Microcontact Printing of P-Selectin Increases the Rate of Neutrophil Recruitment Under Shear Flow. *Biotechnol. Prog.* **2008**, *24*, 1052-1059.

Lee, E.-J.; Chan, E. W. L.; Yousaf, M. N. Spatio-Temporal Control of Cell Coculture Interactions on Surfaces. *ChemBioChem.* **2009**, *10*, 1648-1653.

Lee, J.; Kim, I. S.; Yu, H.-W. Flow Cytometric Detection of Bacillus spoOA Gene in Biofilm Using Quantum Dot Labeling. *Anal. Chem.* **2010**, *82*, 2836-2843.

Lee, K.-B.; Kim, E.-Y.; Mirkin, C. A.; Wolinsky, S. M. The Use of Nanoarrays for Highly Sensitive and Selective Detection of Human Immunodeficiency Virus Type 1 in Plasma. *Nano Lett.* **2004**, *4*, 1869-1872.

Lee, K.-B.; Park, S.-J.; Mirkin, C. A.; Smith, J. C.; Mrksich, M. Protein Nanoarrays Generated By Dip-Pen Nanolithography. *Science.* **2002**, *295*, 1702-1705.

Lee, M.-H.; Chen, Y.-C.; Ho, M.-H.; Lin, H.-Y. Optical recognition of salivary proteins by use of molecularly imprinted poly(ethylene-co-vinyl alcohol)/quantum dot composite nanoparticles. *Anal. Bioanal. Chem.* **2010**, *397*, 1457-1466.

Lee, S. W.; Oh, B.-K.; Sanedrin, R. G.; Salaita, K.; Fujigaya, T.; Mirkin, C. A. Biologically Active Protein Nanoarrays Generated Using Parallel Dip-Pen Nanolithography. *Adv. Mater.* **2006**, *18*, 1133-1136.

Leggett, G. J. Scanning near-field photolithography—surface photochemistry with nanoscale spatial resolution. *Chem. Soc. Rev.* **2006**, *35*, 1150-1161.

Lewandowski, B. R.; Kelley, A. T.; Singleton, R.; Li, J.-R.; Lowry, M.; Warner, I. M.; Garno, J. C. Nanostructures of Cysteine-Coated CdS Nanoparticles Produced with "Two-Particle" Lithography. *J. Phys. Chem. C.* **2009**, *113*, 5933-5940.

Li, B.; Zhang, Y.; Hu, J.; Li, M. Fabricating protein nanopatterns on a single DNA molecule with Dip-pen nanolithography. *Ultramicroscopy.* **2005**, *105*, 312-315.

Li, F.; Li, B.; Wang, Q.-M.; Wang, J. H.-C. Cell Shape Regulates Collagen Type I Expression in Human Tendon Fibroblasts. *Cell Motil. Cytoskel.* **2008**, *65*, 332-341.

Li, H.-W.; Muir, B. V. O.; Fichet, G.; Huck, W. T. S. Nanocontact Printing: A Route to Sub-50-nm-Scale Chemical and Biological Patterning. *Langmuir.* **2003**, *19*, 1963-1965.

Li, J.-R.; Henry, G. C.; Garno, J. C. Fabrication of nanopatterned films of bovine serum albumin and staphylococcal protein A using latex particle lithography. *Analyst.* **2006**, *131*, 244-250.

Li, X.; Liu, Y.; Zhu, A.; Luo, Y.; Deng, Z.; Tian, Y. Real-Time Electrochemical Monitoring of Cellular H2O2 Integrated with In Situ Selective Cultivation of Living Cells Based on Dual Functional Protein Microarrays at Au-TiO2 Surfaces. *Anal. Chem.* **2010**, *82*, 6512-6518.

Li, X.; Wang, T.; Zhang, J.; Yan, X.; Zhang, X.; Zhu, D.; Li, W.; Zhang, X.; Yang, B. Modulating Two-Dimensional Non-Close-Packed Colloidal Crystal Arrays by Deformable Soft Lithography. *Langmuir.* **2010**, *26*, 2930-2936.

Lisboa, P.; Valsesia, A.; Mannelli, I.; Mornet, S.; Colpo, P.; Rossi, F. Sensitivity enhancement of surface-plasmon resonance imaging by nanoarrayed organothiols. *Adv. Mater.* **2008**, *20*, 2352-2358.

Liu, D.; Abdullah, C. A. C.; Sear, R. P.; Keddie, J. L. Cell adhesion on nanopatterned fibronectin substrates. *Soft Matter.* **2010**, *6*, 5408-5416.

Liu, D.; Wang, T.; Keddie, J. L. Protein Nanopatterning on Self-Organized Poly(styrene-b-isoprene) Thin Film Templates. *Langmuir.* **2009**, *25*, 4526-4534.

Liu, J.; Bao, C.; Zhong, X.; Zhao, C.; Zhu, L. Highly selective detection of glutathione using a quantum-dot-based OFF–ON fluorescent probe. *Chem. Commun.* **2010**, *46*, 2971-2973.

Liu, J.; Lau, S. K.; Varma, V. A.; Moffitt, R. A.; Caldwell, M.; Liu, T.; Young, A. N.; Petros, J. A.; Osunkoya, A. O.; Krogstad, T.; Leyland-Jones, B.; Wang, M. D.; Nie, S. Heterogeneity on Clinical Tissue Specimens with Multiplexed Quantum Dots. *ACS Nano.* **2010**, *4*, 2755-2765.

Liu, S. H.; Wang, W. M.; Mannsfeld, S. C. B.; Locklin, J.; Erk, P.; Gomez, M.; Richter, F.; Bao, Z. N. Solution-assisted assembly of organic semiconducting single crystals on surfaces with patterned wettability. *Langmuir.* **2007**, *23*, 7428-7432.

Liu, S. T.; Maoz, R.; Schmid, G.; Sagiv, J. Template guided self-assembly of [Au_{55}] clusters on nanolithographically defined monolayer patterns. *Nano Lett.* **2002**, *2*, 1055-1060.

Liu, X.-h.; Wang, H.-k.; Herron, J. N.; Prestwich, G. D. Photopatterning of Antibodies on Biosensors. *Bioconjugate Chem.* **2000**, *11*, 755-761.

Liu, Y.; Yan, J.; Howland, M. C.; Kwa, T.; Revzin, A. Micropatterned Aptasensors for Continuous Monitoring of Cytokine Release from Human Leukocytes. *Anal. Chem.* **2011**, *83*, 8286-8292.

Lohmüller, T.; Aydin, D.; Schwieder, M.; Morhard, C.; Louban, I.; Pacholski, C.; Spatz, J. P. Nanopatterning by block copolymer micelle nanolithography and bioinspired applications. *Biointerphases.* **2011**, *6*, MR1-MR12.

Lohmüller, T.; Triffo, S.; O'Donoghue, G. P.; Xu, Q.; Coyle, M. P.; Groves, J. T. Supported Membranes Embedded with Fixed Arrays of Gold Nanoparticles. *Nano Lett.* **2011**, *11*, 4912-4918.

Lusker, K. L.; Li, J.-R.; Garno, J. C. Nanostructures of Functionalized Gold Nanoparticles Prepared by Particle Lithography with Organosilanes. *Langmuir.* **2011**, *27*, 13269-13275.

Lussi, J. W.; Tang, C.; Kuenzi, P.-A.; Staufer, U.; Csucs, G.; Vörös, J.; Gaudenz Danuser; Hubbell, J. A.; Textor, M. Selective molecular assembly patterning at the nanoscale: a novel platform for producing protein patterns by electron-beam lithography on SiO2/indium tin oxide-coated glass substrates. *Nanotechnology.* **2005**, *16*, 1781-1786.

Manz, B. N.; Jackson, B. L.; Petit, R. S.; Dustin, M. L.; Groves, J. T-cell triggering thresholds are modulated by the number of antigen within individual T-cell receptor clusters. *P. Natl. Acad. Sci. USA.* **2011**, *108*, 9089-9094.

Mark, S. S.; Bergkvist, M.; Yang, X.; Teixeira, L. M.; Bhatnagar, P.; Angert, E. R.; Batt, C. A. Bionanofabrication of Metallic and Semiconductor Nanoparticle Arrays Using S-Layer Protein Lattices with Different Lateral Spacings and Geometries. *Langmuir.* **2006**, *22*, 3763-3774.

Marquez, M.; Grady, B. P. The use of surface tension to predict the formation of 2D arrays of latex spheres formed via the Langmuir-Blodgett-like technique. *Langmuir.* **2004**, *20*, 10998-11004.

Marquez, M.; Patel, K.; Carswell, A. D. W.; Schmidtke, D. W.; Grady, B. P. Synthesis of Nanometer-Scale Polymeric Structures on Surfaces from Template Assisted Admicellar Polymerization: A Comparative Study with Protein Adsorption. *Langmuir.* **2006**, *22*, 8010-8016.

Maury, P.; Escalante, M.; Péter, M.; Reinhoudt, D. N.; Subramaniam, V.; Huskens, J. Creating Nanopatterns of His-Tagged Proteins on Surfaces by Nanoimprint Lithography Using Specific NiNTA-Histidine Interactions. *Small.* **2007**, *3*, 1584-1592.

McDevitt, T. C.; Woodhouse, K. A.; Hauschka, S. D.; Murry, C. E.; Stayton, P. S. Spatially organized layers of cardiomyocytes on biodegradable polyurethane films for myocardial repair. *J. Biomed. Mater. Res. A.* **2003**, *66*, 586-595.

McEver, R. P.; Beckstead, J. H.; Moore, K. L.; Marshall-Carlson, L.; Bainton, D. F. GMP-140, a Platelet a-Granule Membrane Protein, Is Also Synthesized by Vascular Endothelial Cells and Is Localized in Weibel-Palade Bodies. *J. Clin. Invest.* **1989**, *84*, 92-99.

Mendes, P. M.; Yeung, C. L.; Preece, J. A. Bio-nanopatterning of Surfaces. *Nanoscale Res. Lett.* **2007**, *2*, 373-384.

Merino, S.; Retolaza, A.; Trabadelo, V.; Cruz, A.; Heredia, P.; Alduncín, J. A.; Mecerreyes, D.; Fernández-Cuesta, I.; Borrisé, X.; Pérez-Murano, F. Protein patterning on the micro- and nanoscale by thermal nanoimprint lithography on a new functionalized copolymer. *J. Vac. Sci. Technol. B.* **2009**, *27*, 2439-2443.

Messing, R. A. Adsorption of Protein on Glass Surfaces and Pertinent Parameters for the Immobilizatoin of Enzymes in the Pores of Inorganic Carriers. *J. Non-Cryst. Solids*. **1975**, *19*, 277-283.

Mettlen, M.; Loerke, D.; Yarar, D.; Danuser, G.; Schmid, S. L. Cargo- and adaptor-specific mechanisms regulate clathrin-mediated endocytosis. *J. Cell Biol.* **2010**, *188*, 919-933.

Miao, Y. H.; Helseth, L. E. Adsorption of bovine serum albumin on polyelectrolyte-coated glass substrates: Applications to colloidal lithography. *Colloid. Surface. B.* **2008**, *66*, 299-303.

Miller, E. D.; Li, K.; Kanade, T.; Weiss, L. E.; Walker, L. M.; Campbell, P. G. Spatially directed guidance of stem cell population migration by immobilized patterns of growth factors. *Biomaterials.* **2011**, *32*, 2775-2785.

Miller, J. S.; Bethencourt, M. I.; Hahn, M.; Lee, T. R.; West, J. L. Laser-scanning lithography (LSL) for the soft lithographic patterning of cell-adhesive self-assembled monolayers. *Biotechnol. Bioeng.* **2006**, *93*, 1060-1068.

Miner, J. J.; Xia, L.; Yago, T.; Kappelmayer, J.; Liu, Z.; Klopocki, A. G.; Shao, B.; McDaniel, J. M.; Setiadi, H.; Schmidtke, D. W.; McEver, R. P. Separable requirements for cytoplasmic domain of PSGL-1 in leukocyte rolling and signaling under flow. *Blood.* **2008**, *1112*, 2035-2045.

Mooney, J. F.; Hunt, A. J.; McIntosh, J. R.; Liberko, C. A.; Walba, D. M.; Rogers, C. T. Patterning of functional antibodies and other proteins by photolithography of silane monolayers. *P. Natl. Acad. Sci. USA.* **1996**, *93*, 12287-12291.

Moore, K. L.; Patel, K. D.; Bruehl, R. E.; Fugang, L.; Johnson, D. A.; Lichenstein, H. S.; Cummings, R. D.; Bainton, D. F.; McEver, R. P. P-Selectin Glycoprotein Ligand-1 Mediates Rolling of Human Neutrophils on P-Selectin. *J. Cell Biol.* **1995**, *128*, 661-671.

Mossman, K. D.; Campi, G.; Groves, J. T.; Dustin, M. L. Altered TCR Signaling from Geometrically Repatterned Immunological Synapses. *Science.* **2005**, *310*, 1191-1193.

Mrksich, M.; Chen, C. S.; Xia, Y. N.; Dike, L. E.; Ingber, D. E.; Whitesides, G. M. Controlling cell attachment on contoured surfaces with self-assembled monolayers of alkanethiolates on gold. *P. Natl. Acad. Sci. USA.* **1996**, *93*, 10775-10778.

Muir, B. W.; Fairbrother, A.; Gengenbach, T. R.; Rovere, F.; Abdo, M. A.; McLean, K. M.; Hartley, P. G. Scanning Probe Nanolithography and Protein Patterning of Low-Fouling Plasma Polymer Multilayer Films. *Adv. Mater.* **2006**, *2006*, 3079-3082.

Nalayanda, D. D.; Kalukanimuttam, M.; Schmidtke, D. W. Micropatterned surfaces for controlling cell adhesion and rolling under flow. *Biomed. Microdevices.* **2007**, *9*, 207-214.

Neeves, K. B.; Maloney, S. F.; Fong, K. P.; Schmaier, A. A.; Kahn, M. L.; Brass, L. F.; Diamond, S. L. Microfluidic focal thrombosis model for measuring murine platelet deposition and stability: PAR4 signaling enhances shear-resistance of platelet aggregates. *J. Thromb. Haemost.* **2008**, *6*, 2193-2201.

Nelson, C. M.; Chen, C. S. Cell-cell signalling by direct contact increases cell proliferation via a PI3K-dependent signal. *FEBS Lett.* **2002**, *514*, 238-242.

Netzer, L.; Iscovici, R.; Sagiv, J. Adsorbed Monolayeres Versus Langmuir-Blodgett Monolayers Why and How. 1. From Monolayer to Multilayer, By Adsorption. *Thin Solid Films.* **1983**, *99*, 235-241.

Ngunjiri, J.; Garno, J. C. AFM-Based Lithography for Nanoscale Protein Assays. *Anal. Chem.* **2008**, *80*,

Ngunjiri, J. N.; Daniels, S. L.; Li, J.-R.; Serem, W. K.; Garno, J. C. Controlling the surface coverage and arrangement of proteins using particle lithography. *Nanomedicine.* **2008**, *3*, 529-541.

Nicolau, D. V.; Taguchi, T.; Taniguchi, H.; Yoshikawa, S. Negative and positive tone protein patterning on e-beam/deep-UV resists. *Langmuir.* **1999**, *15*, 3845-3851.

Nishizawa, M.; Takoh, K.; Matsue, T. Micropatterning of HeLa Cells on Glass Substrates and Evaluation of Respiratory Activity Using Microelectrodes. *Langmuir.* **2002**, *18*, 3645-3649.

Nurunnabi, M.; Cho, K. J.; Choi, J. S.; Huh, K. M.; Lee, Y.-k. Targeted near-IR QDs-loaded micelles for cancer therapy and imaging. *Biomaterials.* **2010**, *31*, 5436-5444.

Onclin, S.; Ravoo, B. J.; Reinhoudt, D. N. Engineering silicon oxide surfaces using self-assembled monolayers. *Angew. Chem. Int. Edit.* **2005**, *44*, 6282-6304.

Parajuli, O.; Gupta, A.; Kumar, N.; Hahm, J.-i. Evaluation of Enzymatic Activity on Nanoscale Polystyrene-block-Polymethylmethacrylate Diblock Copolymer Domains. *J. Phys. Chem. B.* **2007**, *111*, 14022-14027.

Park, J. W.; Park, A.-Y.; Lee, S.; Yu, N.-K.; Lee, S.-H.; Kaang, B.-K. Detection of TrkB Receptors Distributed in Cultured Hippocampal Neurons through Bioconjugation between Highly Luminescent (Quantum Dot-Neutravidin) and (Biotinylated Anti-TrkB Antibody) on Neurons by Combined Atomic Force Microscope and Confocal Laser Scanning Microscope. *Bioconjugate Chem.* **2010**, *21*, 597-603.

Park, M.; Harrison, C.; Chaikin, P. M.; Register, R. A.; Adamson, D. H. Block Copolymer Lithography: Periodic Arrays of ~10^{11} Holes in 1 Square Centimeter. *Science.* **1997**, *276*, 1401-1404.

Park, S. H.; Xia, Y. N. Assembly of mesoscale particles over large areas and its application in fabricating tunable optical filters. *Langmuir.* **1999**, *15*, 266-273.

Pattani, V. P.; Li, C.; Desai, T. A.; Vu, T. Q. Microcontact printing of quantum dot bioconjugate arrays for localized capture and detection of biomolecules. *Biomed. Microdevices.* **2008**, *10*, 367-374.

Peng, C.; Li, Z.; Zhu, Y.; Chen, W.; Yuan, Y.; Liu, L.; Li, Q.; Xu, D.; Qiao, R.; Wang, L.; Zhu, S.; Jin, Z.; Xu, C. Simultaneous and sensitive determination of multiplex chemical residues based on multicolor quantum dot probes. *Biosens. Bioelectron.* **2009**, *24*, 3657-3662.

Pesen, D.; Haviland, D. B. Modulation of Cell Adhesion Complexes by Surface Protein Patterns. *ACS Appl. Mater. Interfaces.* **2009**, *1*, 543-548.

Pesen, D.; Heinz, W. F.; Werbin, J. L.; Hoh, J. H.; Haviland, D. B. Electron beam patterning of fibronectin nanodots that support focal
adhesion formation. *Soft Matter.* **2007**, *3*, 1280-1284.

Rakickas, T.; Gavutis, M.; Reichel, A.; Piehler, J.; Liedberg, B.; Valiokas, R. Protein-Protein Interactions in Reversibly Assembled Nanopatterns. *Nano Lett.* **2008**, *8*, 3369-3375.

Ramachandran, V.; Williams, M.; Yago, T.; Schmidtke, D. W.; McEver, R. P. Dynamic alterations of membrane tethers stabilize leukocyte rolling on P-selectin *P. Natl. Acad. Sci. USA.* **2004**, *101*, 13519-13524.

Rauf, S.; Glidle, A.; Cooper, J. M. Application of quantum dot barcodes prepared using biological self-assembly to multiplexed immunoassays. *Chem. Commun.* **2010**, *46*, 2814-2816.

Renault, J. P.; Bernard, A.; Bietsch, A.; Michel, B.; Bosshard, H. R.; Delamarche, E. Fabricating Arrays of Single Protein Molecules on Glass Using Microcontact Printing. *J. Phys. Chem. B.* **2003**, *107*, 703-711.

Retsch, M.; Tamm, M.; Bocchio, N.; Horn, N.; Förch, R.; Jonas, U.; Kreiter, M. Parallel Preparation of Densely Packed Arrays of 150-nm Gold-Nanocrescent Resonators in Three Dimensions. *Small.* **2009**, *5*, 2105-2110.

Reynolds, N. P.; Janusz, S.; Escalante-Marun, M.; Timney, J.; Ducker, R. E.; Olsen, J. D.; Otto, C.; Subramaniam, V.; Leggett, G. J.; Hunter, C. N. Directed Formation of Micro- and Nanoscale Patterns of Functional Light-Harvesting LH2 Complexes. *J. Am. Chem. Soc.* **2007**, *129*, 14625-14631.

Rieger, J. The glass transition temperature of polystyrene. *J. Therm. Anal.* **1996**, *46*, 965-972.

Robel, I.; Subramanian, V.; Kuno, M.; Kamat, P. V. Quantum Dot Solar Cells. Harvesting Light Energy with CdSe Nanocrystals Molecularly Linked to Mesoscopic TiO_2 Films. *J. Am. Chem. Soc.* **2006**, *128*, 2385-2393.

Roberts, T. M.; Streitmatter, G. Membrane-substrate contact under the spermatozoon of Caenorhabditis elegans, a crawling cell that lacks filamentous actin. *J. Cell Sci.* **1984**, *69*, 117-126.

Robin, S.; Gandhi, A. A.; Gregor, M.; Laffir, F. R.; Plecenik, T.; Plecenik, A.; Soulimane, T.; Tofail, S. A. M. Charge Specific Protein Placement at Submicrometer and Nanometer Scale by Direct Modification of Surface Potential by Electron Beam. *Langmuir.* **2011**, *27*, 14968-14974.

Rossi, R. C.; Tan, M. X.; Lewis, N. S. Size-dependent electrical behavior of spatially inhomogeneous barrier height regions on silicon. *Appl. Phys. Lett.* **2000**, *77*, 2698-2700.

Rowe, C. A.; Tender, L. M.; Feldstein, M. J.; Golden, J. P.; Scruggs, S. B.; MacCraith, B. D.; Cras, J. J.; Ligler, F. S. Array Biosensor for Simultaneous Identification of Bacterial, Viral, and Protein Analytes. *Anal. Chem.* **1999**, *71*, 3846-3852.

Rozhok, S.; Shen, C. K.-F.; Littler, P.-L. H.; Fan, Z.; Liu, C.; Mirkin, C. A.; Holz, R. C. Methods for Fabricating Microarrays of Motile Bacteria. *Small.* **2005**, *1*, 445-451.

Rozkiewicz, D. I.; Kraan, Y.; Werten, M. W. T.; Wolf, F. A. d.; Subramaniam, V.; Ravoo, B. J.; Reinhoudt, D. N. Covalent Microcontact Printing of Proteins for Cell Patterning. *Chem.-Eur. J.* **2006**, *12*, 6290-6297.

Ruiz, S. A.; Chen, C. S. Microcontact printing: A tool to pattern. *Soft Matter.* **2007**, *3*, 168-177.

Rundqvist, J.; Mendoza, B.; Werbin, J. L.; Heinz, W. F.; Lemmon, C.; Romer, L. H.; Haviland, D. B.; Hoh, J. H. High Fidelity Functional Patterns of an Extracellular Matrix Protein by Electron Beam-Based Inactivation. *J. Am. Chem. Soc.* **2007**, *129*, 59-67.

Sabella, S.; Brunetti, V.; Vecchio, G.; Torre, A. D.; Rinaldi, R.; Cingolani, R.; Pompa, P. P. Micro/Nanoscale Parallel Patterning of Functional Biomolecules, Organic Fluorophores and Colloidal Nanocrystals. *Nanoscale Res. Lett.* **2009**, *4*, 1222-1229.

Sagiv, J. Organized Monolayers By Adsorption. 1. Formation and Structure of Oleophobic Mixed Monolayers on Solid Surfaces. *J. Am. Chem. Soc.* **1980**, *102*, 92-98.

Salaita, K.; Wang, Y.; Fragala, J.; Vega, R. A.; Liu, C.; Mirkin, C. A. Massively Parallel Dip–Pen Nanolithography with 55000-Pen Two-Dimensional Arrays. *Angew. Chem. Int. Edit.* **2006**, *45*, 7220-7223.

Saux, G. L.; Magenau, A.; Gunaratnam, K.; Kilian, K. A.; Böcking, T.; Gooding, J. J.; Gaus, K. Spacing of Integrin Ligands Influences Signal Transduction in Endothelial Cells. *Biophys. J.* **2011**, *101*, 764-773.

Schmidt, B. J.; Huang, P.; Breuer, K. S.; Lawrence, M. B. Catch Strip Assay for the Relative Assessment of Two-Dimensional Protein Association Kinetics. *Anal. Chem.* **2008**, *80*, 944-950.

Schmidt, R. C.; Healy, K. E. Controlling biological interfaces on the nanometer length scale. *J. Biomed. Mater. Res. A.* **2009**, *90*, 1252-1261.

Schurch, S.; Gehr, P.; Green, F.; Wallace, J. A.; McIver, D. J. L. Cell-substrate adhesion affects intracellular motility of pulmonary macrophages. *Colloid. Surface.* **1989**, *42*, 271-288.

Schvartzman, M.; Nguyen, K.; Palma, M.; Abramson, J.; Sable, J.; Hone, J.; Sheetz, M. P.; Wind, S. J. Fabrication of nanoscale bioarrays for the study of cytoskeletal protein binding interactions using nanoimprint lithography. *J. Vac. Sci. Technol. B.* **2009**, *27*, 61-65.

Schvartzman, M.; Palma, M.; Sable, J.; Abramson, J.; Hu, X.; Sheetz, M. P.; Wind, S. J. Nanolithographic Control of the Spatial Organization of Cellular Adhesion Receptors at the Single-Molecule Level. *Nano Lett.* **2011**, *11*, 1306-1312.

Schvartzman, M.; Wind, S. J. Robust Pattern Transfer of Nanoimprinted Features for Sub-5-nm Fabrication. *Nano Lett.* **2009**, *9*, 3629-3634.

Seisyan, R. P. Nanolithography in Microelectronics: A Review. *Tech. Phys.* **2011**, *56*, 1061-1073.

Senesi, A. J.; Rozkiewicz, D. I.; Reinhoudt, D. N.; Mirkin, C. A. Agarose-Assisted Dip-Pen Nanolithography of Oligonucleotides and Proteins. *ACS Nano.* **2009**, *3*, 2394-2402.

Sengupta, K.; Aranda-Espinoza, H.; Smith, L.; Janmey, P.; Hammer, D. Spreading of Neutrophils: From Activation to Migration. *Biophys. J.* **2006**, *91*, 4638-4648.

Setiadi, H.; Disdier, M.; Green, S. A.; Canfield, W. M.; McEver, R. P. Residues Throughout the Cytoplasmic Domain Affect the Internalization Efficiency of P-selectin. *J. Biol. Chem.* **1995**, *45*, 26818-26826.

Shallcross, R. C.; Chawla, G. S.; Marikkar, F. S.; Tolbert, S.; Pyun, J.; Armstrong, N. R. Efficient CdSe Nanocrystal Diffraction Gratings Prepared by Microcontact Molding. *ACS Nano.* **2009**, *3*, 3629-3637.

Sharma, S.; Johnson, R. W.; Desai, T. A. Evaluation of the stability of nonfouling ultrathin poly(ethylene glycol) films for silicon-based microdevices. *Langmuir.* **2004**, *20*, 348-356.

Shen, K.; Thomas, V. K.; Dustin, M. L.; Kam, L. C. Micropatterning of costimulatory ligands enhances CD4+ T cell function. *P. Natl. Acad. Sci. USA.* **2008**, *105*, 7791-7796.

Shen, K.; Tsai, J.; Shi, P.; Kam, L. C. Self-Aligned Supported Lipid Bilayers for Patterning the Cell-Substrate Interface. *J. Am. Chem. Soc.* **2009**, *131*, 13204-13205.

Shin, D.-S.; Lee, K.-N.; Jang, K.-H.; Kim, J.-K.; Chung, W.-J.; Kim, Y.-K.; Lee, Y.-S. Protein patterning by maskless photolithography on hydrophilic polymer-grafted surface. *Biosens. Bioelectron.* **2003**, *19*, 485-494.

Shuster, M. J.; Vaish, A.; Cao, H. H.; Guttentag, A. I.; McManigle, J. E.; Gibb, A. L.; Martinez, M. M.; Nezarati, R. M.; Hinds, J. M.; Liao, W.-S.; Weiss, P. S.; Andrews, A. M. Patterning small-molecule biocapture surfaces: microcontact insertion printing vs. photolithography. *Chem. Commun.* **2011**, *47*, 10641-10643.

Singh, G.; Gohri, V.; Pillai, S.; Arpanaei, A.; Foss, M.; Kingshottz, P. Large-Area Protein Patterns Generated by Ordered Binary Colloidal Assemblies as Templates. *Nano Lett.* **2011**, *5*, 3542-3551.

Singh, G.; Griesser, H. J.; Bremmell, K.; Kingshott, P. Highly Ordered Nanometer-Scale Chemical and Protein Patterns by Binary Colloidal Crystal Lithography Combined with Plasma Polymerization. *Adv. Funct. Mater.* **2011**, *21*, 540-546.

Singhvi, R.; Kumar, A.; Lopez, G. P.; Stephanopoulos, G. N.; Wang, D. C.; Whitesides, G. M.; Ingber, D. E. Engineering Cell Shape and Function. *Science.* **1994**, *264*, 696-698.

Slater, J. H.; Frey, W. Nanopatterning of fibronectin and the influence of integrin clustering on endothelial cell spreading and proliferation. *J. Biomed. Mater. Res. A.* **2008**, *87*, 176-195.

Son, J. G.; Bae, W. K.; Kang, H.; Nealey, P. F.; Char, K. Placement Control of Nanomaterial Arrays on the Surface-Reconstructed Block Copolymer Thin Films. *ACS Nano.* **2009**, *3*, 3927-3934.

Sorribas, H.; Padeste, C.; Tiefenauer, L. Photolithographic generation of protein micropatterns for neuron culture applications. *Biomaterials.* **2002**, *23*, 893-900.

Stachowiak, A. N.; Irvine, D. J. Inverse opal hydrogel-collagen composite scaffolds as a supportive microenvironment for immune cell migration. *J. Biomed. Mater. Res. A.* **2008**, *85*, 815-828.

Su, X.-L.; Li, Y. Quantum Dot Biolabeling Coupled with Immunomagnetic Separation for Detection of Escherichia coli O157:H7. *Anal. Chem.* **2004**, *76*, 4806-4810.

Subramaniam, V.; Bhattacharya, P. K.; Memon, A. A. Chemical Contamination of Thin Oxides and Native Silicon for Use in Modern Device Processing. *Int. J. Electron.* **1995**, *78*, 519-525.

Sun, F. Q.; Cai, W. P.; Li, Y.; Cao, B. Q.; Lu, F.; Duan, G. T.; Zhang, L. D. Morphology control and transferability of ordered through-pore arrays based on electrodeposition and colloidal monolayers. *Adv. Mater.* **2004**, *16*, 1116-1121.

Swiston, A. J.; Cheng, C.; Um, S. H.; Irvine, D. J.; Cohen, R. E.; Rubner, M. F. Surface Functionalization of Living Cells with Multilayer Patches. *Nano Lett.* **2008**, *8*, 4446-4453.

Tan, J.; Shen, H.; Saltzman, W. M. Micron-Scale Positioning of Features Influences the Rate of Polymorphonuclear Leukocyte Migration. *Biophys. J.* **2001**, *81*, 2569-2579.

Taylor, Z. R.; Patel, K.; Spain, T. G.; Keay, J. C.; Jernigen, J. D.; Sanchez, E. S.; Grady, B. P.; Johnson, M. B.; Schmidtke, D. W. Fabrication of Protein Dot Arrays via Particle Lithography. *Langmuir.* **2009**, *25*, 10932-10938.

Taylor, Z. R.; Sanchez, E. S.; Keay, J. C.; Johnson, M. B.; Schmidtke, D. W. Patterning of Quantum Dot Bioconjugates via Particle Lithography. *Langmuir.* **2010**, *26*, 18938-18944.

Thelen, K.; Wolfram, T.; Maier, B.; Jährling, S.; Tinazli, A.; Piehler, J.; Spatz, J. P.; Pollerberg, G. E. Cell adhesion molecule DM-GRASP presented as nanopatterns to neurons regulates attachment and neurite growth. *Soft Matter.* **2007**, *3*, 1486-1491.

Thibault, C.; Le Berre, V.; S., C.; Trévisiol, E.; François, J.; Vieu, C. Direct microcontact printing of oligonucleotides for biochip applications. *J. Nanobiotechnol.* **2005**, *3*, 7.

Thomas, C. H.; Collier, J. H.; Sfeir, C. S.; Healy, K. E. Engineering gene expression and protein synthesis by modulation of nuclear shape. *P. Natl. Acad. Sci. USA.* **2002**, *99*, 1972-1977.

Thomas, C. H.; Lhoest, J.-B.; Castner, D. G.; McFarland, C. D.; Healy, K. E. Surfaces Designed to Control the Projected Area and Shape of Individual Cells. *J. Biomech. Eng.-T. ASME.* **1999**, *121*, 40-48.

Tinazli, A.; Piehler, J.; Beuttler, M.; Guckenberger, R.; Tampé, R. Native protein nanolithography that can write, read and erase. *Nat. Nanotechnol.* **2007**, *2*, 220-225.

Trau, M.; Saville, D. A.; Aksay, I. A. Field-induced layering of colloidal crystals *Science.* **1996**, *272*, 706-709.

Tuleuova, N.; Revzin, A. Micropatterning of Aptamer Beacons to Create Cytokine-Sensing Surfaces. *Cell. Mol. Bioeng.* **2010**, *3*, 337-344.

Vail, T. L.; Cushing, K.; Ingram, J. C.; Omer, I. S. Micropatterned avidin arrays on silicon substrates via photolithography, self-assembly and bioconjugation. *Biotechnol. Appl. Bioc.* **2006**, *43*, 85-91.

Valsesia, A.; Colpo, P.; Manneill, I.; Mornet, S.; Bretagnol, F.; Ceccone, G.; Rossi, F. Use of nanopatterned surfaces to enhance immunoreaction efficiency. *Anal. Chem.* **2008**, *80*, 1418-1424.

Valsesia, A.; Colpo, P.; Meziani, T.; Lisboa, P.; Lejeune, M.; Rossi, F. Immobilization of Antibodies on Biosensing Devices by Nanoarrayed Self-Assembled Monolayers. *Langmuir.* **2006**, *22*, 1763-1767.

Valsesia, A.; Colpo, P.; Silvan, M. M.; Meziani, T.; Ceccone, G.; Rossi, F. Fabrication of Nanostructured Polymeric Surfaces for Biosensing Devices. *Nano Lett.* **2004**, *4*, 1047-1050.

Valsesia, A.; Mannelli, I.; Colpo, P.; Bretagnol, F.; Rossi, F. Protein Nanopatterns for Improved Immunodetection Sensitivity. *Anal. Chem.* **2008**, *80*, 7336-7340.

Valsesia, A.; Meziani, T.; Bretagnol, F.; Colpo, P.; Ceccone, G.; Rossi, F. Plasma assisted production of chemical nano-patterns by nano-sphere lithography: application to bio-interfaces. *J. Phys. D Appl. Phys.* **2007**, *40*, 2341-2347.

vanBlaaderen, A.; Ruel, R.; Wiltzius, P. Template-directed colloidal crystallization. *Nature.* **1997**, *385*, 321-324.

Veiseh, M.; Zareie, M. H.; Zhang, M. Highly Selective Protein Patterning on Gold-Silicon Substrates for Biosensor Applications. *Langmuir.* **2002**, *18*, 6671-6678.

Velev, O. D.; Jede, T. A.; Lobo, R. F.; Lenhoff, A. M. Microstructured porous silica obtained via colloidal crystal templates. *Chem. Mater.* **1998**, *10*, 3597-3602.

Verma, V.; Hancock, W. O.; Catchmark, J. M. Nanoscale patterning of kinesin motor proteins and its role in guiding microtubule motility. *Biomed. Microdevices.* **2009**, *11*, 313-322.

Verschueren, H. Interference reflection microscopy in cell biology: methodology and applications. *J. Cell Sci.* **1985**, *75*, 279-301.

Vörös, J.; Blättler, T. M.; Textor, M. Bioactive patterns at the 100-nm scale produced using multifunctional physisorbed monolayers. *MRS Bull.* **2005**, *30*, 202-206.

Wadu-Mesthrige, K.; Xu, S.; Amro, N. A.; Liu, G.-y. Fabrication and Imaging of Nanometer-Sized Protein Patterns. *Langmuir.* **1999**, *15*, 8580-8583.

Wagner, H.; Li, Y.; Hirtz, M.; Chi, L.; Fuchs, H.; Studer, A. Site specific protein immobilization into structured polymer brushes prepared by AFM lithography. *Soft Matter.* **2011**, *7*, 9854-9858.

Wang, D.; Kodali, V. K.; II, W. D. U.; Jarvholm, J. E.; Okada, T.; Jones, S. C.; Rumi, M.; Dai, Z.; King, W. P.; Marder, S. R.; Curtis, J. E.; Riedo, E. Thermochemical Nanolithography of Multifunctional Nanotemplates for Assembling Nano-Objects. *Adv. Funct. Mater.* **2009**, *19*, 3696-3702.

Wang, X.; Lou, X.; Wang, Y.; Guo, Q.; Fang, Z.; Zhong, X.; Mao, H.; Jin, Q.; Wu, L.; Zhao, H.; Zhao, J. QDs-DNA nanosensor for the detection of hepatitis B virus DNA and the single-base mutants. *Biosens. Bioelectron.* **2010**, *25*, 1934-1940.

Wang, X. D.; Graugnard, E.; King, J. S.; Zhong, L. W.; Summers, C. J. Large-scale fabrication of ordered nanobowl arrays. *Nano Lett.* **2004**, *4*, 2223-2226.

Wang, Y. C.; Ho, C.-C. Micropatterning of proteins and mammalian cells on biomaterials *FASEB J.* **2004**, *18*, 525-527.

Winzer, M.; Kleiber, M.; Dix, N.; Wiesendanger, R. Fabrication of nano-dot- and nano-ring-arrays by nanosphere lithography. *Appl. Phys. A-Mater.* **1996**, *63*, 617-619.

Wolfram, T.; Belz, F.; Schoen, T.; Spatz, J. P. Site-specific presentation of single recombinant proteins in defined nanoarrays. *Biointerphases.* **2007**, *2*, 44-48.

Xia, Y.; Tien, J.; Qin, D.; Whitesides, G. M. Non-Photolithographic Methods for Fabrication of Elastomeric Stamps for Use in Microcontact Printing. *Langmuir.* **1996**, *12*, 4033-4038.

Xia, Y.; Yin, Y.; Lu, Y.; McLellan, J. Template-Assisted Self-Assembly of Spherical Colloids into Complex and Controllable Structures. *Adv. Funct. Mater.* **2003**, *13*, 907-918.

Xing, C.; Zheng, Z.; Zhang, B.; Tang, J. Nanoscale Patterning of Multicomponent Proteins by Bias-Assisted Atomic Force Microscopy Nanolithography. *ChemPhysChem.* **2011**, *12*, 1262-1265.

Yago, T.; Shao, B. J.; Miner, J. J.; Yao, L. B.; Klopocki, A. G.; Maeda, K.; Coggeshall, K. M.; McEver, R. P. E-selectin engages PSGL-1 and CD44 through a common signaling pathway to induce integrin $\alpha_L\beta_2$-mediated slow leukocyte rolling *Blood.* **2010**, *116*, 485-494.

Yamazoe, H.; Uemura, T.; Tanabe, T. Facile Cell Patterning on an Albumin-Coated Surface. *Langmuir.* **2008**, *24*, 8402-8404.

Yang, S. M.; Jang, S. G.; Choi, D. G.; Kim, S.; Yu, H. K. Nanomachining by colloidal lithography. *Small.* **Small**, *2*, 458-475.

Yoffe, A. D. Semiconductor quantum dots and related systems: electronic, optical, luminescence and related properties of low dimensional systems. *Adv. Phys.* **2001**, *50*, 1-208.

Yu, C.-h.; Wu, H.-J.; Kaizuka, Y.; Vale, R. D.; Groves, J. T. Altered Actin Centripetal Retrograde Flow in Physically Restricted Immunological Synapses. *PLoS ONE.* **2010**, *5*, e11878.

Yu, W. W.; Chang, E.; Drezek, R.; Colvin, V. L. Water-soluble quantum dots for biomedical applications. *Biochem. Biophys. Res. Commun.* **2006**, *348*, 781-786.

Zarbock, A.; Abram, C. L.; Hundt, M.; Altman, A.; Lowell, C. A.; Ley, K. PSGL-1 engagement by E-selectin signals through Src kinase Fgr and ITAM adapters DAP12 and FcRg to induce slow leukocyte rolling. *J. Exp. Med.* **2008**, *205*, 2339-2347.

Zarbock, A.; Lowell, C. A.; Ley, K. Spleen tyrosine kinase syk is necessary for E-Selectin-induced $\alpha_L\beta_2$ integrin-mediated rolling on intercellular adhesion molecule-1 *Immunity.* **2007**, *26*, 773-783.

Zhang, G.; Wang, D.; Möhwald, H. Fabrication of Multiplex Quasi-Three-Dimensional Grids of One-Dimensional Nanostructures via Stepwise Colloidal Lithography. *Nano Lett.* **2007**, *7*, 3410-3413.

Zhang, G. J.; Tanii, T.; Zako, T.; Hosaka, T.; Miyake, T.; Kanari, Y.; Funatsu, T. W.; Ohdomari, I. Nanoscale patterning of protein using electron beam lithography of organosilane self-assembled monolayers. *Small.* **2005**, *1*, 833-837.

Zhang, H.; Xu, T.; Li, C.-W.; Yang, M. A microfluidic device with microbead array for sensitive virus detection and genotyping using quantum dots as fluorescence labels. *Biosens. Bioelectron.* **2010**, *25*, 2402-2407.

Zhao, Y.; Li, M.; Lu, Q. H.; Shi, Z. Y. Superhydrophobic Polyimide Films with a Hierarchical Topography: Combined Replica Molding and Layer-by-Layer Assembly. *Langmuir.* **2008**, *24*, 12651-12657.

Zheng, H.; Berg, M. C.; Rubner, M. F.; Hammond, P. T. Controlling Cell Attachment Selectively onto Biological Polymer-Colloid Templates Using Polymer-on-Polymer Stamping. *Langmuir.* **2004**, *20*, 7215-7222.

Zhou, D.; Bruckbauer, A.; Ying, L.; Abell, C.; Klenerman, D. Building Three-Dimensional Surface Biological Assemblies on the Nanometer Scale. *Nano Lett.* **2003**, *3*, 1517-1520.

Zhu, H.; Macal, M.; Jones, C. N.; George, M. D.; Dandekar, S.; Revzin, A. A miniature cytometry platform for capture and characterization of T-lymphocytes from human blood. *Anal. Chim. Acta.* **2008**, *608*, 186-196.

Zhu, H.; Stybayeva, G.; Silangcruz, J.; Yan, J.; Ramanculov, E.; Dandekar, S.; George, M. D.; Revzin, A. Detecting Cytokine Release from Single T-cells. *Anal. Chem.* **2009**, *81*, 8150-8156.

Zou, Y.; Yeh, P.-Y. J.; Rossi, N. A. A.; Brooks, D. E.; Kizhakkedathu, J. N. Nonbiofouling Polymer Brush with Latent Aldehyde Functionality as a Template for Protein Micropatterning. *Biomacromolecules.* **2010**, *11*, 284-293.

Zou, Z.; Du, D.; Wang, J.; Smith, J. N.; Timchalk, C.; Li, Y.; Lin, Y. Quantum Dot-Based Immunochromatographic Fluorescent Biosensor for Biomonitoring Trichloropyridinol, a Biomarker of Exposure to Chlorpyrifos. *Anal. Chem.* **2010**, *82*, 5125-5133.